УНИВЕРЗИТЕТ У НОВОМ САДУ

ФАКУЛТЕТ ТЕХНИЧКИХ НАУКА

ЕНЕРГЕТИКА, ЕЛЕКТРОНИКА И ТЕЛЕКОМУНИКАЦИЈЕ

СТОХАСТИЧКИ ДИНАМИЧКИ ОПИС ISI ВРЕМЕНСКИХ НИЗОВА: МАРКОВЉЕВИ МОДЕЛИ

ДОКТОРСКА ДИСЕРТАЦИЈА

Ментор: проф. др Драгана Бајић Кандидат: Јанош Миницх

Нови Сад, 2018. године

УНИВЕРЗИТЕТ У НОВОМ САДУ

UNIVERSITY OF NOVI SAD

FACULTY OF TECHNICAL SCIENCES

POWER ENGINEERING, ELECTRONICS AND TELECOMMUNICATIONS

STOCHASTIC DYNAMICAL DESCRIPTION OF THE ISI TIME SERIES: MARKOV MODELS

PhD THESIS

Mentor: prof. dr Dragana Bajic

Candidate: János Minich

Novi Sad, 2018.

UNIVERSITY OF NOVI SAD

УНИВЕРЗИТЕТ У НОВОМ САДУ
ФАКУЛТЕТ ТЕХНИЧКИХ НАУКА
KLJUČNA DOKUMENTACIJSKA INFORMACIJA

Redni broj: RBR	
Identifikacioni broj: IBR	
Tip dokumentacije: TD	Monografska dokumentacija
Tip zapisa: TZ	Tekstualni štampani materijal
Vrsta rada (dipl., mag., dokt.): VR	Doktorska disertacija
Ime i prezime autora: AU	Janoš Minich
Mentor (titula, ime, prezime, zvanje): MN	Prof. dr Dragana Bajić, redovni profesor
Naslov rada: NR	Stohastički dinamički opis ISI vremenskih nizova: Markovljevi modeli
Jezik publikacije: JP	Engleski
Jezik izvoda: JI	srp. / eng.
Zemlja publikovanja: ZP	Srbija
Uže geografsko područje: UGP	Vojvodina, Novi Sad
Godina: GO	2018

Izdavač: IZ	autorski reprint
Mesto i adresa: MA	Trg Dositeja Obradovića 6, Novi Sad
Fizički opis rada: FO	broj poglavlja 7 / stranica 91/ slika 80/ tabela 26/ referenci 27/ priloga 0
Naučna oblast: NO	Elektrotehničko i računarsko inženjerstvo
Naučna disciplina: ND	Telekomunikacije i obrada signala
Predmetna odrednica, ključne reči: PO	ISI vremenski nizovi, slučajni procesi, Markovljevi modeli
UDK	
Čuva se: ČU	U biblioteci
Važna napomena: VN	
Izvod: IZ	**Cilj:** Brzina ispaljivanja neuralnih impulsa u kori velikog mozga je veoma promenljiva što ukazuje da bi Poasonov tačkasti proces mogao da bude pogodan za modelirqnje takvog procesa. Međutim, brojna istraživanja su pokazala da statistika ispaljivanja ne sledi Poasona. Uprkos tome, još uvek se nije iskristalisao ni alternativni mehanizam koji bi opisao generisanje spajkova, ni raspodela koja bi opisala raspodelu intervala između spajkova (ISI). Ključni cilj ove disertacije je statistička analiza koja će omogućiti modelovanje ISI vremenskih nizova snimljenih u različitim delovima kore velikog mozga dok su majmuni rešavali različite probleme. **Metoda:** Primenjena je robusna neparametarska statistika da bi se odredila funkcija gustine raspodele (PDF) ISI vremenskih nizova. Rezultati su verifikovani butstrep metodom i iskorišćeni za kreiranje Markovljevog modela. **Rezultati:** Pokazalo se da se raspodela ISI intervala ne može opisati samo jednom funkcijom i da se statistika ne može da poveže isključivo sa već postojećim modelima, uključujući i eksponencijalni. Pokazalo se, zatim, da ISI statistika ne zavisi od regije u kori velikog mozga, niti, unutar jedne regije, od problema koji je budni majmun rešavao. Međutim, ISI mizovi

	snimani dok je majmun rešavao isti problem ali u različitim vremenskim intervalima nisu statistički slični, što ukazuje na postojanje varijabiliteta u ISI vremenskim nizovima u zavisnosti od problema koji se rešava. **Zaključak:** Rezultati analize signala ukazuju da je neuralna aktivnost posledica komplesnih generišućih mehanizama sa značajnom međuzavisnošću i da process zavisi od zadatka koji se rešava.
Datum prihvatanja teme od strane Senata: DP	
Datum odbrane: DO	
Članovi komisije: (ime i prezime / titula / zvanje / naziv organizacije / status) KO	predsednik: dr Fülöp Bazsó, naučni savetnik, Wigner Research Centre for Physics of the Hungarian Academy of Sciences, Department of Computational Sciences, Theoretical Neuroscience and Complex Systems Group član: dr László Négyessy, naučni savetnik, Wigner Research Centre for Physics of the Hungarian Academy of Sciences, Department of Computational Sciences, Theoretical Neuroscience and Complex Systems Group član: dr Vojin Šenk, redovni profesor, Fakultet tehničkih nauka, Univerzitet u Novom Sadu član: dr Vlado Delić, redovni profesor, Fakultet tehničkih nauka, Univerzitet u Novom Sadu mentor: dr Dragana Bajić, redovni profesor, Fakultet tehničkih nauka, Univerzitet u Novom Sadu

UNIVERSITY OF NOVI SAD
FACULTY OF TECHNICAL SCIENCES
KEY WORD DOCUMENTATION

Accession number: ANO	
Identification number: INO	
Document type: DT	Monograph documentation
Type of record: TR	Textual printed material
Contents code: CC	PhD Thesis
Author: AU	János Minich
Mentor: MN	Prof. dr Dragana Bajić
Title: TI	Full professor
Language of text: LT	English
Language of abstract: LA	eng. / srp.
Country of publication: CP	Serbia
Locality of publication: LP	Vojvodina, Novi Sad
Publication year: PY	2018.
Publisher: PU	

Publication place: PP	Novi Sad
Physical description: PD	Chapters 7 / Pages 91/ Figures 80/ Tables 26/ References 27/ Appendices 0
Scientific field SF	Electrptechnical and computer engineering
Scientific discipline SD	Communications and Signal Processing
Subject, Key words SKW	ISI time series, stochastic processes, Markov models
UC	
Holding data: HD	
Note: N	
Abstract: AB	**Objectives:** High variability of neuronal firing patterns in the cerebral cortex points towards spiking activity models based on Poisson point processes. In spite of growing evidence that firing behavior may fail Poisson statistics, an alternate spike generating mechanisms and the resulting inter-spike interval (ISI) distributions have not been clarified yet. The key objective of this thesis is to perform a statistical analysis that would yield a model of ISI time series recorded from different from different cortical areas of awake monkeys performing various behavioral tasks. **Methods:** A robust and non-parametrical statistics to determine ISI probability density functions (PDF-s) of extracellularly recorded cerebral cortical neurons of behaving macaque monkeys is performed. The results were validated using the bootstrap method. The obtained statistics were used to create a Markov model of ISI time series. **Results:** It turned out that there is no single ISI distribution, but many, and that the underlying statistics is not associated exclusively to the current established models including the exponential. Distribution of types of ISI statistics obtained from different cortical areas are statistically similar and the same applies to the statistics obtained from the same cortical area by ignoring ongoing behavior. However, particular ISI time series observed during the time epochs of the same

	behavioral task did not show statistical similarity, suggesting a task dependent variation of spike generating dynamics. **Conclusion:** In summary, the results indicate that neuronal firing activity is resulted by complex generative mechanisms with significant dependency and that this process is contingent upon the behavior.
Accepted on Senate on: AS	
Defended: DE	
Thesis Defend Board: DB	president: dr Fülöp Bazsó, senior research fellow, Wigner Research Centre for Physics of the Hungarian Academy of Sciences, Department of Computational Sciences, Theoretical Neuroscience and Complex Systems Group member: dr László Négyessy, senior research fellow, Wigner Research Centre for Physics of the Hungarian Academy of Sciences, Department of Computational Sciences, Theoretical Neuroscience and Complex Systems Group member: dr Vojin Šenk, full professor, Faculty of Technical Sciences, University of Novi Sad member: dr Vlado Delić, full professor, Faculty of Technical Sciences, University of Novi Sad mentor: dr Dragana Bajić, full professor, Faculty of Technical Sciences, University of Novi Sad

In memory of my father

János Minich

Acknowledgment

I wish to express my appreciation to my mentor Professor Dr. Dragana Bajić for her support and patience.

I thank colleagues and friends Laszló Négyessy, Fülöp Bazsó, Zoltán Somogyvári and László Zalányi from the Department of Theory, Institute for Particle and Nuclear Physics, Wigner RCP of the Hungarian Academy of Science, for useful suggestions and discussions during the development of this work.

Thanks to Emmanule Procyk from the Inserm, Stem Cell and Brain Research Institute and Pascal Barone from CerCo (CNRS-UT3), TMBI (Univ. Toulouse) who have given me access to and work on their data.

I wish to thank the members of my dissertation committee.

This research is supported by the Hungarian-Serbian (TET_10-1-2011-0001) and Hungarian-French (TET_14_FR-1-2015-0030) bilateral programs of the National Research, Development and Innovation Office of Hungary and Ministry of Education, Science and Technological Development (national grant TR32040).

I thank my mother, Jolán Minich, for the conditions without which this thesis has not been completed. And I also thank the patience of my son, Bertalan Olivér Minich. I hope that I will have the opportunity to make up for the time I took from them.

Contents

List of Figures

List of Tables

List of Abbreviation

CT	Computer Thomography
MRT	Magnetic Resonance Tomography
MRI	Magnetic Resonance Imagening
fMRI	Functional MRI
PET	Positron Emission Tomography
EEG	ElectroEncephaloGraphy
ECoG	ElectroCorticoGraphy
CDF	Cumulative Distribution Function
PDF	Probablity Densitie Function
ISI	Interspike Interval
CV	Coefficient of Variation
LV	Local coefficient of Variation

1. Introduction

1.1. The basics of neurology

The human brain is central part of the human nervous system. It is also the center of the control of the peripheral nervous system. Its function is to control the low level of unconsciousness activity such as the hart beet, breath rhythm and other metabolic functions, and to control higher level aware activity such as thought, reasoning, abstraction, etc. Consciousness is a mutual interaction of many systems in the brain. Final and detailed description of consciousness based on the biological ground has not been given jet.

Neurophysiology is medical science which exploring the activity of the healthy brain. There are several methods to explore the activity of the human brain. These methods belong to the scientific discipline called Neuroimaging. Methods are divided in two categories. One of them tries to gives a structural description while the other one gives a functional description of the human brain. Functional description is very important not only in case of diagnosis of the metabolic disease, wound, lesion, but also in exploring of the cognitive functions of the human brain. Since the information processing processes are followed by increased metabolism of specific region of the brain, functional description makes it possible to directly visualize the activity of different brain center.

1.2. Methods of reading neural signals

Computer tomography (**CT**) is a method used for quick examination of the brain. Computer algorithms processing the amount of x-rays absorbed in the relatively small volume of the brain, and visualize the results as cross section of the brain.

The method of *magnetic resonance tomography* (**MRT**) uses magnetic fields and radio waves to make a two or three dimensional image of the structure of the brain. The main advantage of this method that it dos not use any radioactive tracers to imaging. Because of the sophisticated mechanism of signal detection, the MRI is capable of depth and surface imaging with a high level of resolution, and tracking the temporal changes of the structure of the brain.

Functional MRI (**fMRI**) is based on the feature of the hemoglobin. It imaging the changes in the bloodstream in the brain caused by the neural activity. This method is capable of visualizing in which way and which structure of the brain was activated during solving some specific task. Since the method is very sensible of bloodstream changes, fMRI is used in the early diagnosis of the stroke.

Positron emission tomography (**PET**) uses radioactive tracers injected in the bloodstream to show the structure of the brain. The absorbed radioactive tracers in the different brain region are detected to get a two or three dimensional picture. Because of the fast decomposition of the radioactive tracers PET allows only a short time examination of the brain.

Electroencephalography (**EEG**) is a method which turns the brain activity into electrical signals. By placing electrodes on the skull it is possible to record collective activities of neurons in the near area of the electrodes. The main disadvantage of the method is its poor spatial resolution.

Electrocorticography (**ECoG**) is an invasive measuring method. It uses electrodes implanted by chirurgical procedure directly into or near the neural cell of the cerebral cortex. There are depth and surface electrodes. The depth electrode could measure the neural activity of dipper structure of the brain.

1.3. The neuron, the membrane potencial and the action potencial

The rule of the nervous system of humans and animals is to harmonize and adjust organism to the outer environment depending on the stimulation coming from it. The nervous system of the vertebrates makes:

- the central nervus system; it makes the brain and the spinal cord,

- the peripheral nervous system; it composes the nerves and ganglia.

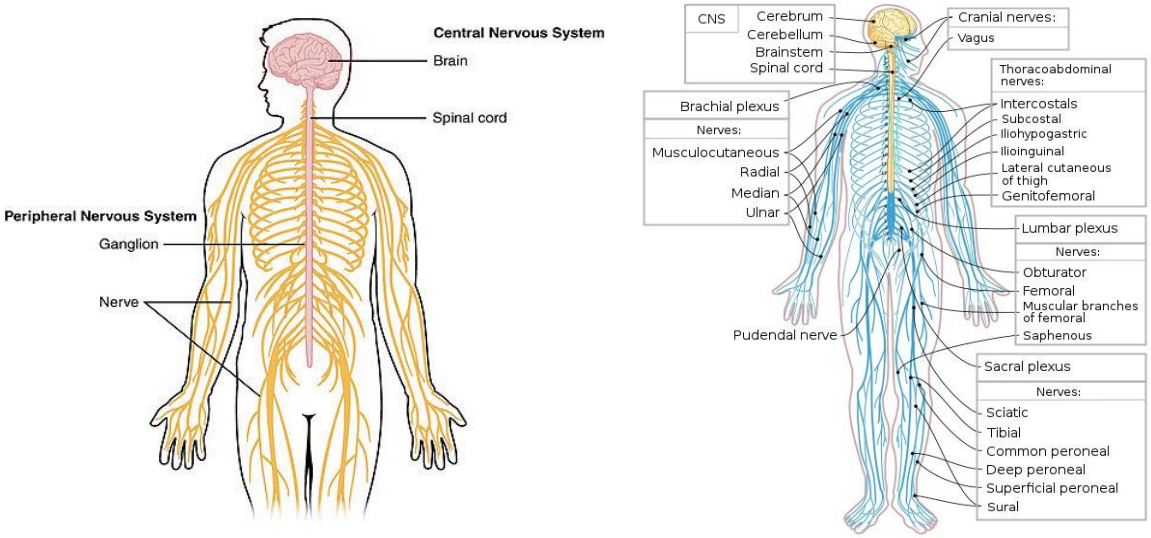

Figure 1 The diagram of the nervus system, Error! Reference source not found.

The components of typical neuron are:

- the body or *soma* of the neuron; it contains the nucleus which takes place the biggest part of the protein synthesis,
- the *dendrites* or the tree of the neuron which provides with its many branches a one-way supply of the stimuli to the body of the cell,
- the *axon*; it supplies the transfer of the neural impulses from the body of the cell to other neurons,
- the *axon terminal*; it contains synapses which excretes neurotransmitters doing communication with other neuron or neurons.

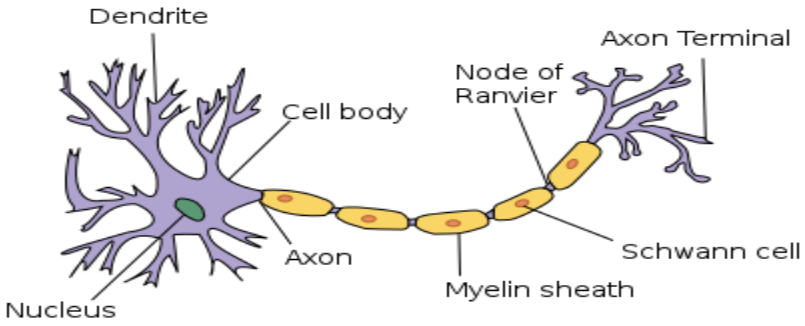

Figure 2 The typical neuron, [2]

There are many aspects which could be used for neuron classification. The two most important are based on:

- the effect or influence on other neurons:
  - *excitatory neurons*; they excite the targeted neurons,
  - *inhibitory neurons*; they suppress the neural impulses,
  - *modulatory neurons*.
- the way of spiking:
  - tonic or regular spiking,
  - phasic or bursting,
  - fast spiking,
  - thin-spike.

Neurons communicate by *neural impulses*. The neural impulse is a change of the *membrane potential* of the neuron which caused by the stimulation of the neuron. In the resting state, the membrane potential is called *resting potential*. Stimulating the neuron the resting potential rapidly changes. During this process a specific ion channels open and the concentration of the positive and negative charges change inside and outside of the cell. This phenomenon is called *action potential*.

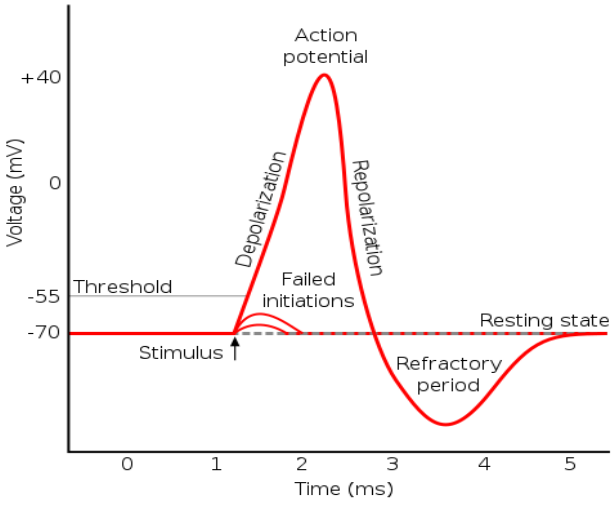

Figure 3 The action potential, [3]

The parameters of the action potential are:

- the time of the *stimulus*,
- the *resting potential*,
- the *rising phase*,
- the *falling phase*,
- the *peek*,
- the *overshoot* and the *undershoot*,
- the threshold level.

The neurons generate neural impulses on *all or nothing* basis. The stimulus of the cell needs to be large enough to force the membrane potential above the threshold level. When it happens the action potential appears. It has been observed that in the central nervous system the peek of the action potential is always the same and it does not change with the strength of the stimulus, but the frequency of the appearance of the action potential does. Action potential or neural impulse occurs at the beginning of the axon, and it carries it to the targeted neurons.

1.4. Measuring electrical impulses of neurons

Electrophysiology as science deals with methods which could measure the changes of the membrane potential of the neural cells especially action potential. The electrical activity of the neural cell could be measured in its natural environment (*in vivo*) or in laboratory controlled condition (*in vitro*). Both methods imply invasive surgical operation. To measure the membrane potential very fine micropipettes is used. They are placed into the cell (*intra cellular*) or near the cell (*extra cellular*). Today's application uses micropipettes made by glass. These are filled with solution with ion composition which is very similar to the composition of the interior of the cell. Appropriate conductor placed in the solution of the micropipette provides a closed electrical circuitry between the interior of the cell and the signal processing circuitry.

Voltage clamp

The advantage of the method is that it allows to the experimenter the possibility to hold the membrane potential on predetermined level. Considering that most ion channels of the cell membrane works as a voltage controlled gateway, it is possible to measure the ion current trough the cell membrane for given membrane potential. These channels pass ion currents only if the membrane potential reaches specific level. The apparatus essentially makes a current source with electrodes. The membrane voltage is measured trough voltage electrodes and it applied to the amplifier. The amplified membrane voltage has been compared with a determined membrane potential level. By the negative feedback the error signal drives the current into the cell trying to reduce the error to zero. Recording the sign and the intensity of the feedback current it is possible to determine the ion current trough the membrane of the tested cell.

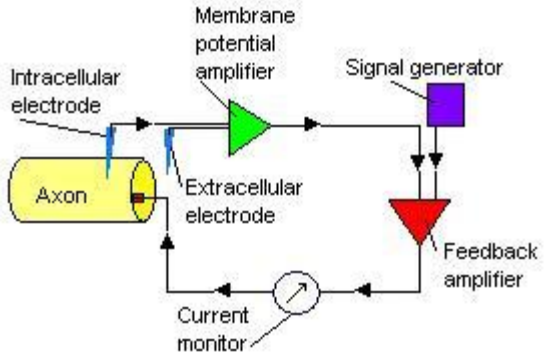

Figure 4 The voltage clamp method, [4]

Current clamp method

With this method it is possible to track and record the changes of the membrane potential caused by the cell him self or by stimuli. It is a good method to test the influence of the ion current trough the membrane on the generation of the membrane potential. This method commonly used to examine and understand the influence of neurotransmitters on the opening and permeability of the ion channels of the membrane. The instrumentation is the same as in the voltage clamp method. The difference is that the control is made trough the current electrode.

Patch clamp method

Micropipette with a relatively large opening is placed as near as possible to the tested cell. With gentile sanction a small part of the membrane surface is drown into the opening of the patch pipette. The main advantage of the method is that allows direct examination of the activity of a

specific ion channel. If the sanction force is strong enough to remove a small part of the membrane surface, than it is possible to monitor the activity inside of he cell. The disadvantage of the removing process is that the solution of the pipette is mixed with the ion composition of the interior of the cell causing dilution of the essential ingredients in the cell. This could change the condition of the action potential generation process and lead to the measurement error. There are many variation of this method.

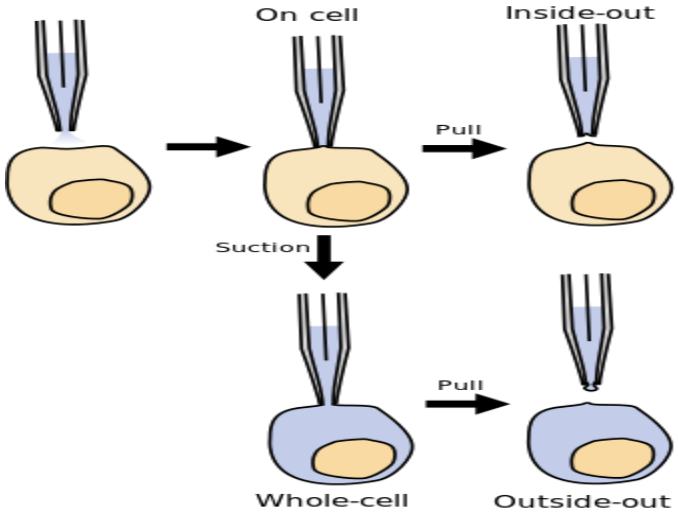

Figure 5 The patch clamp method, [5]

New methods

The disadvantages of the aforementioned classical methods are that they measure neural activity only one cell. Significant problems occur due to artifacts caused by the subject movement. Parallel measurement of the neural activity of more than one cell requires more implanted micropipettes which lead to significant tissue damage and complicated surgical intervention. The precise technological procedures, knew signal processing methods and cluster algorithms create the possibility of parallel measurement of electrical activity of the interior or the exterior of multiple cells. The structure of the neural network shows uneven spatial distribution of the neural cells in the brain. They are divided in *layers* of different depths. With these knew methods is possible to measure neural activity of different layers. Figure 6 shows the shape of a glass micropipette with eight different measuring positions. Every position measures electrical activity of the environment over eight parallel measuring channels. This configuration gives sixty four parallel recorded signals.

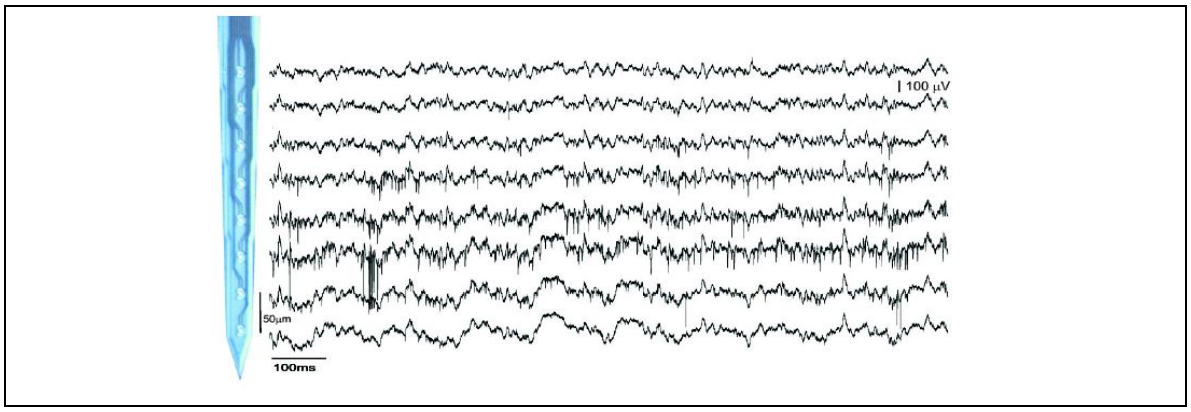

Figure 6 The micropipette with eight measuring position, [6]

2. The state of the art

2.1. The basic deterministic model of the neural cell

Integrate-and-fire neuron model

Lapicuque was the first who managed to model the neural cell membrane characteristics using parallel connected resistor and capacity. This simplified electrical circuit could mimic the action potential if the membrane capacitor is charged to some initial potential. When the level of threshold potential is reached the action potential generated, the capacitor discharged resetting the membrane potential. Lapicque used his model to compute the firing frequency of a nerve fiber resistively coupled to a stimulating electrode held at fixed voltage.

These types of neuron models do not describe the exact form of the action potential. The action potential is taken as an event which appears in some epoch. The integrate-and-fire model describes the neuron dynamics by two components:

- an equation to describe the form of action potential,
- a mechanism to generate spikes.

In the class of integrate-and-fire models the following elements are used:

- a linear differential equation to describe the form of the membrane potential,
- a threshold for spike firing.

This model is called the "leaky integrate-and-fire" model. Its basic electrical circuit consist a capacitor C and a resistor R driven by an input current $I(t)$, Figure . The voltage on the capacitor is given by the equation

$$RC \cdot \frac{dv(t)}{dt} + v(t) - v_{rest} = R \cdot I(t) \qquad \text{EQ 2-1}$$

This equation is a linear differential equation. It represents a leaky integrator or RC-circuit with parallel connected resistor R and capacitor C. From the point of view of the neuroscientist it is called the equation of a passive membrane. If the initial condition is $v(t_0) = v_{rest} + \Delta v$ the solution of the equation is

$$v(t) - v_{rest} = \Delta v \cdot e^{-\frac{t-t_0}{RC}}, \quad t > t_0 \qquad \text{EQ 2-2}$$

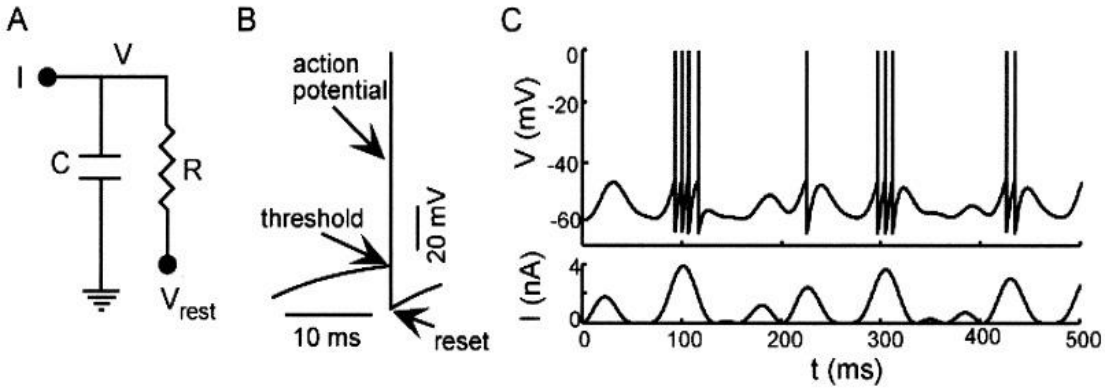

Figure 7 The leake integrate and fire model of the neuron

The benefit of this model lies in the separation of time scales between the extremely rapid action potential and slower process that affect synaptic integration, bursting, and adaptation. It has been used in the studies ranging from analyzing synaptic integration by single neurons to simulations of networks containing relatively complex connected

neurons. This model found to be useful in understanding the properties of large neural networks and the implications of large numbers of synaptic connections.

However, the leaky integrate-and-fire model is not capable to explain many aspects of neuronal dynamics:

- the input is integrated linearly, independently of the state of the postsynaptic neuron,

- after the action potential was generated the membrane potential is reset and the spikes before has been forgotten, no memory present and adaptation process, fast-spiking and bursting processes can not be captured,

- nonlinear interactions between different presynaptic spikes are neglected.

Hodgkin-Huxley model of neuron

As it has been described earlier, the action potential is a result of the difference of the potential of the interior and exterior of the cell. This difference is caused by the flow of charged ions trough the ion channel of the cell membrane. Analyzing the giant axon of the squad, Hodgkin and Huxley succeeded to measure these currents and described their dynamics in terms of differential equations. Originally, the Hodgkin–Huxley model describes only three types of ion channel. It can be extended to include many other ion channel types. The cell membrane separates the interior of the cell from the extracellular liquid and acts as a capacitor. If an input current $I(t)$ is injected into the cell, it may add further charge on the capacitor, or leak through the channels in the cell membrane. Each channel type is represented by a variable resistor. The unspecific channel has a leak resistance R, the sodium channel a resistance R_{Na} and the potassium channel a resistance R_K. The value of the resistance changes depending on whether the ion channel is open or closed. Because of the flow of the ions through the cell membrane, there is a different ion concentration between the inside and the outside of the cell. This difference of ion concentration generates the Nernst potential. Every specific difference of ion type is presented as a separate battery. There are voltage source for sodium, potassium, and

the unspecific third channel, labeled as E_{Na}, E_K, and E_L respectively. The equation which describes the membrane potential is

$$C \cdot \frac{dv_m(t)}{dt} = I(t) - \sum_k I_k(t)$$

where the sum $\sum_k I_k(t)$ is the sum of all currents trough the membrane ion channels. To model the open and closed uncertainty of the ion channels, Hodgkin and Huxley introduced additional variable m, n and h. The combined action of m and h controls the N_a^+ channels while the K^+ gates are controlled by n. Hodgkin and Huxley formulated the three ion currents on the right-hand side as

$$\sum_k I_k = g_{Na} m^3 h(v - E_{Na}) + g_K n^4 (v - E_K) + g_L (v - E_L)$$

The three gating variables m, n and h change according to differential equations of the form

$$\frac{dm(t)}{dt} = -\frac{m - m_0(u)}{\tau_m(u)}, \quad \frac{dn(t)}{dt} = -\frac{n - n_0(u)}{\tau_n(u)}, \quad \frac{dh(t)}{dt} = -\frac{h - h_0(u)}{\tau_h(u)}$$

The number of ion channels is finite, and the specific ion channels open and close stochastically. The ion current over the patch of membrane for every repeated experiment is never the same. The Hodgkin–Huxley equations describe the opening and closing of ion channels with deterministic equations correspond to the current density through an extremely large patch of membrane containing an infinite number of channels or, alternatively, to the current through a small patch of membrane but averaged over many repetitions of the same experiment. To model the stochastic characteristic appropriate noise could be added to the model.

The Hodgkin–Huxley model describes the generation of action potentials on the level of ion channels. It could be used to analyze sophisticated biophysical neuron models with more than three types of ion currents. Electrophysiologists have described an overwhelming richness of different ion channels and the set of ion channels is different

from one neuron to the next. The precise channel configuration in each individual neuron determines a good deal of its overall electrical properties.

Some of the disadvantages of the Hodgkin–Huxley model are:

- adding new ion currents to model a specific membrane are makes the universality of the Hodgkin-Huxley equations questionable,

- Hodgkin-Huxley equation is not derived based on the microscopic behavior of the opening and closing of ion channels,

- the analysis of collective phenomena in neuronal networks often rely on much simpler and more tractable models of the single neuron than that used by Hodgkin and Huxley.

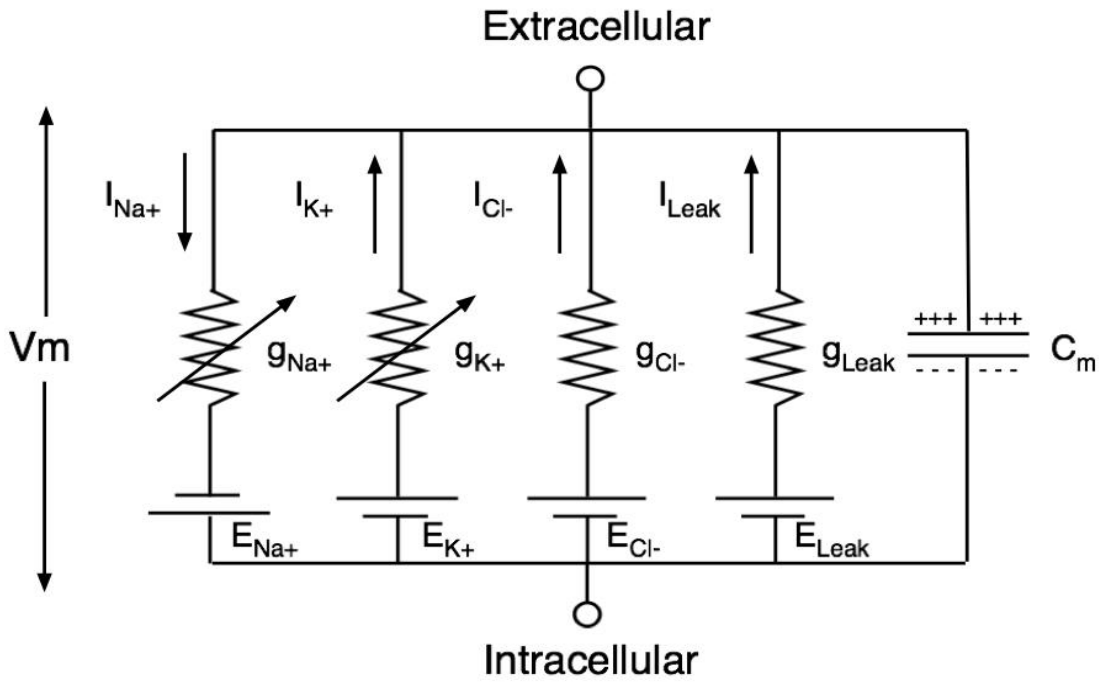

Figure 8 Hodgkin–Huxley model of the neuron

Dendrites and synapses.

The Hodgkin–Huxley model disregards the spatial structure of the neuron and reduces it to a point-like spike generator. However, the spatial structure of a neuron could

potentially be important for signal processing in the brain. The electrical properties of neurons have been described as a capacitor that is charged by synaptic currents and other ion currents across the membrane. A non-uniform distribution of the membrane potential on the dendritic tree and the soma induces additional longitudinal current along the dendrite. To describe these phenomena cable equation has been derived. This model of neuron is known as the cable theory model. It describes the membrane potential along a dendrite as a function of time and space.

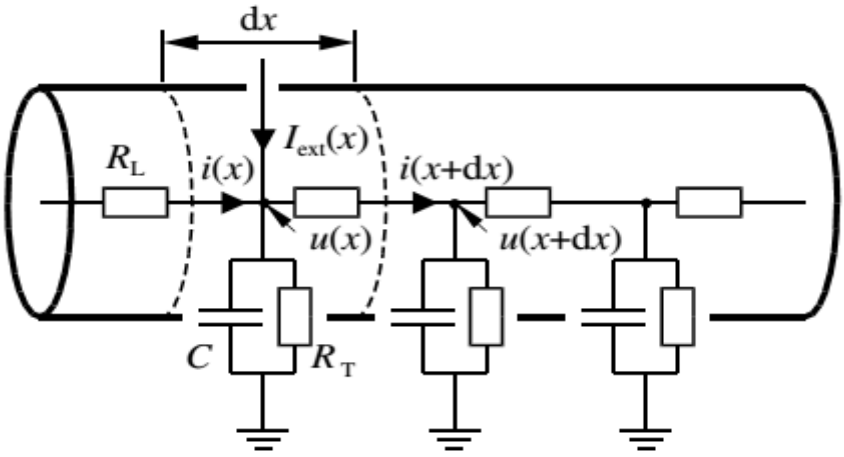

Figure 9 cable theory model of the neuron

The compartment model

The cable theory model supposes that the dendritic tree is at most locally equivalent with a uniform cable. The different kind of diameter and electrical property along of the dendrite makes the solution of the cable equation not so easy. Discretization of the dendritic tree by dividing it in smaller element makes the solution of the cable equation easier. This model is known as the compartment model of the neuron.

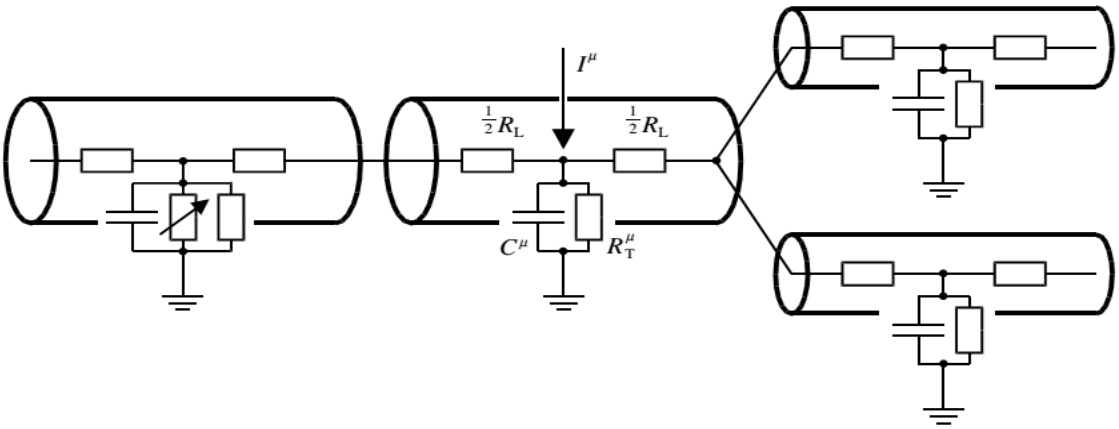

Figure 10 The compartment model of the neuron

2.2. The basic statistical assumption of neural activity

The detailed analysis of the action potential generation process shows that the appearance of the action potential is irregular. This is also true for the laboratory conditions. The nature and the causing effect of this phenomenon is still a subject of many research works. The questions such as "Is there a *neural noise* in the neural system and what is its role in the system?", "Can the neural noise causes a significant irregularity in the appearance of the neural impulses?" are still should be answered.

As possible source of this neural noise two sources are usually mentioned. One of them is thermal noise which could be explained and analyzed by Hodgkin-Huxley model. The second one explains the source of the noise as a variable number of membrane channels dedicated to specific ions, [8]. However, theoretical researches on the field of neural systems modeling, where the neural connections made randomly, show that the irregularity in the timing of the neural impulses is not conditioned to the neural noise. The irregularity is the feature of the system as a whole and not of the element or elements of the system, [9].

To explain and interpret the irregularity of the spike timings usually states two not so different kind of interpretation. These are also used to try to explain the information coding process in the brain, [10].

In the work of Adrian et. al. sensory neural cell were examined, [11]. They found that the strength of the stimulus is coded by the variable flow of the spikes and the irregular timing is due to neural noise. This type of information coding and irregularity is called *rate coding*. The rate of the neural impulses is determined by the number of generated impulses in a unit time interval. This parameter is the crucial datum in the information coding process. However, irregularity caused by the noise limits the amount of information proceeded by sensory neurons. In stabile physiology characteristics, the estimation of the rate parameter is possible even in the relatively low level of noise. But, high level of noise causes significant changes in the impulse timings and the accuracy of the estimated rate parameter decreases.

It is interesting to ask, whether the rate of the generated neural impulses in unit time is the only parameter which describes the information coding processes in sensory and motor event? The search for the answer created the second interpretation of information coding known as *temporal coding*, [11]. By this interpretation, if the timing of neural impulses presents important factor in information coding process, than the irregular feature of these events is the crucial part of the signal sequences. In this case, the noise accompanied by the signal in form of irregular timing could amplify the sensibility to the relatively small signals. This type of phenomenon is known as *stochastic resonance*, [13].

Regardless of the interpretation accepted, irregular feature of the neural spikes generation process comes to the statistical and stochastic analysis of the Interspike Interval (*ISI*) sequences of two consecutive neural impulses. One of the interesting observations shows, that the analysis made on the *ISI* time series dos not mentions the confirmed feature of statistical stationarity, randomness or independency. The second one is that most of the published research works based on the assumption that the neural spikes are generated by Poisson process, [14], [15], [16] . If this assumption would be true than the empirical probability density function of the log *ISI* values shows a straight line. In the recent years a lot of published research works have questioned this assumption, [17], [18], [19], [20]. The author of this doctoral thesis shows in his master thesis, that the Poisson process is not the appropriate model to describe the statistical characteristic of the *ISI* time series. The results show that many different kind of

probability density function can be fitted to the random, independent and unimodal *ISI* time series. But, the most frequent type of functions is the Generalized-Pareto, Generalized-Extreme Value and Log-Normal [27].

3. The theory of Markov processes

3.1. Stochastic processes, [21]

Suppose that $X(t)$ is a random variable for every value of $t \in T$. The set of random variables for different value of $t \in T$ is a random function in time. This random function is a stochastic or random process. The value of stochastic process at every epoch $t \in T$ changes randomly. Let denote the probability space of possible values of stochastic process as (Ω, A, P). At every epoch $t \in T$ the value of stochastic process is from the set R. So, (R, B) is a phase space of stochastic process at t.

Definition 3-1.: Let (Ω, A, P) be a probability space and T a set of parameters t. The real valued stochastic process on (Ω, A, P) with (R, B) phase space and index set T is a family of

$$X = \{X(t), \quad t \in T\}$$

measurable functions

$$X(t): \ (\Omega, \mathrm{A}) \ \rightarrow \ (R, \mathrm{B}).$$

For a given $X = \{X(t), \quad t \in T\}$ stochastic process the value of $X(t)$ for a given t is a random variable. It has a one dimensional cumulative density function (cdf)

$$F_1(x;t) = P(X(t) < x)$$

The set of t with n given elements $(t_1, t_2, \ldots, t_n)$ defines a set of random variables $(X(t_1), X(t_2), \ldots, X(t_n))$. The n-dimensional cdf of the set $(X(t_1), X(t_2), \ldots, X(t_n))$ is

$$F_n(x_1, x_2, \ldots, x_n; t_1, t_2, \ldots, t_n) = P(X(t_1) < x_1, X(t_2) < x_2, \ldots, X(t_n) < x_n).$$

For a different set of t we have a family of different n-dimensional cdf function. The family of all n-dimensional cdf $F(x_1, x_2, \ldots, x_n; t_1, t_2, \ldots, t_n)$, $n = 1, 2, \ldots$ is a family of n-dimensional cdf of the stochastic process X. These cdf underlies the symmetry and consistency condition.

The n-dimensional cdf is symmetric if it is invariant of the permutation of all n pairs of (x_i, t_i), that is for all permutation of $(t_1, t_2, \ldots, t_n)$ stay

$$F_n(x_{j_1}, x_{j_2}, \ldots, x_{j_n}; t_{j_1}, t_{j_2}, \ldots, t_{j_n}) = F_n(x_1, x_2, \ldots, x_n; t_1, t_2, \ldots, t_n)$$

The n-dimensional cdf is consistent if

$$F_n(x_1, x_2, \ldots, x_{n-1}, +\infty; t_1, t_2, \ldots, t_{n-1}, t_n) = F_{n-1}(x_1, x_2, \ldots, x_{n-1}; t_1, t_2, \ldots, t_{n-1}).$$

The definition of stochastic process says, that $X(\omega, t)$ is a function of two variables, $\omega \in \Omega$ and $t \in T$. This function has following properties:

1. for variable ω and given t it is a random variable,

2. for given ω and variable t it is a real valued deterministic function,

3. for given ω and given t it is a real number,

4. for variable ω and variable t it is a real valued random function.

Property 2 is a realization of the stochastic process. It is also called the *trajectory* of the stochastic process. If the experiment consists of recording the values at different time, than the outcome will be one of the possible realization or trajectory of the stochastic process. If the experiment repeated again, a different trajectory will be obtained.

Some examples of stochastic processes, [22].

1. Stochastic processes with independent values.

The stochastic process is with independent values if for every $n \in \square$ and $(t_1, t_2, \ldots, t_n) \in T^n$ is true

$$F_n(x_1, x_2, \ldots, x_n; t_1, t_2, \ldots, t_n) = F_1(x_1; t_1) \cdots F_1(x_n; t_n) = \prod_{i=1}^{n} F_1(x_i; t_i)$$

Stochastic processes with independent values are connected with the class of processes with uncorrelated values and the class of processes with orthogonal values.

The stochastic process is with uncorrelated values if

$$\operatorname{cov}(X(t), X(s)) = E\left[\left(X(t) - E[X(t)]\right) \cdot \overline{\left(X(s) - E[X(s)]\right)}\right] = 0, \quad \forall t \neq s$$

The stochastic process is with orthogonal values if $E\left[X(t) \cdot \overline{X(s)}\right] = 0, \quad \forall t \neq s$.

2. Stochastic processes with independent increments.

The stochastic process is with independent increments if for any given set of

$t_0 \leq t_1 \leq \cdots \leq t_n$ the sequence of random variables

$$X(t_0), X(t_1) - X(t_0), X(t_2) - X(t_1), \ldots, X(t_n) - X(t_{n-1})$$

are independent. To describe this process it is enough to know the functions

$$F_1(x; t) = P(X(t) < x), \text{ and } G(x; t, s) = P(X(t) - X(s) < x).$$

This implies that the knowledge of cdf of the second order is fully describes the characteristics of these processes.

3. Stochastic processes with finite moment of second order.

These are the complex valued processes $X(t) = a(t) + i \cdot b(t)$, where $a(t)$ and $b(t)$ are real valued stochastic processes and for every $t \in T$

$$E\left[\left|X(t)\right|^2\right] = E\left[X(t)\overline{X(t)}\right] = E\left[a^2(t)\right] + E\left[b^2(t)\right] < \infty$$

4. Stochastic processes with orthogonal increments.

These stochastic processes satisfy the condition

$$E\left[\left|X(t) - X(s)\right|^2\right] < \infty, \quad t, s \in T$$

5. Stationary stochastic processes.

The stochastic process is strictly stationary if its all n-dimensional cdf are invariant of the time shift, i.e.

$$F_n(x_1, x_2, \ldots, x_n; t_1 + h, t_2 + h, \ldots, t_n + h) = F_n(x_1, x_2, \ldots, x_n; t_1, t_2, \ldots, t_n)$$

If the strictly stationary stochastic process has mean and its moments of second order are finites, than i.e.

$$E\left[X(t)\right] = E\left[X(t+h)\right] = m = const.$$

$$k(t,s) = E\left[\left(X(t) - m\right) \cdot \overline{\left(X(s) - m\right)}\right] = E\left[\left(X(t-s) - m\right) \cdot \overline{\left(X(s-s) - m\right)}\right] =$$
$$= E\left[\left(X(t-s) - m\right) \cdot \overline{\left(X(0) - m\right)}\right] = B(t-s)$$

The stochastic process is weekly stationary (wide-sense stationary) if its all moments of up to second order are finites, its mean is constant and its correlation function is a function of the difference of its arguments.

6. Gaussian stochastic processes.

The Gaussian stochastic process has a family of n-dimensional Gaussian cdf. These stochastic processes have a characteristic function

$$f_{t_1, t_2, \ldots, t_n}(\lambda_1, \lambda_2, \ldots, \lambda_n) = E\left[e^{i \cdot \sum_{j=1}^{n} \lambda_j X(t_j)}\right] = e^{i \cdot \sum_{j=1}^{n} \lambda_j m_j - \frac{1}{2} \sum_{j,k=1}^{n} \lambda_j \lambda_k r_{j,k}}$$

Where

$$m_j = E\left[X\left(t_j\right)\right], \quad r_{j,k} = E\left[\left(X\left(t_j\right) - m_j\right)\left(X\left(t_k\right) - m_k\right)\right]$$

It follows, that the functions $m(t) = E\left[X\left(t\right)\right]$ and $K(t,s)$ are sufficient to describe the Gaussian stochastic process.

7. Markov processes.

The stochastic process is a Markov process if for every nondecreasing set $t_1, t_2, \ldots, t_n \in T$ if it satisfies

$$P\left(X\left(t_n\right) < x_n \mid X\left(t_1\right) < x_1, \ldots, X\left(t_{n-1}\right) < x_{n-1}\right) = P\left(X\left(t_n\right) < x_n \mid X\left(t_{n-1}\right) < x_{n-1}\right)$$

This equation states that the future $X\left(t_n\right)$ of the Markov process depends only on the knowledge of the present and independent of the knowledge of the past.

In the mathematical study of stochastic processes the concept of continuity is one of the most important properties.

Definition 3-2: Stochastic process $\left\{X\left(t\right), \quad t \in T\right\}$ is stochastically continues at the point t_0 if

$$P\left(\left|X\left(t\right) - X\left(t_0\right)\right| \geq \varepsilon\right) \to 0, \quad t \to t_0$$

This definition describes the local behavior of the stochastic process at the point t_0. It could be extended on the interval $[a,b]$ if the above definition applies for any point in the given interval. Another form of definition of stochastic continuity states

Definition 3-3: Stochastic process $\left\{X\left(t\right), \quad t \in T\right\}$ is almost sourly continues in the interval $[a,b] \subset T$ if its almost all trajectory are continues in that interval.

The stochastic continuity of the stochastic process is its local property, while the almost sourly continuity is its global characteristic.

3.2. Markov processes

Let (Ω, A, P) be the probability space of the stochastic process $\{X(t), \quad t \in T\}$ with phase space (R, B). For $s \in T$ denote F_s the σ-field generated by the family of random variables $X(u), \quad u \le s, u \in T$.

Denote $\mathrm{F}_s = \sigma\{X(u); \quad u \le s, \quad u, s \in T\}$ the σ-field generated by the family of random variables $X(u), \quad u \le s, \quad u, s \in T$. Denote $\mathrm{F}_s^+ = \sigma\{X(v); \quad v \ge s, \quad v, s \in T\}$ the σ-field generated by the family of random variables $X(v), \quad v \ge s, \quad v, s \in T$. Denote $P(A \mid X(s))$ the conditional probability of the event A conditioned of the σ-field generated by the random variable $X(s)$.

Definition 3-4: The stochastic process $\{X(t), \quad t \in T\}$ has a Markov property if it satisfies the equation

$$P(X(t) \in B \mid \mathrm{F}_s) = P(X(t) \in B \mid X(s))$$

In the study of Markov processes the parameter t is interpreted as time. In this context, $X(t)$ describes the time evolution of some stochastic system. The random variable $X(s)$ is the present state of the system. If $u < s$, than the family of $X(u)$ represents the evolution of the system in the past. If $v > s$, than the family of $X(v)$ represents the future of the system. In this context, the Markov property says that the evolution in the future depends only on the present state and independent of the past.

The conditional probability $P(X(t) \in B \mid X(s)) = f(s, X(s), t, B)$ is a measurable function of $x \in$ and it is a function of the parameters s, t, B. This function is the transition probability of the Markov process. If the system in epoch $s < t$ is in state $X(s)$ than the transition probability gives a probability that it will be in one of the state from set B at epoch t. The transition probability has following properties:

1. as function of B it is a probability of (R,B)

$$P(s,X(s),t,B)\geq 0,\quad P(s,X(s),t,R)=1$$

2. as a function of x it is B-measurable,

3. $P(X(t)\in B\mid X(t)=x)=1,\quad x\in B$

4. Chapman-Kolmogorov equation

$$P(X(t)\in B\mid X(s))=\int_R P(X(t)\in B\mid X(\tau)=y)P(X(\tau)=dy\mid X(s))$$

Suppose that Markov process has finite or denumerable set of states. To define the measure in (R,B) it is enough to give finite or denumerable number of transition probabilities $P(X(t)=x_k\mid X(s)=x_j)=p_{jk}(s,t)$. The Chapman-Kolmogorov equation becomes

$$p_{jk}(s,t)=\sum_v p_{jv}(s,\tau)\,p_{vk}(\tau,t),\quad s<\tau<t$$

Using matrix notation $\mathbf{P}(s,t)=\left[p_{jk}(s,t)\right]$, $s<t$, the matrix form of Chapman-Kolmogorov equation is

$$\mathbf{P}(s,t)=\mathbf{P}(s,\tau)\mathbf{P}(\tau,t),\quad s<\tau<t$$

The transition matrix $\mathbf{P}(s,t)$ is a stochastic matrix with the following properties:

- $\mathbf{P}(s,t)\geq 0$,

- $\sum_k p_{jk}(s,t)=1$,

- $\mathbf{P}(t,t)=\mathbf{I}$

To describe the n-dimensional cdf it is enough to know the initial probability $P(X(t_0)\in B_0),\quad B_0\in\mathrm{B}$ and the transition probabilities $P(X(t)\in B\mid X(s)=x)$. This implies that the Markov process is fully characterized by its two-dimensional cdf. If the

transition probability $P\left(X\left(t\right)\in B\,|\,X\left(s\right)=x\right)$ is only a function of the difference $t-s$ for any x and B, than the Markov process satisfy the homogeny condition. Than the Chapman-Kolmogorov equation describes the evolution of the process as

$$P\left(X\left(t\right)\in B\right)=\int_{-\infty}^{\infty}P\left(X\left(t\right)\in B\,|\,X\left(0\right)=x\right)P\left(X\left(0\right)\in dx\right).$$

In case of Markov process with finite states, the matrix equation has a form

$$\mathbf{P}\left(t+s\right)=\mathbf{P}\left(t\right)\cdot\mathbf{P}\left(s\right)$$

3.3. Markov chain [23]

Let the parameter t takes integer values and denote it with n. Let the phase space be a finite set of countable elements called states. We recall that, finite stochastic process is an independent process if the knowledge of any sequence of observations up to n-th observation does not affect the prediction of the next observation. In case of Markov processes, this condition is weakened to allow the immediate past to influence on the prediction of the next observation. The Markov property has a form

$$P\left(X\left(n\right)=s_j\,|\,X\left(n-1\right)=s_i,X\left(n-2\right)=s_k,\ldots\right)=P\left(X\left(n\right)=s_j\,|\,X\left(n-1\right)=s_i\right)$$

Definition 3-5: Denote with $p_{ij}\left(n\right)$ the conditional probabilities which corresponds to Markov property. The n-th step transition probabilities of the Markov process are

$$p_{ij}\left(n\right)=P\left(X\left(n\right)=s_j\,|\,X\left(n-1\right)=s_i\right)$$

Definition 3-6: A finite Markov chain is a finite Markov process such that the transition probabilities do not depend on n, i.e. $p_{ij}\left(n\right)=p_{ij}$.

Definition 3-7: The transition matrix of the Markov chain is a matrix $\mathbf{P}$ which elements are p_{ij}. The vector of initial probability p_0 is the vector which contains the probabilities of the set of states at initial or starting time.

The initial probabilities and the transition matrix are enough to determine the Markov chain process, since they are sufficient to give a probability measure of any sequence of the process. Given any probability vector p_0 and any probability matrix $\mathbf{P}$, there is a unique Markov chain with initial probability vector p_0 and transition matrix $\mathbf{P}$.

Let s_j denote the state of the process at time n. Denote F the sequence of states after n and P the sequence of the states up to n. The Markov property could be expressed in a following form

$$P\left(F \cap P \mid s_j\right) = \frac{P\left(F \cap P \cap s_j\right)}{P\left(s_j\right)} = \frac{P\left(F \mid P \cap s_j\right) \cdot P\left(P \cap s_j\right)}{P\left(s_j\right)} =$$
$$= \frac{P\left(F \mid s_j\right) \cdot P\left(P \cap s_j\right)}{P\left(s_j\right)} = P\left(F \mid s_j\right) \cdot P\left(P \mid s_j\right)$$

This form says that for the known present state the future and past are independent of each anther.

For finite Markov process, the probability that the process at time n will be in state s_j is equal to the sum of all possible state sequences ending in state s_j, i.e for a given transition probabilities $p_{ij}(n)$

$$P\left(X(n) = s_j\right) = \sum_k P\left(X(n-1) = s_k\right) \cdot p_{kj}(n)$$

Let denote $p^{(n)}$ the vector of the probabilities of the different states at time n. For a given initial probability vector p_0 and transition matrix $\mathbf{P}$, the matrix form of the above statement is

$$p^{(n)} = p^{(n-1)} \cdot \mathbf{P}(n) = p^{(n-2)} \cdot \mathbf{P}(n-1) \cdot \mathbf{P}(n) = p^{(n-3)} \cdot \mathbf{P}(n-2) \cdot \mathbf{P}(n-1) \cdot \mathbf{P}(n) =$$
$$= p_0 \cdot \mathbf{P}(1) \cdot \mathbf{P}(2) \cdots \mathbf{P}(n-2) \cdot \mathbf{P}(n-1) \cdot \mathbf{P}(n)$$

In case of Markov chain the transition matrix $\mathbf{P}(n)$ does not depend on n. The above expression takes the form $p^{(n)} = p_0 \cdot \mathbf{P}^n$. It shows, that the study of the probabilities of the different state of the Markov chain is reduced to the study of the power of the transition matrix $\mathbf{P}$.

State Classification

The classification of the state of the Markov chain could be made by inspecting whether it is possible to go from a given state to another given state. In this context states can be divided into equivalence classes. Two states are elements of the same class if they communicate, i.e. it is possible to go from either state to another one in the class. The equivalence classes define equivalence relations. The basic property of the equivalence relation is that it partitions the set of states. It is reflexive, symmetric and transitive. The week ordering relation holds only the reflexive and transitive properties. By the week ordering relation it is possible to order the states. If the equivalence relation is the identity relation, than the week ordering relation is a partial ordering.

Definition 3-8: A subset of states of the whole set of states is a minimal element of the partial ordering if its members cannot contact members of other classes. A subset of states of the whole set of states is a maximal element of the partial ordering if its members cannot be contacted by embers of any other class.

Definition 3-9: The minimal elements of the partial ordering of equivalence classes are called ergodic sets. Its elements are called ergodic states. The remaining elements are called transient states and they make a transient sets.

For every finite Markov chain there must be at least one ergodic set, however there need be no transient set. If the finite Markov chain has no transient set, than its states make one ergodic set or there are several ergodic sets which do not communicate with others. If the ergodic set contains one state, it is called absorbing state. If the state s_i is absorbing state than its transition probabilities are

$$p_{ij} = \begin{cases} 1, & i = j, \\ 0, & i \neq j. \end{cases}$$

The equivalence classes can be divided into cyclic classes. If there is only one cyclic class it is called regular. Otherwise it is called cyclic. In case of regular classes after sufficient time the process can be in any state of the class independently of its starting state in class. It also means that the sufficiently high power of its transition matrix must be positive. If the class is cyclic, than no power of the transition matrix can be positive.

Based on the above state classification it is possible to classify Markov chain.

I. Chains without transient sets.

If this chain has more than one ergodic set, than there is no connection between them, hence there is two or more unrelated Markov chains lumped together. They could be studied separately.

a. If the ergodic set is regular it is called regular Markov chain. No matter where the process starts, after sufficient time passed it could be in any state.

b. If the ergodic set is cyclic it is called cyclic Markov chain. This type of chain has period d. For a given starting state it move trough the cyclic sets in a definite order, and returning to the set of he starting state after d steps.

II. Chain with transient sets.

In this case if the process starts from the transient set it moves toward the ergodic sets. After the process enters in the ergodic set it cannot escape from it. So, the classification of the chains will be made by their ergodic sets.

a. If all ergodic sets are unit sets, the Markov chain is called absorbing chain.

b. All ergodic sets are regular, but not all are absorbing sets.

c. All ergodic sets are cyclic.

d. There are cyclic and regular sets simultaneously.

Let us focus our attention on ergodic chain. In case of ergodic chain, it is possible to go from any every state to every other state. This is true when the ergodic chain has a single ergodic class i.e. $d=1$. If $d>1$, this kind of transition is possible for special number of steps. The transition matrix has zero elements and their position change cyclically in the matrix with the power of the transition matrix. Hence $\mathbf{P}^n$ does not converge.

Theorem 3-1: For any ergodic chain the sequence of powers $\mathbf{P}^n$ is Euler-summable to limiting matrix $\mathbf{A}$, and this limiting matrix is of the form $\mathbf{A}=\xi\cdot\alpha$, with α a positive probability vector.

Theorem 3-2: If $\mathbf{P}$ is an ergodic transition matrix,

a) the sequence $\mathbf{P}^n$ is Cesaro-summable to $\mathbf{A}$,

b) the series $\mathbf{I}+\sum_{i=1}^{\infty}\left(\mathbf{P}^i-\mathbf{A}\right)$ is Ceasaro-summable to $\mathbf{Z}$.

Theorem 3-3: The transition matrix $\mathbf{P}$ is regular if and only if for some N the matrix $\mathbf{P}^N$ is positive i.e. it has nonzero elements.

Theorem 3-4: If $\mathbf{P}$ is a regular matrix then

a) the limit $\lim_{n\to\infty}\mathbf{P}^n=\mathbf{A}$ exist,

b) each row of the matrix $\mathbf{A}$ is the some probability vector $\alpha=\{a_1,a_2,\ldots,a_n\}$, that is $\mathbf{A}=\xi\cdot a$ where ξ is a unit column vector,

c) the elements of α is a positive vector.

Theorem3-5: If $\mathbf{P}$ is a regular matrix and $\mathbf{A}$ and α are given as in *Theorem 3-4*, then

a) for a probability vector π the product $\lim_{n\to\infty}\pi\cdot\mathbf{P}^n=\alpha$,

b) the vector α is a unique probability vector such that $\alpha\cdot\mathbf{P}=\alpha$,

c) $\mathbf{A}\cdot\mathbf{P}=\mathbf{P}\cdot\mathbf{A}=\mathbf{A}$.

The matrix $\mathbf{A}$ and the vector α will be called as the limiting matrix and limiting probability vector for the Markov chain determined by $\mathbf{P}$. It is also called stationary vector or stationary matrix of the Markov chain. The last theorem says that for the regular Markov chain the long range predictions are independent of the initial vector. The fundamental matrix $\mathbf{Z}$ of the regular Markov chain plays basic quantity in determining the properties of the chain.

Theorem 3-6: Let $\mathbf{P}$ be the transition matrix and $\mathbf{A}$ stationary matrix for a regular Markov chain. Then the matrix

$$\mathbf{Z} = \mathbf{I} + \sum_{k=1}^{\infty} \left(\mathbf{P}^n - \mathbf{A} \right) = \left(\mathbf{I} - \mathbf{P} + \mathbf{A} \right)^{-1}$$

exists and it is referred as the fundamental matrix of the regular Markov chain. It has the following properties

a) $\mathbf{P} \cdot \mathbf{Z} = \mathbf{Z} \cdot \mathbf{P}$,

b) $\mathbf{Z} \cdot \xi = \xi$,

c) $\alpha \cdot \mathbf{Z} = \alpha$,

d) $\mathbf{I} - \mathbf{Z} = \mathbf{A} - \mathbf{P} \cdot \mathbf{Z}$.

Definition 3-10: For a regular Markov chain, the first passage time n_k is a function whose value is the number of steps before entering state s_k for the first time after the initial position.

Definition 3-11: The mean first passage matrix, denoted by $\mathbf{M}$, is the matrix with entries $m_{ij} = E_i \left[n_j \right]$.

Let us collect all the properties of the matrix $\mathbf{M}$ in the following theorem.

Theorem 3-7: Properties of the mean first passage matrix $\mathbf{M}$ are

a) it satisfy the equation $\mathbf{M} = \mathbf{P} \cdot \left(\mathbf{M} - \mathbf{M}_{dg} \right) + \mathbf{E}$,

b) for the stationary distribution α of the matrix $\mathbf{P}$, then $m_{ij} = \frac{1}{a_i}$,

c) it is given by $\mathbf{M} = \left(\mathbf{I} - \mathbf{Z} + \mathbf{E} \cdot \mathbf{Z}_{dg}\right) \cdot \mathbf{D}$,

d) $\alpha \cdot \mathbf{M} = \eta \cdot \mathbf{Z}_{dg} \cdot \mathbf{D}$.

Theorem 3-8: Let us define matrix $\overline{\mathbf{M}} = \mathbf{M} - \mathbf{D}$. Than, for any regular Markov chain

a) the matrix $\mathbf{M}$ has an inverse,

b) $\alpha = (c-1) \cdot \left(\overline{\mathbf{M}} \cdot \xi\right)^T$,

c) $\mathbf{P} = \mathbf{I} + (\mathbf{D} - \mathbf{E}) \cdot \overline{\mathbf{M}}^{-1}$.

Theorem 3-9: The variance of the mean first passage time is $\mathrm{var}_i\left[n_j\right] = \mathbf{W} - \mathbf{M}_{sq}$ where $\mathbf{W} = \mathbf{M}\left(2 \cdot \mathbf{Z}_{dg} \cdot \mathbf{D} - \mathbf{I}\right) + 2 \cdot \left(\mathbf{Z} \cdot \mathbf{M} - \mathbf{E} \cdot \left(\cdot \mathbf{M}\right)_{dg}\right)$.

Reverse Markov chain

Recall, that if the forward process is a Markov chain, the reverse process will be a Markov chain if $P\left(X(n) = s_j\right)$ does not dependent on n regardless of the starting state. It is an obvious property if the process starts from the equilibrium.

Definition 3-12: Let $\mathbf{P}$ be the transition matrix for an ergodic Markov chain. Let α be the fixed probability vector for $\mathbf{P}$. Then the reverse Markov chain for $\mathbf{P}$ is a Markov chain with transition matrix given by $\mathbf{P} = \mathbf{D} \cdot \mathbf{P}^T \cdot \mathbf{D}^{-1}$.

Definition 3-13: A Markov chain is reversible if $\mathbf{P} = \mathbf{P}$.

Theorem 3-10: A Markov chain is reversible if and only if $\mathbf{D}^{-1} \cdot \mathbf{P}$ is a symmetric matrix.

Theorem 3-11: The fixed probability vector for $\mathbf{P}$ and $\mathbf{P}$ is the same.

Theorem 3-12: The fundamental matrix for the reverse Markov chain is $\overline{\mathbf{Z}} = \mathbf{D} \cdot \mathbf{Z}^T \cdot \mathbf{D}^{-1}$.

Theorem 3-13: $\overline{\mathbf{M}} - \mathbf{M} = (\mathbf{Z} \cdot \mathbf{D}) - (\mathbf{Z} \cdot \mathbf{D})^T$

Theorem3-14: $\overline{\mathbf{W}} - \mathbf{W} = \left(\mathbf{Z} \cdot \mathbf{D} - (\mathbf{Z} \cdot \mathbf{D})^T\right) \cdot \left(2 \cdot \mathbf{Z}_{dg} \cdot \mathbf{D} - 3 \cdot \mathbf{I}\right) + 2 \cdot \left(\mathbf{Z}^2 \cdot \mathbf{D} - (\mathbf{Z}^2 \cdot \mathbf{D})^T\right)$

4. Data description and the statistical properties

This chapter contains descriptions of the datasets which were used in the data analysis procedure. The chapter describes the experimental condition used in the process of the signal recording. All experimental protocols, such as care, surgery, and training of animals, were done according to the Public Health Service policy on the use of laboratory animals and complied with guidelines of the European Ethics Committee on Use and Care of Animals.

The basic empirical statistical properties are given for both dataset. These includes the mean, median, mode, geometrical mean, harmonical mean, the kurtosis and skewness coefficients. The different coefficient of variation (CV) and local coefficient of variation (LV) are also given.

The variability of the neural firing patterns in the cerebral cortex was analyzed by exemining statistical properties of the interspike interval (ISI) between two consecutive action potencial. In order to describe these random variabilities of the values of the ISI sequences, the probabilitie densitie function (PDF) given in Table 1 were used. The PDF s which were selected are the most common functions in the scientific and mathematical literature. In the fitting procedure robust statistical methods were used.

To measure the time dependency of the adjacent ISI values, the Poincare plots were used. Combining it with the theory of copula function, the results show that the adjacent

ISI samples are highly dependent and these dependencies can not be described by *PDF* function.

Table 1 The list of probabilitie densitie fuction

CODE	PDF TYPE	DATA TYPE
1	Log-Normal (LN)	ISI
2	Exponential (E)	ISI
3	Weibull (W)	ISI
4	Chi-square (C2)	ISI
5	Gamma (G)	ISI
6	Noncentral Chi-square (NcC2)	ISI
7	Rayleigh (R)	ISI
8	Uniform (U)	ln ISI
9	Fisher (F)	ISI
10	Noncentral Fisher (NcF)	ISI
11	Noncentral Student (NcT)	ln ISI
12	Student (T)	ln ISI
13	Extreme Value (EV)	ln ISI
14	Generalized Extreme Value (GEV)	ln ISI
15	Generalized Pareto (GP)	ISI
16	Generalized Beta-2	ln ISI

4.1. *IM* dataset, [24], [25]

4.1.1. Recording from *ACC* brain area

EXPERIMENTAL PROCEDURES

Housing, surgical, electrophysiological, and histological procedures were carried out according to the European Community Council Directive (1986) (Ministe `re de l'Agriculture et de la Fore ˆt, Commission nationale de l'expe ´rimentation animale) and Direction De´partementale des Services Ve´te ´rinaires (Lyon, France). Each animal was seated in a primate chair within arm's reach of a tangent touch-screen (Microtouch System) coupled to a TV monitor. An arm-projection window was opened in the front panel of the chair, allowing

the monkey to touch the screen with one hand. A computer recorded the position and accuracy of each touch. It also controlled the presentation via the monitor of visual stimuli (color shapes), which served as light targets (CORTEX software, NIMH Laboratory of Neuropsychology, Bethesda, MD). Eye movements were monitored using an infrared system (Iscan Inc., USA). Four target items (disks of 5 mm in diameter) were used: upper left (UL), upper right (UR), lower right (LR), lower left (LL). A central white disk served as fixation point (FP). The lever was disposed just below the FP.

Task

Two male rhesus monkeys were trained in the problem solving task (PS). Monkeys had to find by trial and error which target, presented in a set of four, was rewarded. Each trial started by the onset of a starting target named ‘‘lever.’’ The animal had to start a trial by touching the lever and holding his touch. The FP appeared, and the animal had to fixate it with his gaze. A delay period (2 s) followed, and ended by the simultaneous onset of the four targets. At the FP offset, the animal made a saccade toward a target, fixated it (0.5 s), and then touched it following the GO signal. All targets switched off at the touch, and a 0.6 s delay followed before the feedback was given. A reward (fruit juice) was delivered for choosing the correct target (positive feedback; white arrowhead). If a choice in one trial was incorrect (no reward, negative feedback; black arrowhead), the monkey could select another target in the following trial and so on until the solution was discovered (search period). Each touch was followed by an interval of 2 s. The animal had to search for the correct target by trial and error. After discovery, the animal was allowed to repeat the response. In 90% of cases, after the third repetition, a red flashing signal (the four targets in red) indicated the start of a new problem, i.e., a search for a new correct target. In 10% of cases, the repetition lasted for 7 or 11 trials. A problem was composed of two periods: a ‘‘search’’ period that included all incorrect trials up to the first correct touch, and a ‘‘repetition’’ period wherein the animal was required to repeat the correct touch.

Recordings

Monkeys were implanted with a head-restraining device, and an atlas-guided craniotomy was done to expose an aperture over the prefrontal cortex. Neuronal activity was recorded using epoxy-coated tungsten electrodes (1–4 MOhm at 1 kHz; FHC Inc, USA). One to four microelectrodes were placed in stainless-steel guide tubes and independently advanced into the cortex through a set of micromotors (Alpha-Omega Engineering, Israel). Neuronal activity was sampled at 13 kHz resolution and LFP at 900 Hz. Recordings were referenced on the guide tubes in contact with the dura and containing the microelectrodes. Recording sites covered an area extending over about 6 mm (anterior to posterior), in the dorsal bank of the anterior cingulate sulcus, at stereotaxic antero-posterior levels superior to A+30, and at depths superior to 4.5 mm from cortical surface. Locations were confirmed by anatomical MRI and histology.

Unit Activity

Single activity was identified using online spike sorting (MSD, AlphaOmega). The activity of single neurons was compared with respect to different events and outcomes resulting from different conditions by using averaged peristimulus histograms (PSTH) and trial-by-trial spike counts (NeuroExplorer, Nex Technology, USA, and MatLab—The MathWorks Inc.—home-made scripts). PSTHs had a binning of 0.01 s and were boxcar averaged. Neural activity was considered to be significantly different between conditions if it exceeded 5 standard deviations of the mean difference between trial types taken during the window -600/-200 ms preceding event alignment time and remained above this threshold for more than six 0.01 s bins.

4.1.2. Recording from *dlPFC* brain area

Behavioral task

Data from three monkeys (Macaca mulatta) are reported here. Two monkeys were trained in the two following tasks.

Delayed response task.

The monkey sat in a primate chair in front of a vertical touch screen (Elo-Touch; 19 inches, 48 cm) positioned at arm reach distance. Eye movements were monitored and digitized at 100 Hz using an Iscan (Burlington, MA) infrared system.

The animal touched a central target (lever) to trigger the appearance of a fixation point (FP). An FP fixation of 700 ms triggered the appearance of a 500 ms light cue at one of the four possible locations (targets were positioned at the corners of a virtual square 10 cm from the FP. After an ensuing delay period of 2–2.5 s (during which the monkey was required to maintain fixation on the FP), all four possible targets were illuminated and, 100 ms later, the FP was extinguished. The monkey then had to make a saccade toward the remembered target. After the monkey fixated on the remembered target for 390 ms, all the targets turned white (go signal), indicating that the monkey was required to touch the target. A juice reward was delivered 600 ms after a correct touch. The trial aborted in case of an incorrect or a premature touch, or a break in eye fixation.

For the first sessions of the experiment, cues were delivered by blocks of three consecutive trials. Thus, in the second and third trials of each block the animals could predict the location of the next cue. This design was then abandoned. It concerns five cells included in the pool of data.

Problem-solving task.

Task events were similar to the DR task, except that the correct target location was not specified by a cue. Monkeys had to find it via trial and error. A problem was composed of two periods: a “search period” that included all incorrect trials up to the first correct touch, and a “repetition period” wherein the animal was required to repeat the correct touch three times.

In the case of an incorrect touch, all targets disappeared, and in the next trial the animal was required to continue his search for the correct target. A juice reward was delivered 600 ms after a correct touch. After the third repetition, a red flashing signal (circle of 8 cm in diameter centered on the FP position) indicated the start of a new

problem (i.e., a search for a new correct target). Two consecutive problems never had the same solution.

A third monkey was trained in the PS task with a variation concerning reward size. For each problem, the size of the reward was randomly selected between two sizes (small, 0.25 ml; large, 0.5 ml). At the beginning of each trial, the color of the lever indicated whether the reward would be small (red lever) or large (green lever).

Electrophysiological recordings.

Monkeys were implanted with a head-restraining device, and a magnetic resonance imaging-guided craniotomy was done to expose a circular aperture over the prefrontal cortex. Neuronal activity was recorded using varnish-coated tungsten electrodes (1– 4 Mohm at 1 kHz). One or two electrodes were placed in stainless-steel guide tubes and independently advanced into the cortex through a set of micromotors (Alpha-Omega, Nazareth, Israel). Neuronal activity was sampled with 30ms resolution and recorded waveforms were sorted into separate units using a template-matching algorithm (CED, Cambridge, UK). All animal training, surgeries, and experimental procedures were done in accordance with National Institutes of Health guidelines, and approved by the Yale Animal Care and Use Committee. The third animal was recorded using an AlphaLab system (Alpha-Omega).

4.1.3. Statistical properties of the *IM* dataset

From data obtained 698 *ISI* sequences is extracted for further analysis. Since the exact probability density function of the individual data has not been known, most of the tests used in the analysis are distribution free tests. At first the randomness of the data has been tested using Wald-Wolfowitz non-parametric test. The result shows that $53.58\%(374/698)$ of the data has random and independent, identically distributed characteristics. Using the dip test the percentage of the unimodal sequences is $70.91\%(495/698)$. The percentage of the data that are random and unimodal is $34.24\%(239/698)$, Table 2.

Table 2 The percentage of data with different kind of statistical properties

Dataset	Number of ISI sequences	Data type			
		random, independent	unimodal	random, independent, unimodal	random, independent, unimodal, convergent ML estimation
IM	698	374 (53.58%)	495 (70.91%)	252 (36.1%)	239 (34.24%)

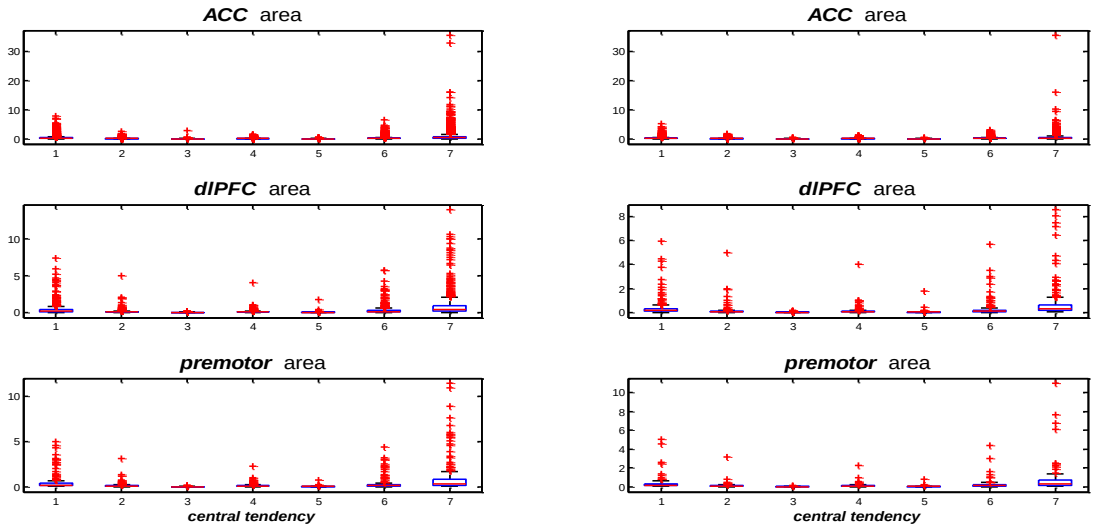

Figure 11 The descriptive statistics of the *IM* dataset; 1-mean, 2-median, 3-mode, 4-geometric mean, 5-harmonic mean, 6-trimmed mean (10%), 7-square root

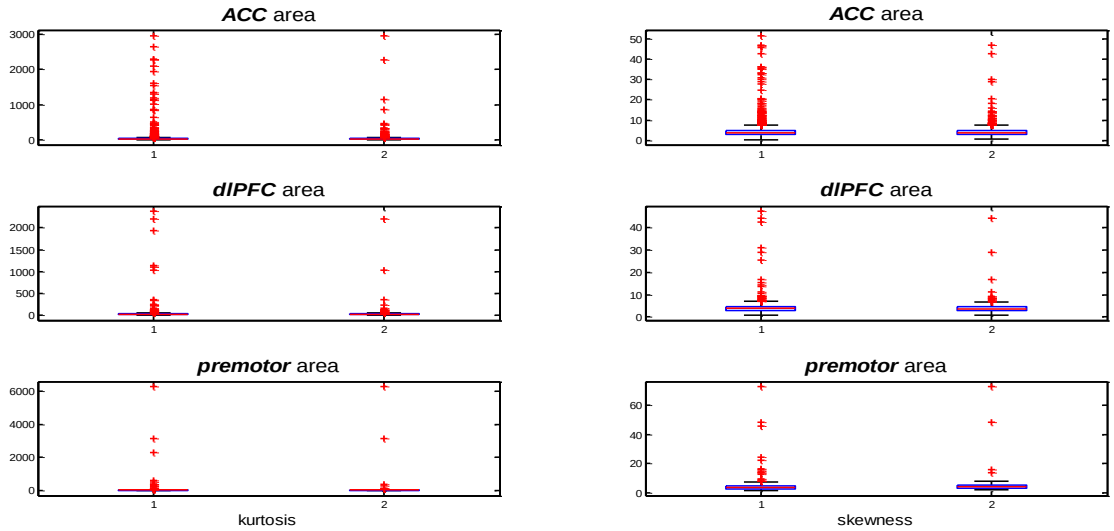

Figure 12 The kurtosis and skewness coefficient of the *IM* dataset

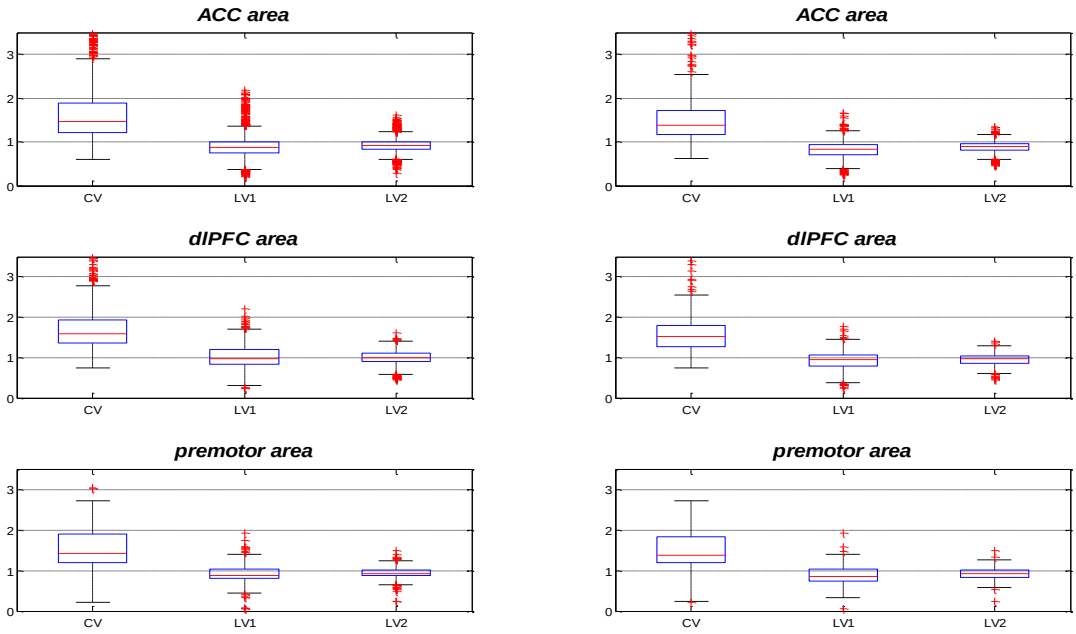

Figure 13 The different coefficients of the *IM* dataset

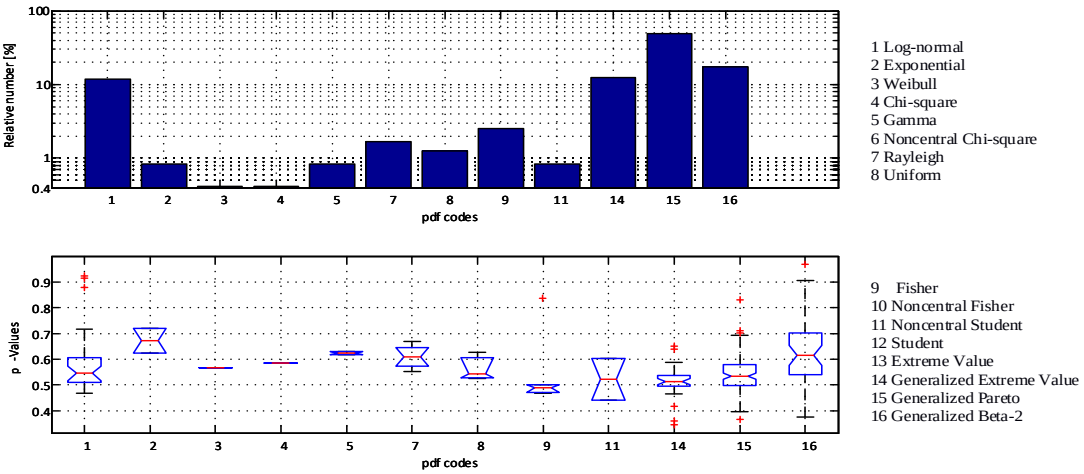

Figure 14 The results of the fitting procedure of the IM dataset. The number of data sequences with convergent fitting results is 239. Upper panel: a relative number of particular PDF types. Lower panel: box plot of the corresponding p-values. PDF code numbers are listed in the right (from Table 1). Note that a small number of neural units with Weibull and Chi-squared distribution (code 3 and 4) cause a narrow box plot. Code numbers 6, 10, 12 and 13 dose not appeared as a winner PDF in the estimation process.

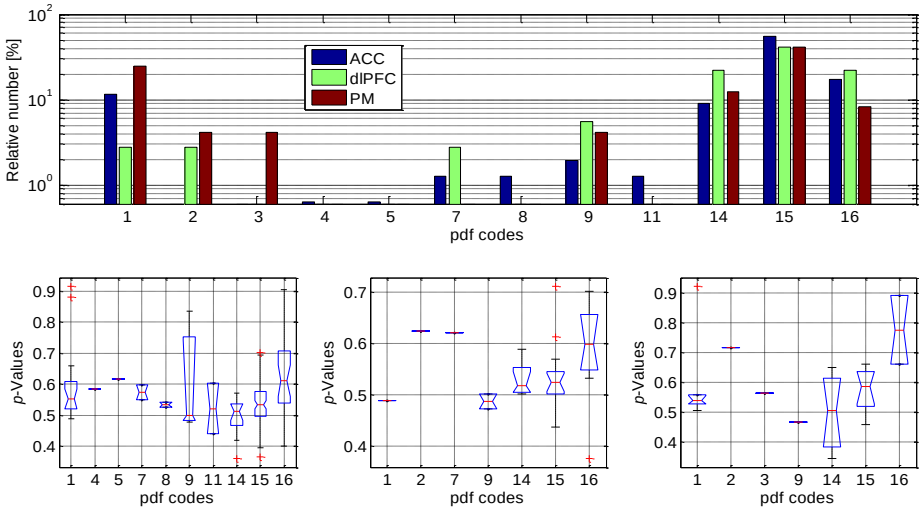

Figure 15 The results of the fitting procedure of the IM dataset within the different brain areas. Upper panel: the relative number of PDF-s in the ACC, dlPFC and PM brain area. Lower panel: the corresponding p-values.

4.2. *IP* dataset, [26]

4.2.1. recording

Behavioral task

The core of the present study concerns two monkeys (Mk1 and Mk2) trained to perform a visually guided saccadic task during which the visual target could be accompanied by an auditory stimulus (V/VA active task). A trial was initiated by the appearance of a fixation point (FP) located at the center of the video screen and of a size of 0.2 degree. The monkey had to direct its gaze and to maintain fixation at this central point. The duration of presentation of the FP was randomized between trials and lasted between 1500 to 1800 ms. Simultaneously, with the extinction of the FP, a peripheral visual target was flashed for 50 ms. The monkey was required to perform a saccade in the direction to the locus of the visual target within 250 ms of its appearance. Responses

were considered as correct when the saccades were performed within a window of 4 × 4 degrees centered on the visual target, and in these cases a few drops of fruit juice were delivered to the monkeys as a reward. In half of the trials, presented randomly, a 25 ms sound (a white noise) was delivered from a speaker located at the same eccentricity on the azimuth as the visual stimulus. In such visuo-auditory trials (VA), the visual and the auditory stimuli were presented at the exactly same time. In both conditions (V and VA) the monkey was required to perform a saccade directed toward the visual target and consequently, the auditory stimulus had no behavioral meaning for the animal. Note that we did not train the monkeys to perform a saccade toward the auditory stimulus alone.

The first monkey engaged in the present study (Mk1) was first trained to perform two control tasks before the V/VA active task. In a first stage, the monkey was trained to perform a simple passive fixation task (V/VA passive task). Following the presentation of the FP (of variable duration from 1500 to 1800 ms), a visual or visuo-auditory stimulus was presented for 500 ms together with the FP. To get rewarded, the monkey had to maintain its fixation until the FP was extinguished.

Further, Mk1 was trained in a visual control task (V-only control task), during which the color of the FP informed the animal whether he had to maintain a central fixation (blue FP) or to make a saccade toward a visual peripheral stimulus (Red FP). In this case the visual stimulus was never accompanied by an auditory stimulus. The timing of stimulus presentation was identical to that described for the active task (50 ms).

The monkey Mk1 was engaged successively in each of these different protocols for several months, a period during which electrophysiological recordings were performed in the primary visual cortex (see below). Mk2 was trained from the beginning to do the VA active task.

4.2.2. Statistical properties of the *IP* datase

From data obtained 1234 *ISI* sequences is extracted for further analysis. The distribution-free results show that $86.22\%(1064/1234)$ of the data has random and independent, identically distributed characteristics. The percentage of the unimodal

sequences is $63.53\%(784/1234)$. The percentage of the data that are random and unimodal is $16.61\%(205/1234)$, Table 3.

Table 3 The percentage of data with different kind of statistical properties

Dataset	Number of ISI sequences	Data type			
		random, independent	unimodal	random, independent, unimodal	random, independent, unimodal, convergent ML estimation
IP	1234	1064 (86.22%)	784 (63.53%)	688 (55.75%)	205 (16.61%)

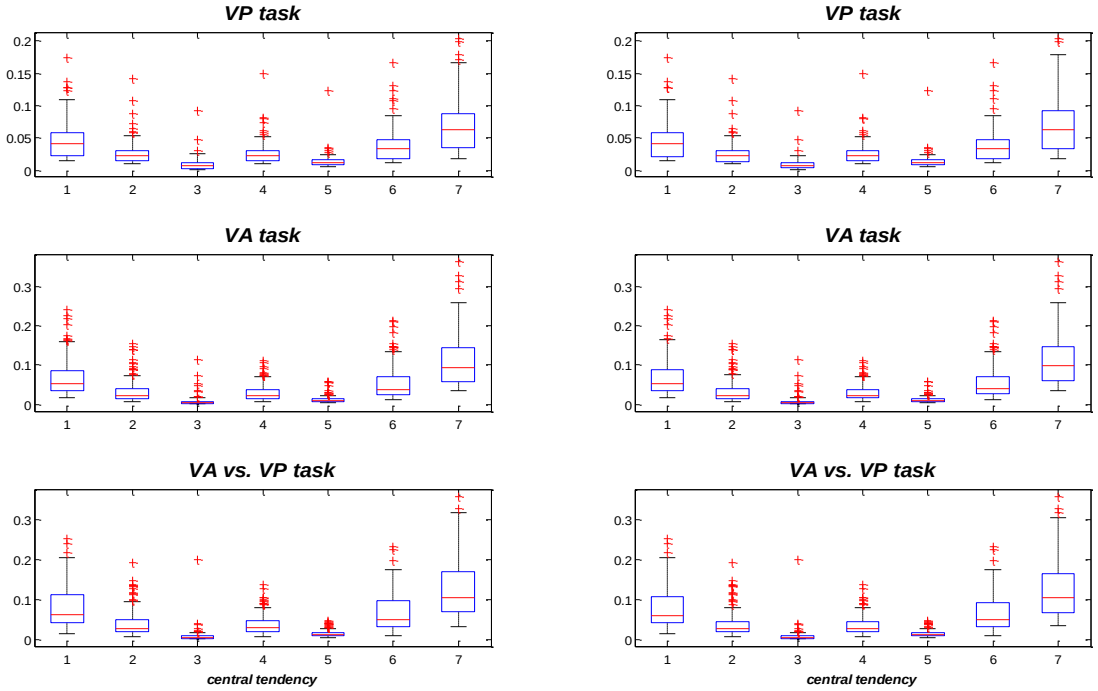

Figure 16 The descriptive statistics of the IP dataset; 1-mean, 2-median, 3-mode, 4-geometric mean, 5-harmonic mean, 6-trimmed mean (10%), 7-square root

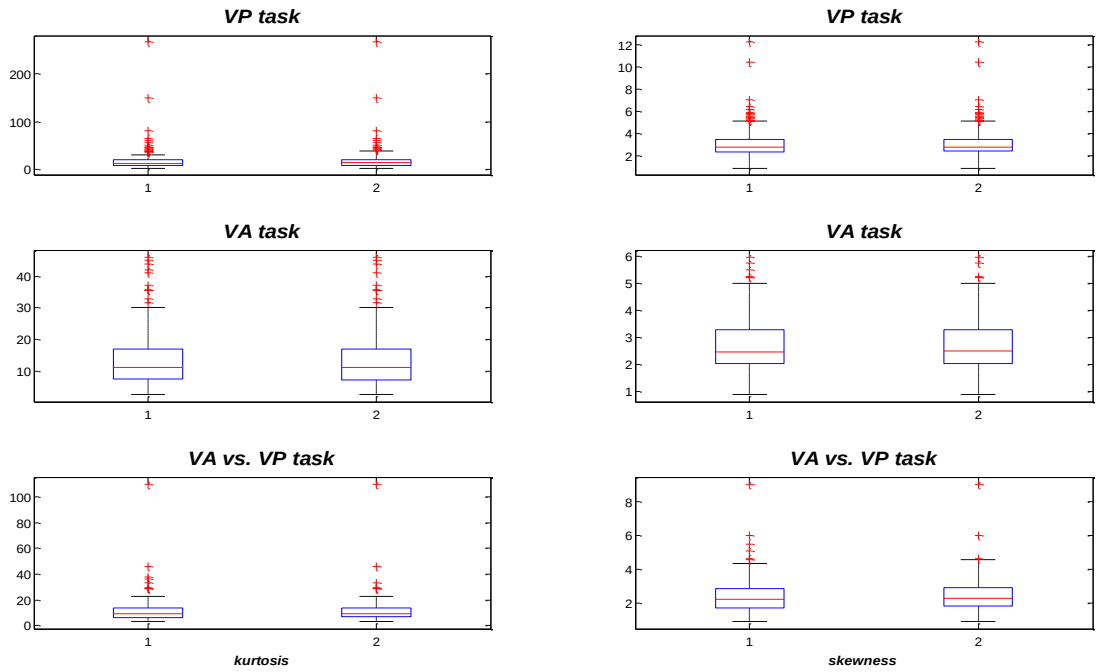

Figure 17 The kurtosis and the skewness coefficients of the IP dataset

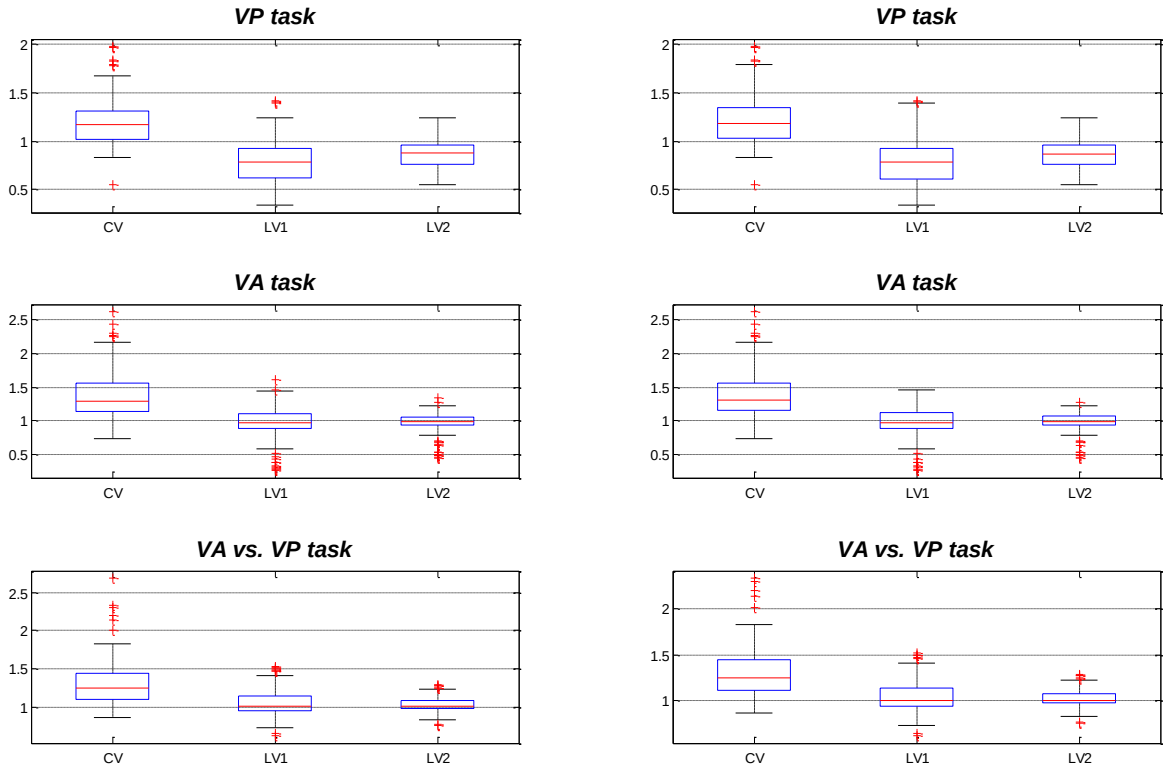

Figure 18 The different coefficient of variation of the IP dataset.

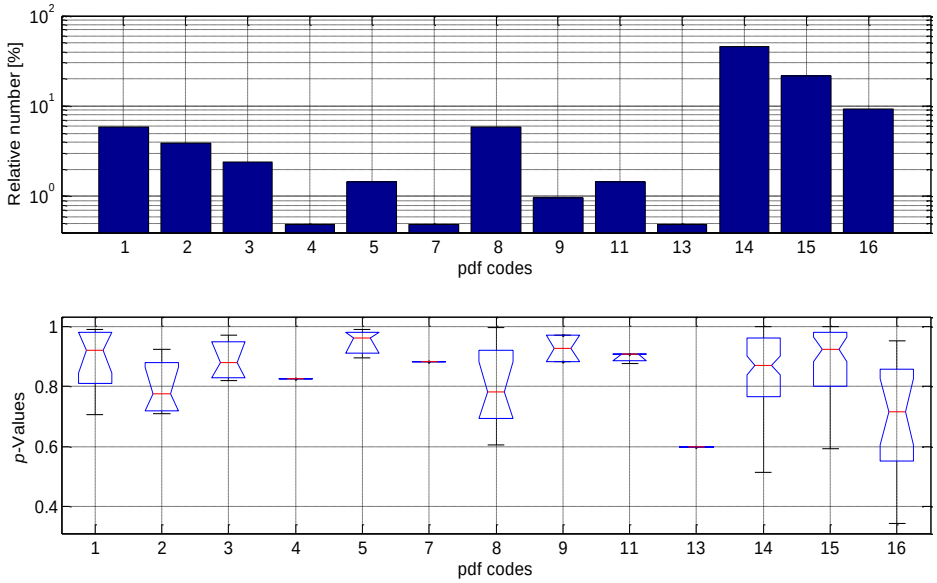

Figure 19 The results of the fitting procedure of the IP dataset consisting of 209 data sequences. Upper panel: a relative number of particular PDF types. Lower panel: box plot of the corresponding p-values.

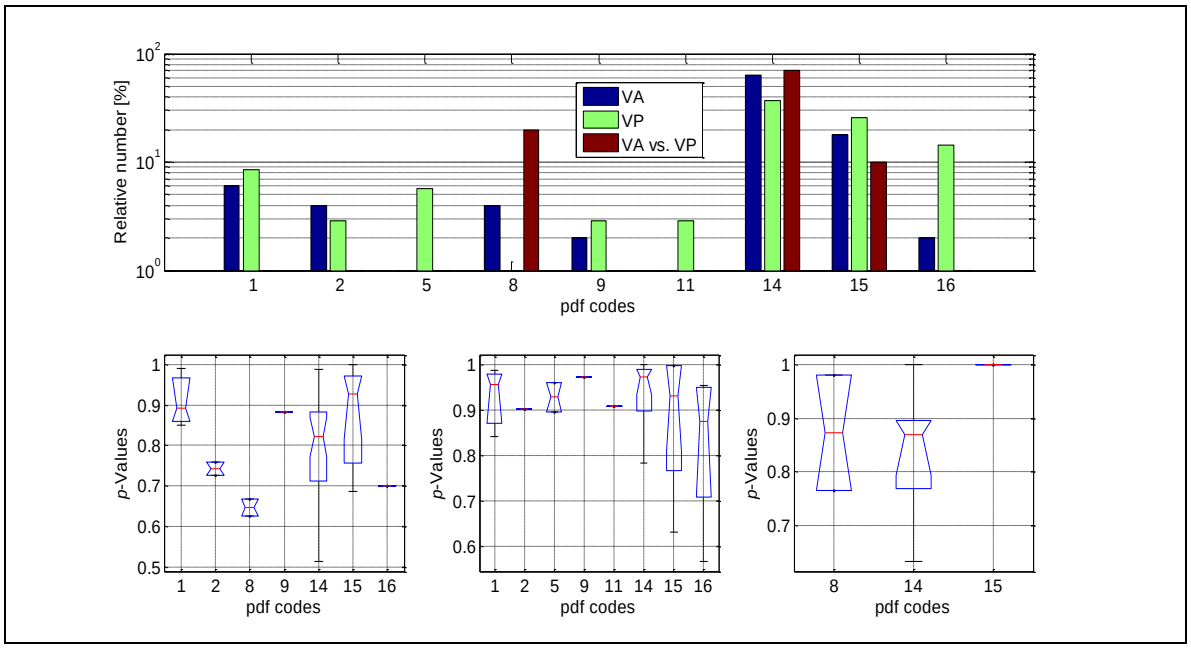

Figure 20 The results of the fitting procedure of the IP dataset for different tasks. percentage of PDF-s corresponding to VA, VP and VA vs. VP tasks. Lower panel: box plot of the corresponding p-values.

5. The Markov model

5.1. The three state Markov chain model

Based on the observational study of the Interspike Interval (ISI) it is possible to generalize their characteristic behavior. In some time intervals there are ISI values which successively increasing. In these intervals the differences of the successive ISI values have positive sign. In some intervals there are ISI values which successively decreasing. In these intervals the differences of the successive ISI values have negative sign. There are some intervals where the successively appearing ISI values have difference which change its sign.

Let us define the following states of the neural cell.

Definition 5-1: Let us take three successively appearing ISI values $ISI_{n-1}, ISI_n, ISI_{n+1}$. The neural cell has following states:

a) decreasing state (D) if $\cdots > ISI_{n-1} > ISI_n > ISI_{n+1} > \cdots,$

b) alternating state (x) if

$\cdots < ISI_{n-1} > ISI_n < ISI_{n+1} > \cdots$ *or* $\cdots > ISI_{n-1} < ISI_n > ISI_{n+1} < \cdots,$

a) c) increasing state (I) if $\cdots < ISI_{n-1} < ISI_n < ISI_{n+1} < \cdots.$

Definition 5-2: The sequence of the states is determined by the sequence of the observed ISI values. The first state is determined by (ISI_1, ISI_2, ISI_3), the second

by (ISI_2, ISI_3, ISI_4), the third by (ISI_3, ISI_4, ISI_5), and so on. In every step the new state is determined by the newly observed ISI values and its two presiding.

Notice that from the definition of the states, there is no possibility to go from state D to state I directly or visa versa. The estimated sequence of the states does not have patterns like $\ldots DI \ldots$ or $\ldots ID \ldots$. Because of the finite representation of the ISI values, it is possible to observe two identical values $ISI_{n-1} = ISI_n$ called ties. In this case the weakened definition of the states could be

Definition 5-3: Let us take three successively appearing ISI values $ISI_{n-1}, ISI_n, ISI_{n+1}$. The neural cell has following states:

a) decreasing state (D) if $\cdots > ISI_{n-1} > ISI_n \geq ISI_{n+1} > \cdots$,

b) alternating state(x) if

$\cdots < ISI_{n-1} > ISI_n < ISI_{n+1} > \cdots$ *or* $\cdots > ISI_{n-1} < ISI_n > ISI_{n+1} < \cdots$,

c) increasing state (I) if $\cdots < ISI_{n-1} \leq ISI_n < ISI_{n+1} < \cdots$.

This definition allows patterns of states like $\ldots DI \ldots$ or $\ldots ID \ldots$.

If we take the stronger definition than the transition matrix has a form

$$\mathbf{P} = \begin{bmatrix} p_{11} & p_{12} & 0 \\ p_{21} & p_{22} & p_{23} \\ 0 & p_{32} & p_{33} \end{bmatrix}, \quad 0 \leq p_{ij} \leq 1 .$$

Definition 5-4: The percentage ISI values of the specific state pattern are the normalized ISI values with respect to the time duration of that state pattern.

Definition 5-5: The state of alternation can be devided into two further states:

a) state A with propertie $\cdots ISI_{n-1} < ISI_n > ISI_{n+1} \cdots$,

b) state a with propertie $\cdots ISI_{n-1} > ISI_n < ISI_{n+1} \cdots$.

5.2. The empirical results

Based on the definitions of the Paragraph 5.1, this chapter contains the empirical statistical results of the set of state sequencies. First, the results of the *IM* data set presented and than the results of the *IP* data set. For both data sets the results of the analysis comprise type subset of results and they are given in the same order.

The first set of results contains descriptive statistics of the state sequences such as time duration of the increasing I, decreasing D states and the alternation state x, the relative number of appearances of these states, two way tables to test independence with minimum discrimination information statistic, the distribution of the different length of I, D and x.states.

The second set of results contains the results of statistical comparison of the defined states by comparing ISI values which defined them. The distribution free two samples Kolmogorov-Smirnov test was used, $KS2$ test. The hypothesis is that the two samles are generated by identical probability function. The test was used to compare percentage ISI values and raw ISI values too. The results are given in colored table format. The colored parts of the tables present the weigthed average of the number of those state sequences which KS2 test accepted the hypothesis of indentical probability function. The weigth was the observed pV value of the KS2 test results. Formaly

$$R = \frac{\sum_k I_k \cdot pV_k}{number\ of\ \ state\ sequences}, \quad I_k = \begin{cases} 1, & accepted, \\ 0, & rejected \end{cases}$$

5.2.1. The empirical results of the *IM* data set

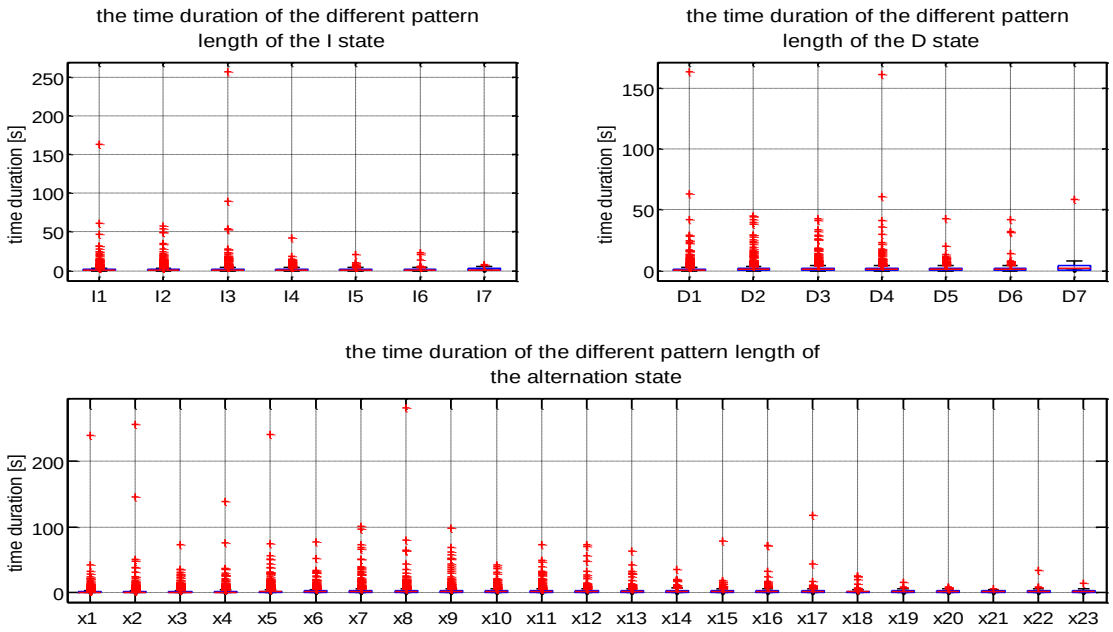

Figure 21 Boxplot diagrams of time durations of different state patterns of the whole data set; I -increasing state; D -decreasing state; x -aternation state

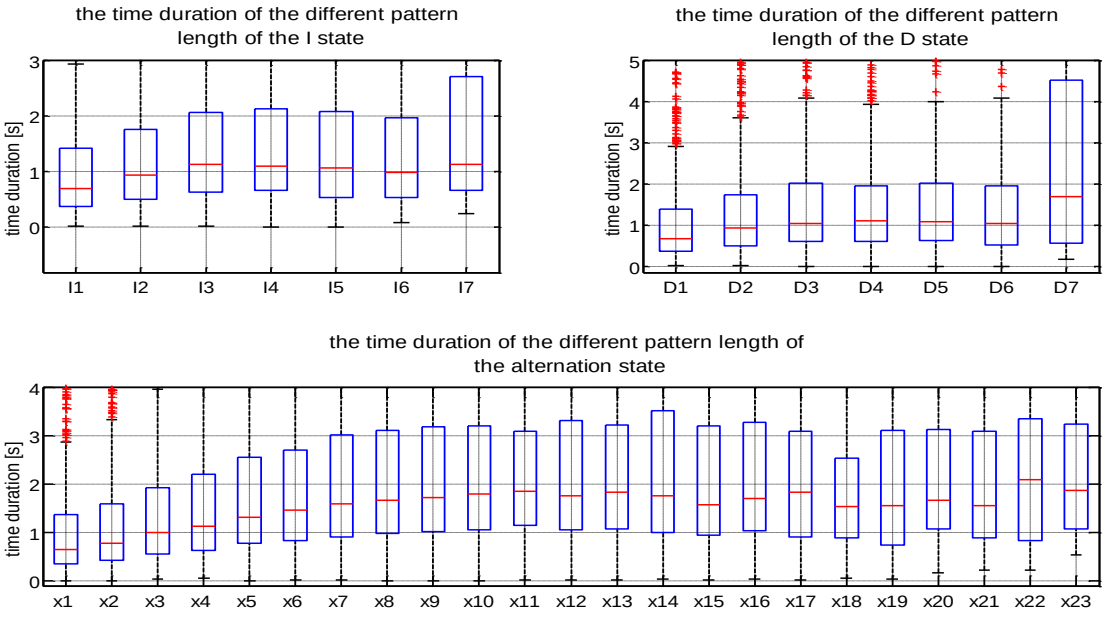

Figure 22 Boxplot diagrams of time duration of different state pattern; the panels show the most frequent range of time durations; I -increasing state; D -decreasing state; x -alternation state

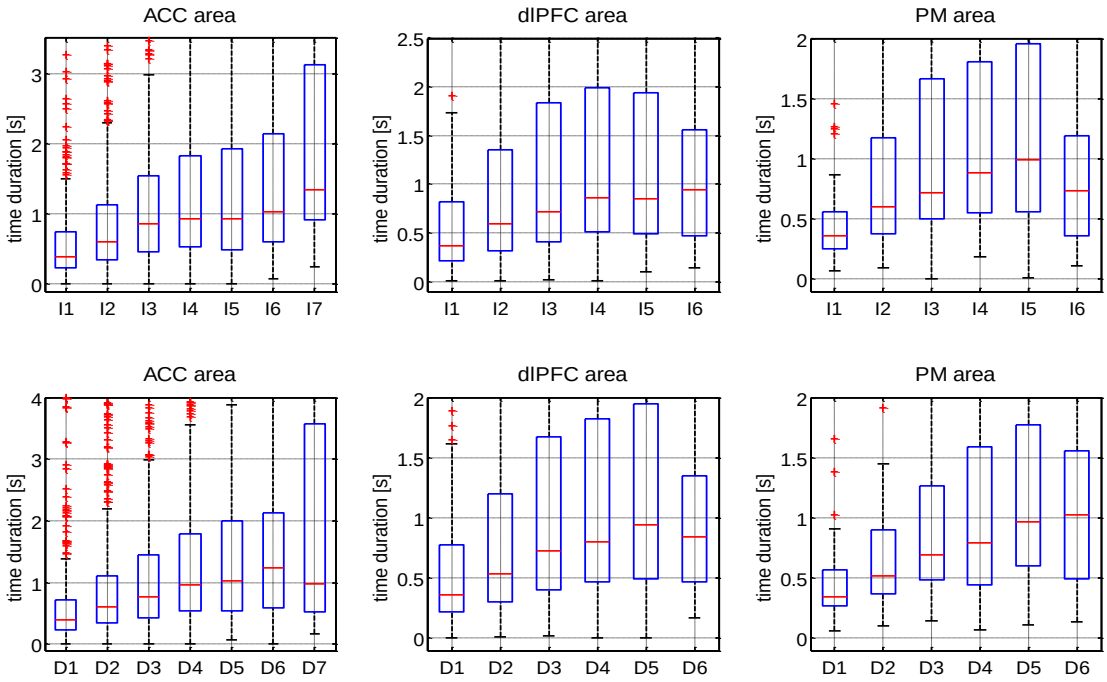

Figure 23 Boxplot diagrams of time durations in different brain area; I -increasing state; D -decreasing state

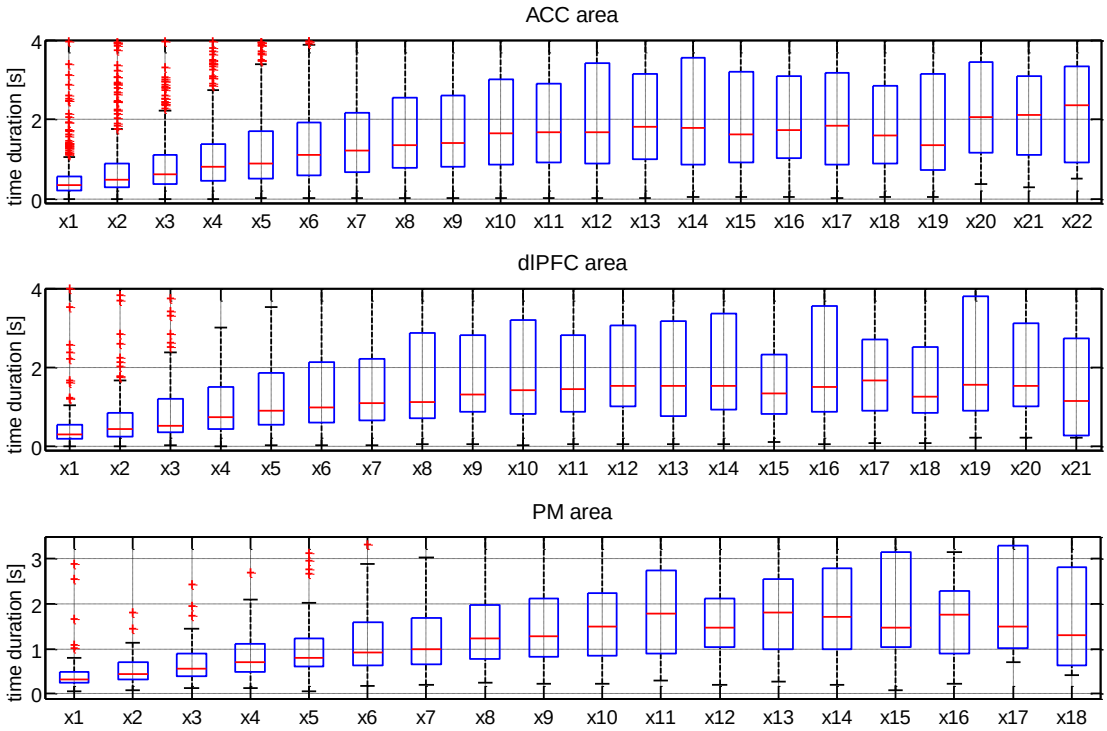

Figure 24 Boxplot diagrams of time durations in different brain area; x -alternation state

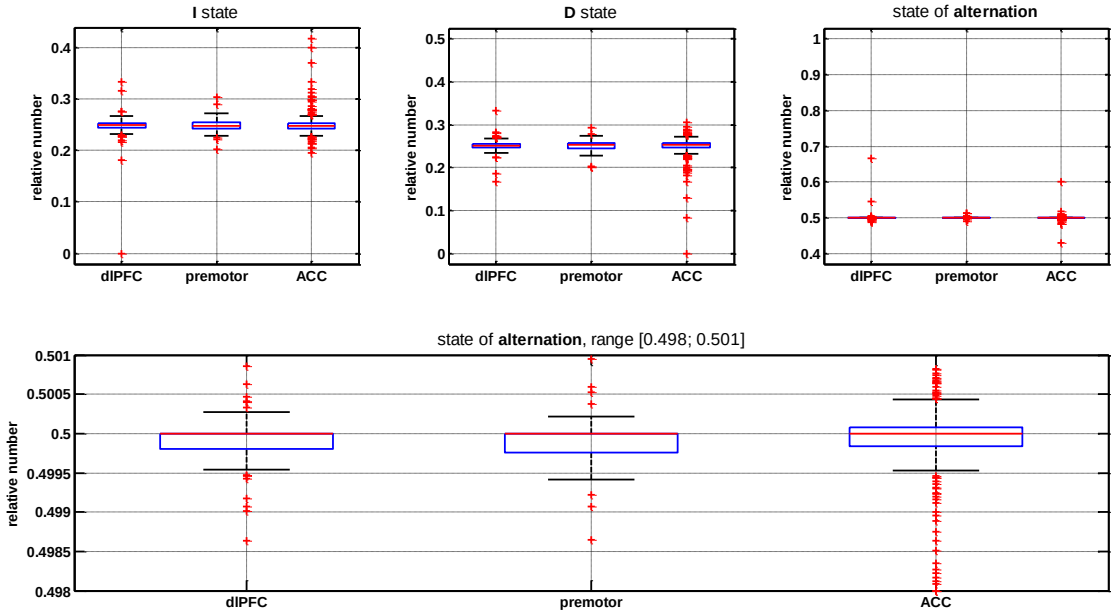

Figure 25 The relative number of appearances of the I, D and x states in different brain area; I -increasing state; D -decreasing state; x -state of alternation; the lower panel shows the magnified range around 0.5

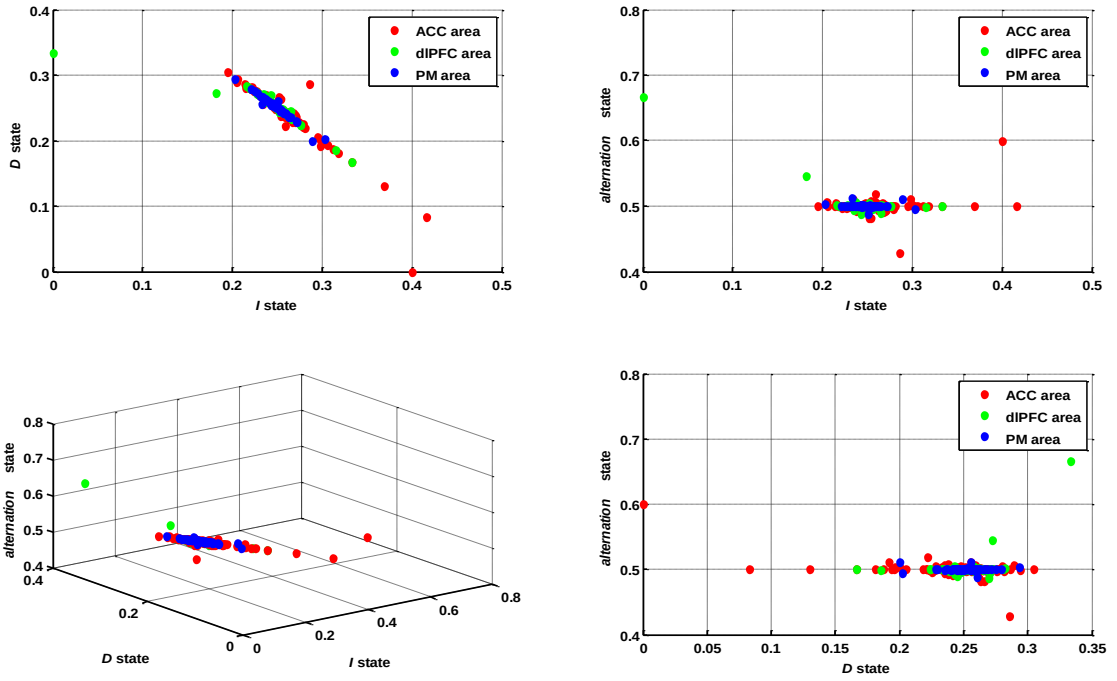

Figure 26 The 3-dimensional presentation of the set of state sequences by the relative number of they I, D and x state contents. Every single point presents a state sequences belonging to one of the three brain area

Table 4 The cross-table statistic to test the independency and homogeneity

CrossTable results $\alpha = 0.05$	degrees of freedom	$\chi^2_{df,\alpha}$	test statistic	Hypothesis
ACC area	$df = (433-1)\cdot(3-1) = 864$	933.5	4564.5	Rejected
dlPFC area	$df = (139-1)\cdot(3-1) = 276$	316	12686	Rejected
PM area	$df = (70-1)\cdot(3-1) = 138$	166.42	558.64	Rejected

CrossTable statistics to test the independency and homogeneity of ACC, dlPFC and PM area, $T = 47.037 > 9.488$. The hypothesis of the independence is rejected.

$df = (3-1)\cdot(3-1) = 4$ $\alpha = 0.05$	I state	D state	State of alternation
ACC brain area	475294	488980	1868320
dlPFC brain area	210914	214873	828079
PM brain area	66559	68913	257409

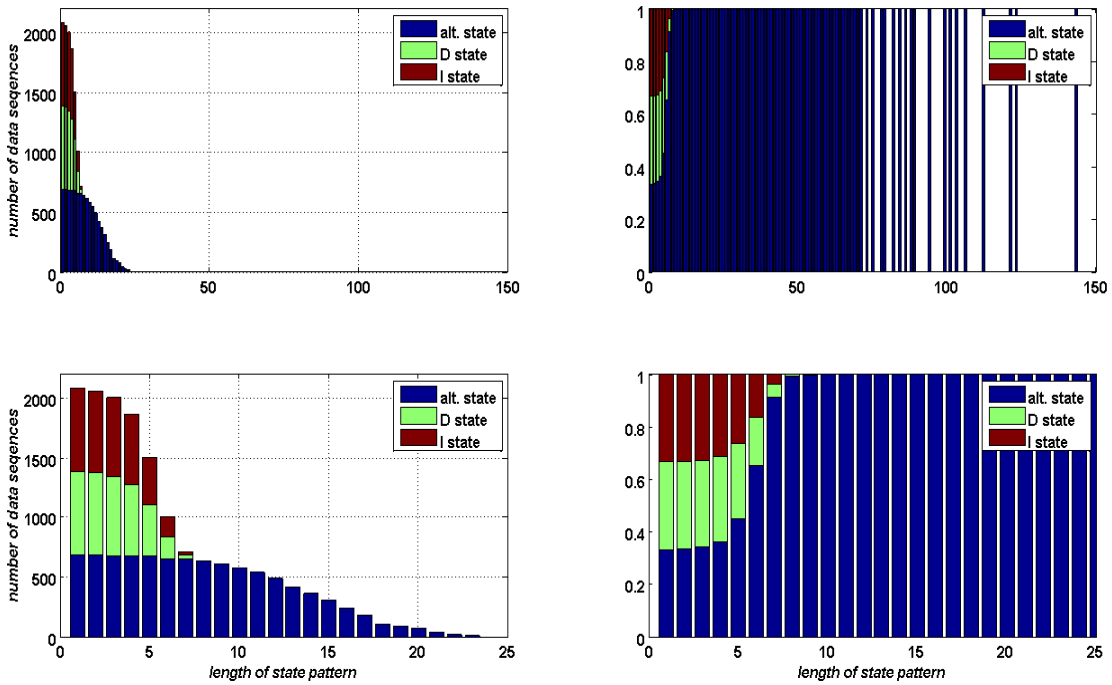

Figure 27 Bar plot of the number of state sequences which contain a specific state pattern; panels at the wrigth column show the relative numbers of these state sequences with the specific state pattern

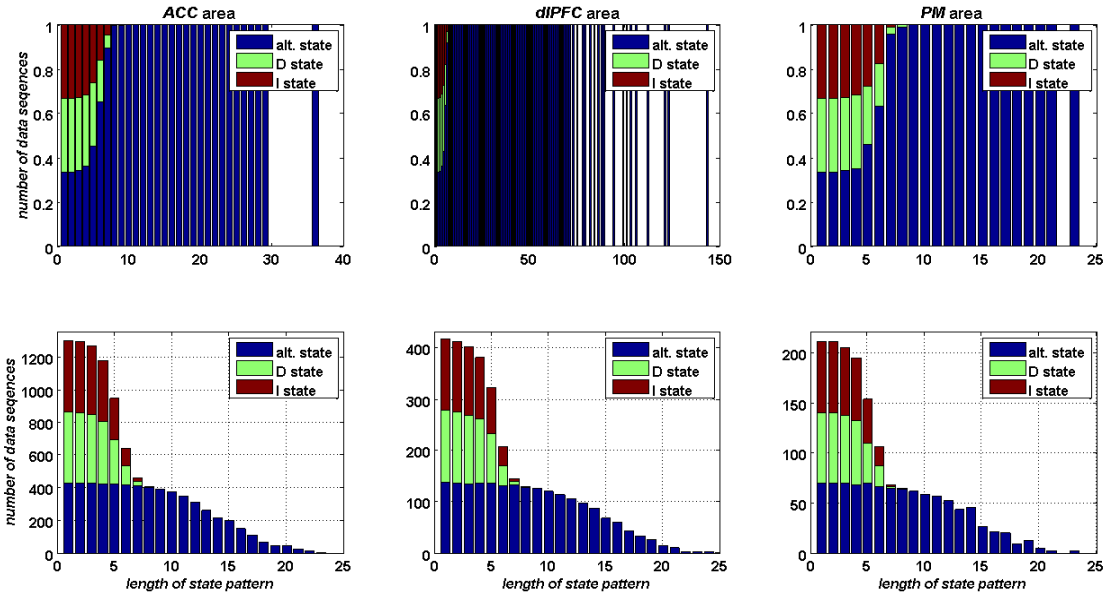

Figure 28 Bar graphs of the state pattern length distribution in different brain area.

Table 5 Cross Table analysis by the different I state pattern length

$\alpha = 0.05$	degrees of freedom	$\chi^2_{df,\alpha}$	test statistic	Hypothesis
ACC area	$df = (433-1)\cdot(8-1) = 3024$	3160.2	2100	Accepted
dlPFC area	$df = (139-1)\cdot(8-1) = 966$	1046.7	1055.6	Rejected
PM area	$df = (70-1)\cdot(7-1) = 414$	468.78	538.02	Rejected

Table 6 Cross Table analysis by the different D pattern length

$\alpha = 0.05$	degrees of freedom	$\chi^2_{df,\alpha}$	test statistic	Hypothesis
ACC area	$df = (433-1)\cdot(10-1) = 3888$	4043.3	2310.4	Accepted
dlPFC area	$df = (139-1)\cdot(8-1) = 966$	1046.7	1402.9	Rejected
PM area	$df = (70-1)\cdot(8-1) = 483$	542.6	656.66	Rejected

Table 7 Cross Table analysis of the different I , D pattern length and x state

$\alpha = 0.05$	degrees of freedom	$\chi^2_{df,\alpha}$	test statistic	Hypothesis
ACC area	$df = (433-1)\cdot(19-1) = 7776$	8000.5	5123	Accepted
dlPFC area	$df = (139-1)\cdot(17-1) = 2208$	2334.8	2771.5	Rejected
PM area	$df = (70-1)\cdot(16-1) = 1035$	1126.5	1397.9	Rejected

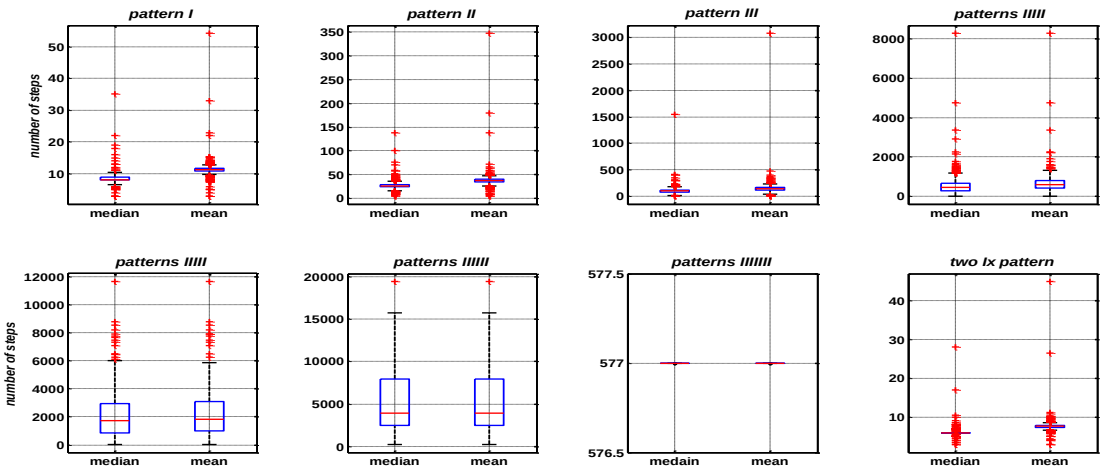

Figure 29 Boxplot diagrams of the number of steps between the same I pattern length; the panel at the lower-wright corner shows the number of steps between any two I state pattern

Table 8 The crosstable test results of independency and homogeneity by the number of steps between different I pattern lenght

$\alpha = 0.05$	degrees of freedom	$\chi^2_{df,\alpha}$	test statistic	Hypothesis
ACC area	$df = (431-1)\cdot(8-1) = 3010$	3138.75	896891.98	Rejected
dlPFC area	$df = (137-1)\cdot(7-1) = 816$	883.56	349573.38	Rejected
PM area	$df = (70-1)\cdot(7-1) = 414$	462.44	138113.66	Rejected

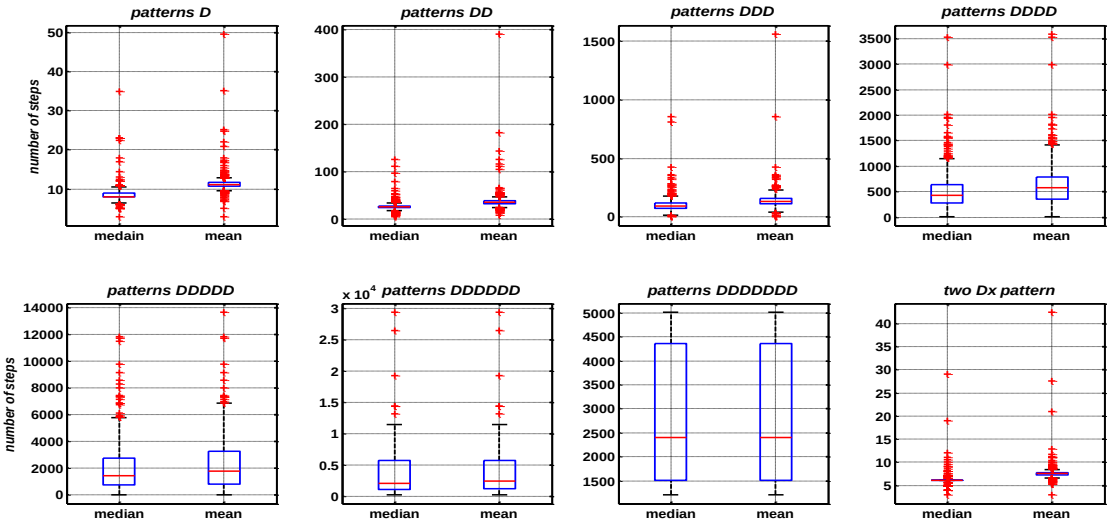

Figure 30 Boxplot diagrams of the number of steps between the same D pattern length; the panel at the lower-wright corner shows the number of steps between any two D state pattern

Table 9 The crosstable test results of independency and homogeneity by the number of steps between different D pattern length

$\alpha = 0.05$	degrees of freedom	$\chi^2_{df,\alpha}$	test statistic	Hypothesis
ACC area	$df = (428-1)\cdot(8-1) = 2989$	3117.3	9339907.3	Rejected
dlPFC area	$df = (137-1)\cdot(8-1) = 952$	1024.89	412893.55	Rejected
PM area	$df = (70-1)\cdot(7-1) = 414$	462.44	110028.56	Rejected

Table 10 Table of the median and the mean number of steps between different I and D state pattern legth

median	D	Dx2	Dx3	Dx4	Dx5	Dx6	Dx7
I	4	5	6	7	7	6	6
Ix2	5	11	19	21	24	20	23
Ix3	6	18	47	79	89	89	105
Ix4	6	21	77	213,5	326	392	307
Ix5	6	22	78	320	808	1199	1157
Ix6	7	23	76	459	1245	2690,5	0
Ix7	7,5	23,5	32,5	592	1450	4770	0

mean	D	Dx2	Dx3	Dx4	Dx5	Dx6	Dx7
I	5,01	7,37	8,82	9,45	9,56	9,64	10,13
Ix2	7,40	16,57	26,84	31,59	33,82	34,25	31,21
Ix3	8,71	26,31	69,99	116,88	135,56	136,04	135,97
Ix4	9,21	30,28	115,07	330,58	525,94	602,20	554,25
Ix5	9,35	31,29	125,53	477,75	1383,57	2058,07	1600,77
Ix6	10,00	33,55	118,64	623,35	2049,86	4212,93	0,00
Ix7	11,00	37,60	97,37	751,07	1837,32	3969,09	0,00

Table 11 The median of the number of steps between I and D pattern in different brain area

ACC	D	Dx2	Dx3	Dx4	Dx5	Dx6	Dx7
I	4	5	6	6	7	6	6
Ix2	5	11	19	22	26	18	23,5
Ix3	6	18	48,5	79	88	80	89
Ix4	6	21	78	223	300	364,5	371
Ix5	6	22	74	337,5	841	1556,5	1148,5
Ix6	8	22	76	400	1260	2840,5	0
Ix7	7	22	42	611	1521	4770	0

dlPFC	D	Dx2	Dx3	Dx4	Dx5	Dx6
I	4	5	6	7	8	5,5
Ix2	5	11	18	21	22	20
Ix3	6	17	46	79	98	89
Ix4	6	20	76	203	371	414
Ix5	7	22	88	286	944	1312
Ix6	6	27	77	530	1310	2917,5

PM	D	Dx2	Dx3	Dx4	Dx5	Dx6
I	4	5	6	7	6	6,5
Ix2	5	11	17	20,5	22	28
Ix3	6	18	45	77	83	110
Ix4	6	22	73	185	336	456
Ix5	6	23	97	303	678	447
Ix6	10	24	94,5	409	912	0

Table 12 The mean number of steps between I and D pattern in different brain area

ACC	D	Dx2	Dx3	Dx4	Dx5	Dx6	Dx7
I	4,98	7,35	8,78	9,29	9,37	9,35	9,96
Ix2	7,35	16,62	27,17	32,04	34,99	31,89	30,14
Ix3	8,75	26,60	70,27	117,58	132,82	129,72	147,88
Ix4	9,30	30,82	116,93	342,32	513,22	618,97	627,29
Ix5	9,11	31,72	121,53	492,17	1521,80	2190,73	1766,43
Ix6	9,92	31,48	124,17	601,75	2189,27	4078,32	0,00
Ix7	9,96	37,13	117,17	782,78	1869,35	3969,09	0,00

dlPFC	D	Dx2	Dx3	Dx4	Dx5	Dx6
I	5,07	7,37	8,81	9,86	9,98	9,84
Ix2	7,47	16,59	26,55	30,95	31,94	39,09
Ix3	8,69	25,74	70,00	116,32	140,04	125,83
Ix4	8,88	29,51	113,87	322,71	558,46	494,40
Ix5	10,17	29,65	138,42	458,86	1367,14	2034,93
Ix6	9,65	36,23	116,51	712,81	2197,51	5266,31

PM	D	Dx2	Dx3	Dx4	Dx5	Dx6
I	5,05	7,42	8,94	9,34	9,67	8,90
Ix2	7,56	16,02	26,17	30,79	32,52	38,13
Ix3	8,44	26,17	68,79	111,79	137,32	174,27
Ix4	9,65	29,94	111,24	278,72	553,60	597,52
Ix5	8,91	32,06	121,32	442,49	803,34	1004,94
Ix6	11,41	36,48	109,85	505,09	1178,11	0,00

Table 13 The median and the mean number of steps between D and I state pattern legth

median	I	Ix2	Ix3	Ix4	Ix5	Ix6	Ix7
D	4	5	6	6	6	7	12,5
Dx2	5	11	18	21	20	24	30
Dx3	6	18	48	75	89	86	66,5
Dx4	6	22	78	215	332	348	299,5
Dx5	7	22	94,5	357	869	1265	1279
Dx6	6	25	101	353	1135,5	3347,5	0
Dx7	6	30	75	325	1060,5	0	0

mean	I	Ix2	Ix3	Ix4	Ix5	Ix6	Ix7
D	5,00	7,40	8,73	9,30	9,37	9,50	13,43
Dx2	7,41	16,68	26,56	30,42	29,96	29,52	34,97
Dx3	8,76	26,74	72,11	112,90	127,34	133,14	105,10
Dx4	9,35	31,81	120,62	328,27	507,88	515,21	399,50
Dx5	9,91	33,00	135,37	523,76	1508,07	1959,59	1873,90
Dx6	8,95	33,71	148,50	549,36	1828,38	3981,52	0,00
Dx7	8,84	36,95	107,31	518,48	2543,29	0,00	0,00

Table 14 The median of the number of steps between D and I pattern in different brain area

ACC	I	Ix2	Ix3	Ix4	Ix5	Ix6	Ix7
D	4	5	6	6	6	7	11
Dx2	5	11	19	21	20	27,5	26,5
Dx3	6	19	48	78	90	97	66,5
Dx4	6	22	81	210,5	327	374	241
Dx5	7	22,5	89	364	867	1187,5	1279
Dx6	5	22	104,5	347	1136	2934	0
Dx7	6	22	71	359	1024	0	0

dlPFC	I	Ix2	Ix3	Ix4	Ix5	Ix6
D	4	5	6	6	6	8
Dx2	5	11	18	21	20	22
Dx3	6	18	50	74	88	73
Dx4	6	21	75	222	365	351,5
Dx5	6	22	109	370	882,5	1266,5
Dx6	6	25	85	390,5	1071	3398

PM	I	Ix2	Ix3	Ix4	Ix5	Ix6
D	4	5	6	7	4,5	7
Dx2	5	12	17	20	25	13
Dx3	6	18	45	67	105,5	93
Dx4	7	21	75,5	204	291	257
Dx5	8	22	91	319,5	795	944,5
Dx6	6,5	29,5	142,5	448	1113	0

Table 15 The mean number of steps between *D* and *I* pattern in different brain area

ACC	I	Ix2	Ix3	Ix4	Ix5	Ix6	Ix7
D	4,98	7,40	8,69	9,32	9,51	9,63	13,17
Dx2	7,45	16,72	26,97	30,72	29,94	32,58	34,79
Dx3	8,83	27,09	72,44	116,13	131,15	145,35	99,29
Dx4	9,37	32,25	121,19	327,30	513,86	613,63	400,55
Dx5	10,02	34,20	136,05	550,05	1482,09	1803,05	1987,93
Dx6	8,74	33,29	160,51	550,58	1817,30	3828,26	0,00
Dx7	8,07	35,30	113,62	451,96	2917,65	0,00	0,00

dlPFC	I	Ix2	Ix3	Ix4	Ix5	Ix6
D	5,03	7,43	8,75	9,11	9,35	9,58
Dx2	7,40	16,55	25,90	29,46	30,33	27,23
Dx3	8,64	26,15	73,55	109,22	118,75	117,98
Dx4	8,97	31,49	120,96	330,74	538,64	419,07
Dx5	9,43	30,60	138,51	479,82	1574,96	2417,61
Dx6	8,81	35,37	127,18	538,92	1909,33	4189,47

PM	I	Ix2	Ix3	Ix4	Ix5	Ix6
D	4,95	7,36	9,02	9,58	7,94	8,85
Dx2	7,20	16,65	26,18	30,40	31,88	20,85
Dx3	8,67	26,31	67,64	104,67	128,09	123,89
Dx4	9,78	30,24	114,89	311,53	415,50	363,00
Dx5	9,86	31,48	128,93	491,97	1258,86	1716,06
Dx6	9,63	33,73	138,63	584,71	1881,86	0,00

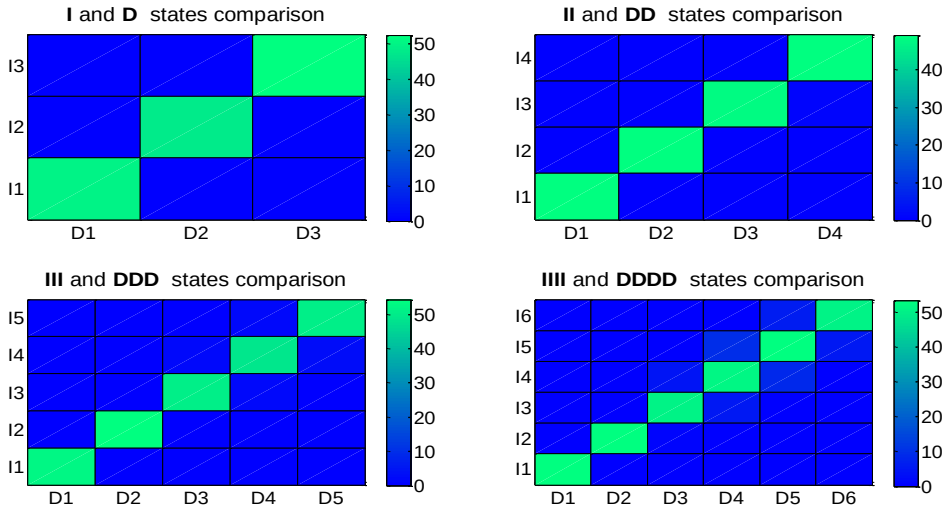

Figure 31 The results of the Kolmogorov-Smirnov twoo sample test (KS2 test) of the percentage of the *ISI* values comparison

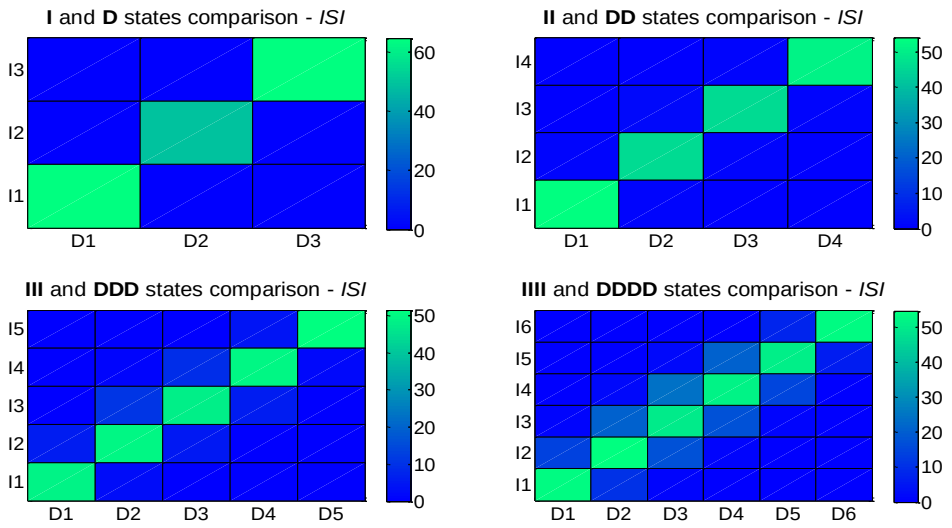

Figure 32 The results of the Kolmogorov-Smirnov twoo sample test (KS2 test) of the raw *ISI* values comparison

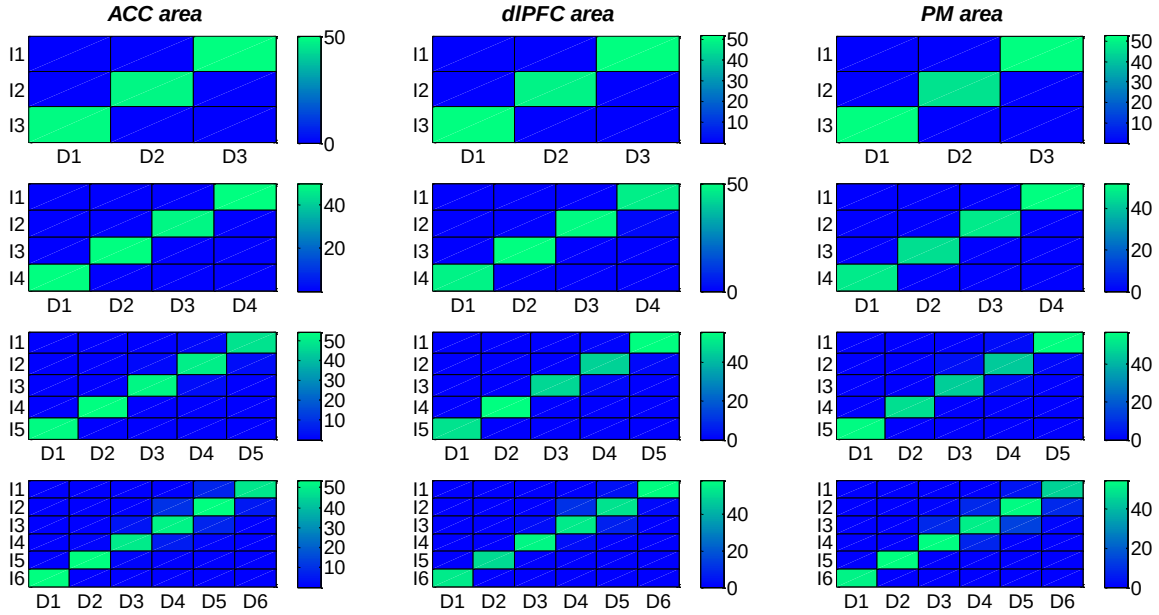

Figure 33 The results of the Kolmogorov-Smirnov twoo sample test (KS2 test) of the percentage of the *ISI* values comparison in different brain area

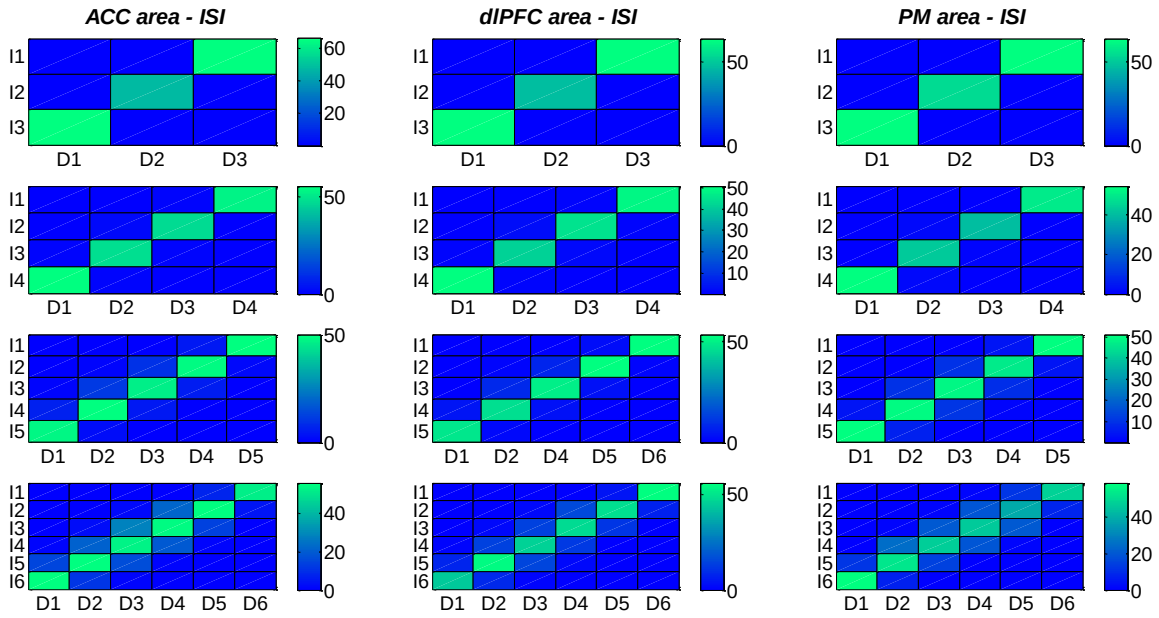

Figure 34 The results of the Kolmogorov-Smirnov twoo sample test (KS2 test) of the raw *ISI* values comparison in different brain area

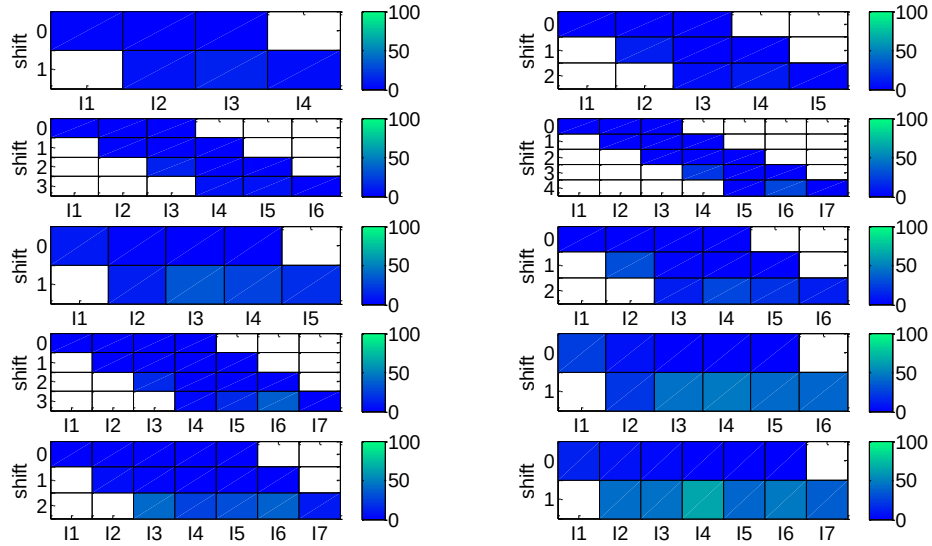

Figure 35 The KS2 test results of comparison between to different legth of *I* states; the y-axes represents the amount of shift of the shorter type state to compare the different percentage *ISI* values.

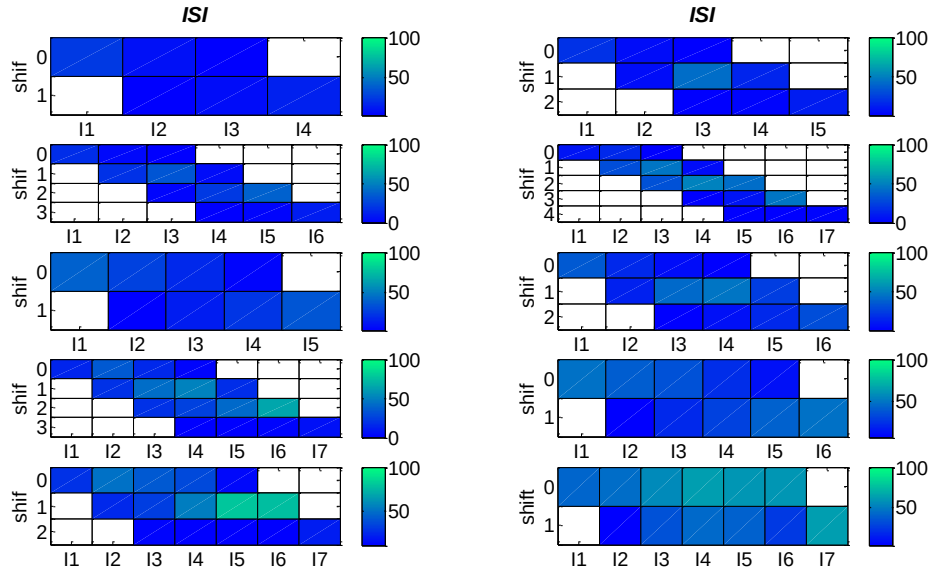

Figure 36 The KS2 test results of comparision between to different legth of *I* states; the y-axes represents the amount of shift of the shorter type to compare the different raw *ISI* values.

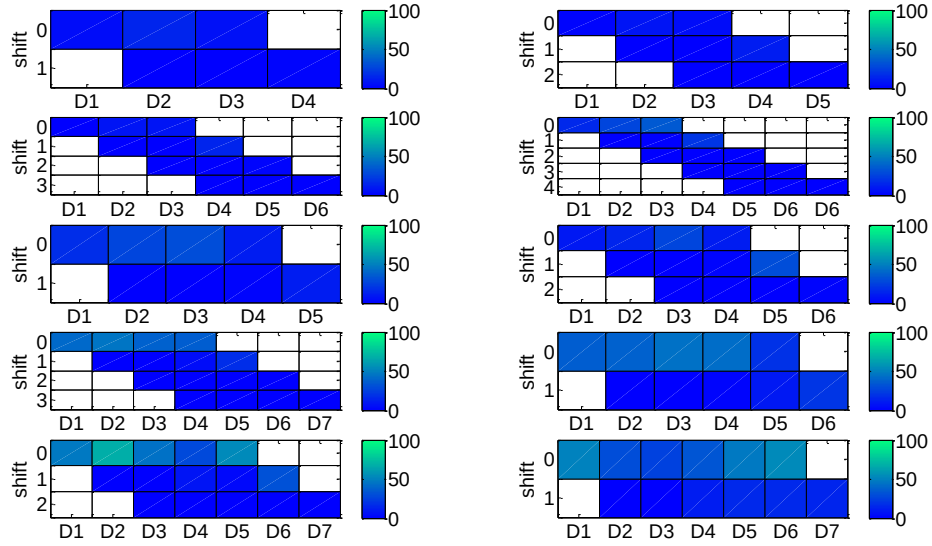

Figure 37 The KS2 test results of comparision between to different legth of *D* states; the y-axes represents the amount of shift of the shorter type to compare the different percentage *ISI* values.

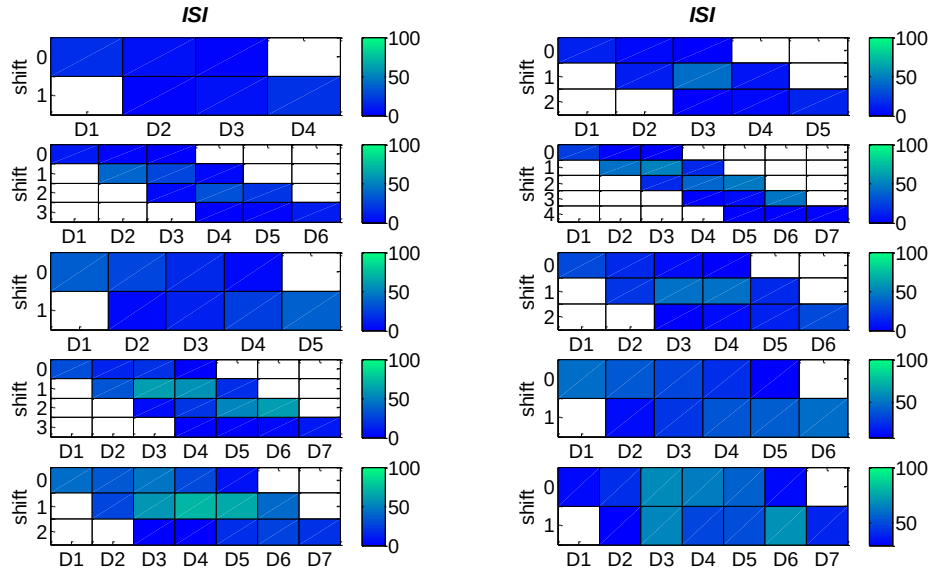

Figure 38 The KS2 test results of comparision between to different legth of *D* states; the y-axes represents the amount of shift of the shorter type to compare the different raw *ISI* values.

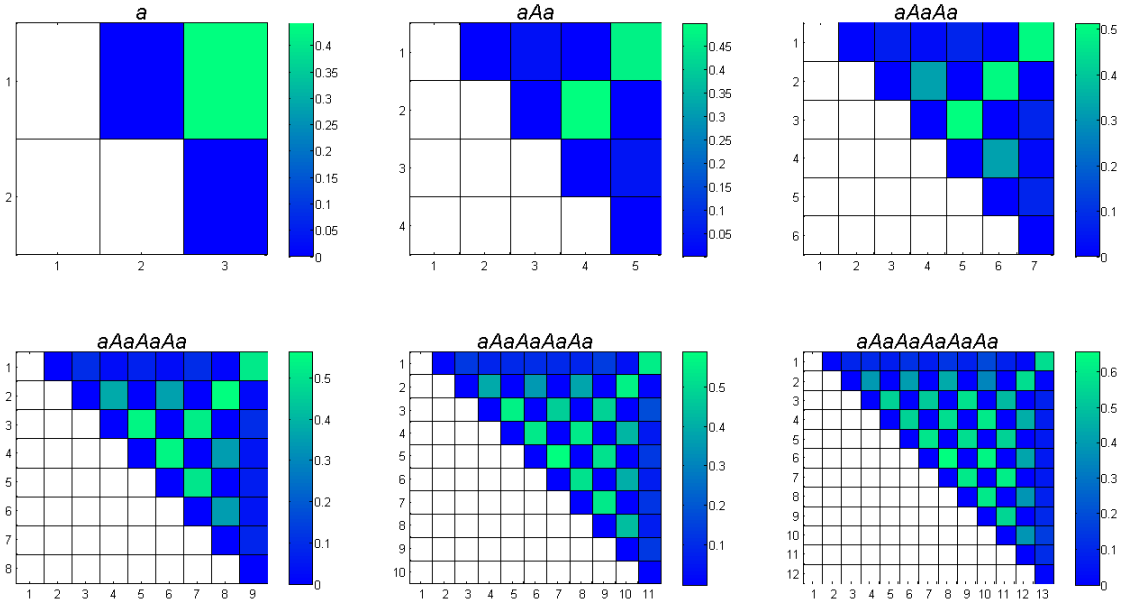

Figure 39 The KS2 test results of the self comparison of the alternate state pattern with odd number of length starting with alternation state *a*; the coordinate of the colored patch presents the order numbers of the *ISI* values wich were tested

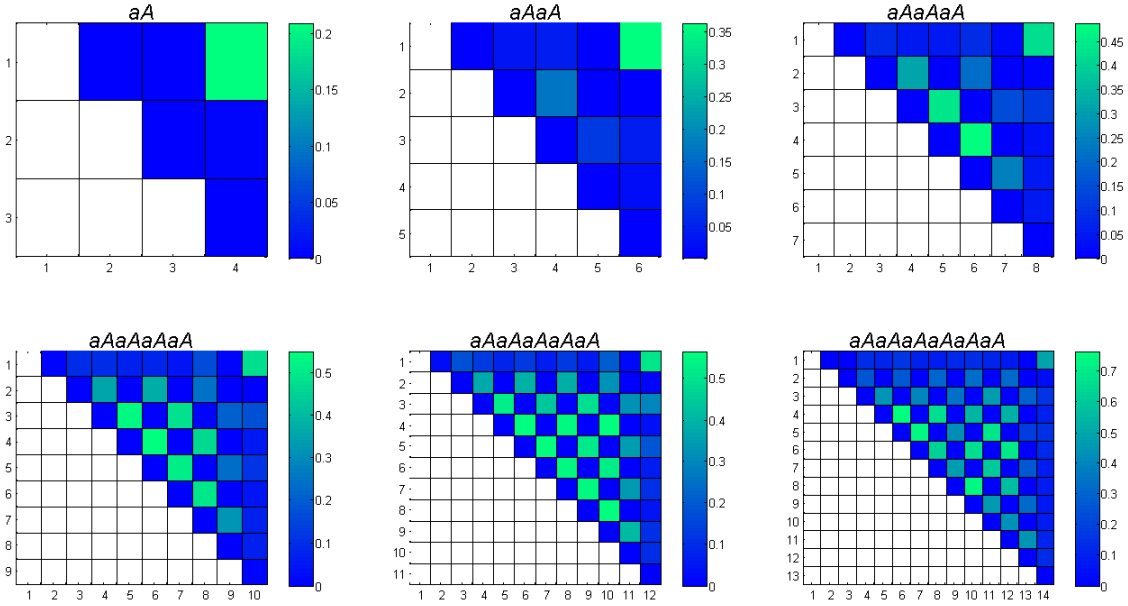

Figure 40 The KS2 test results of the self comparison of the alternate state pattern with even number of length starting with alternation state *a*; the coordinate of the colored patches present the order number of *ISI* values which were tested

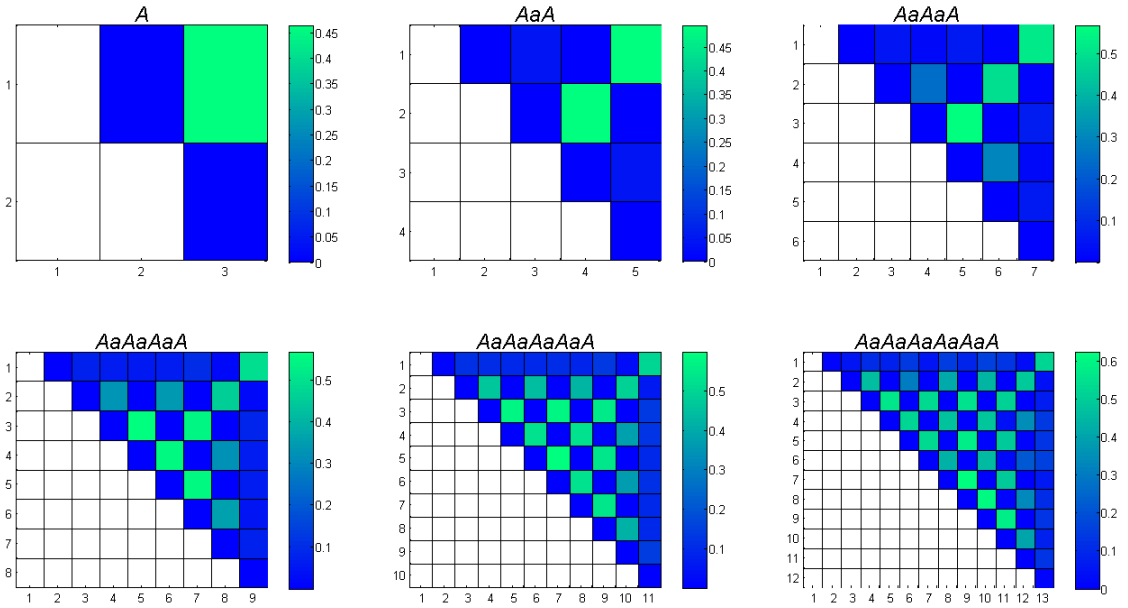

Figure 41 The KS2 test results of the self comparison of the alternation state pattern with odd number of length starting with alternation state *A*; the coordinate of the colored patches present the order number of the *ISI* values which were tested

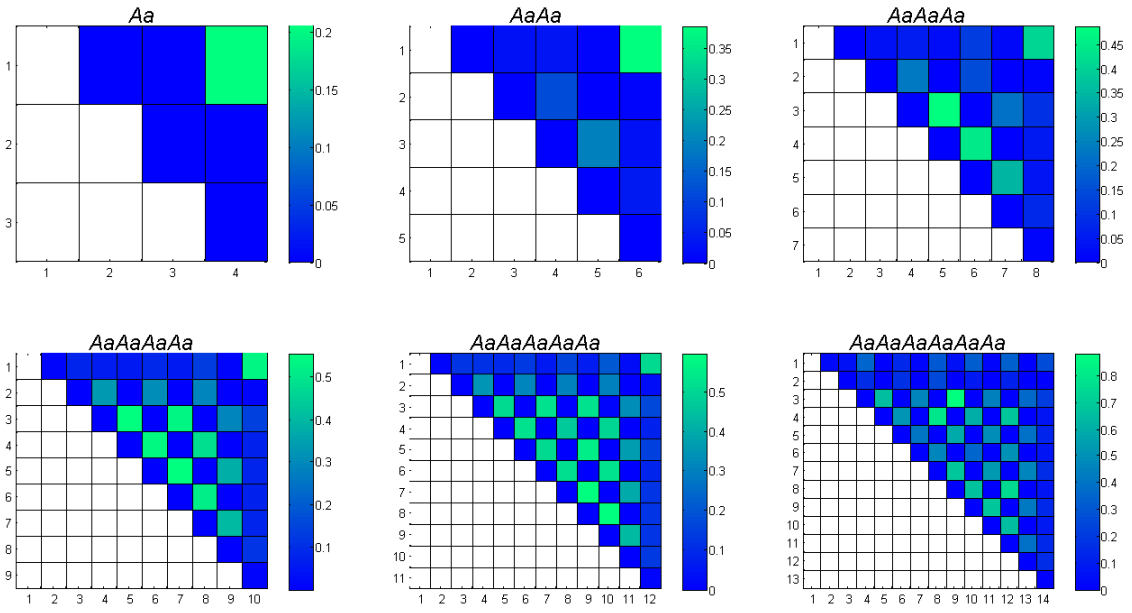

Figure 42 The KS2 test results of the self comparison of the alternation state pattern with even number of length starting with alternation state A ; the coordinate of the colored patches present the order number of the ISI values which were tested

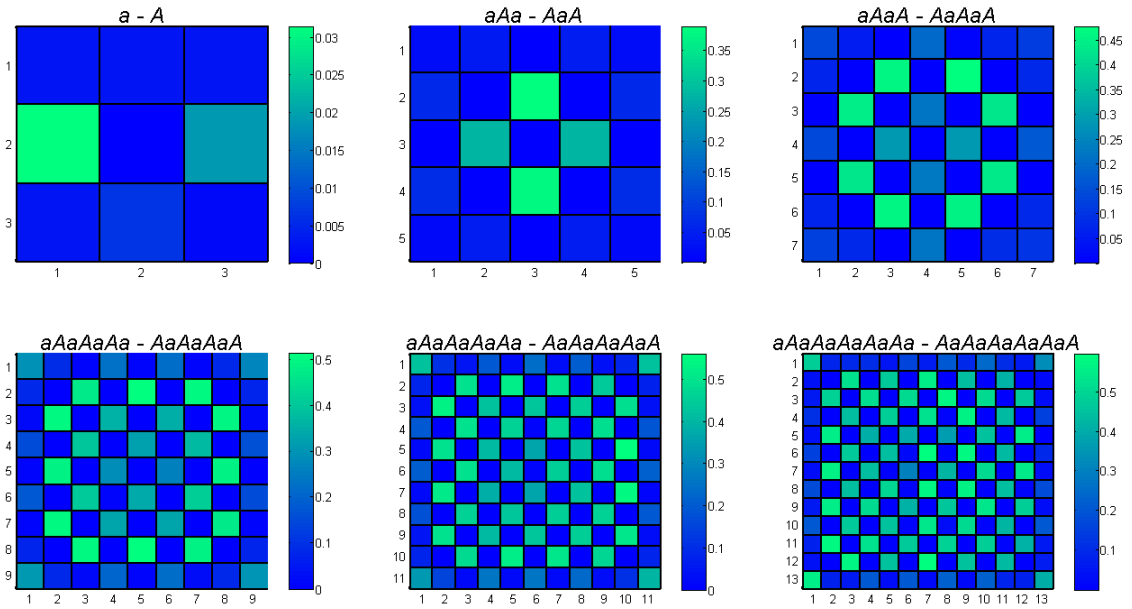

Figure 43 The KS2 test results of the cross comparison of the a and A alternate state pattern with odd number of length; the coordinate of the colored patches present the order number of the ISI values which were tested

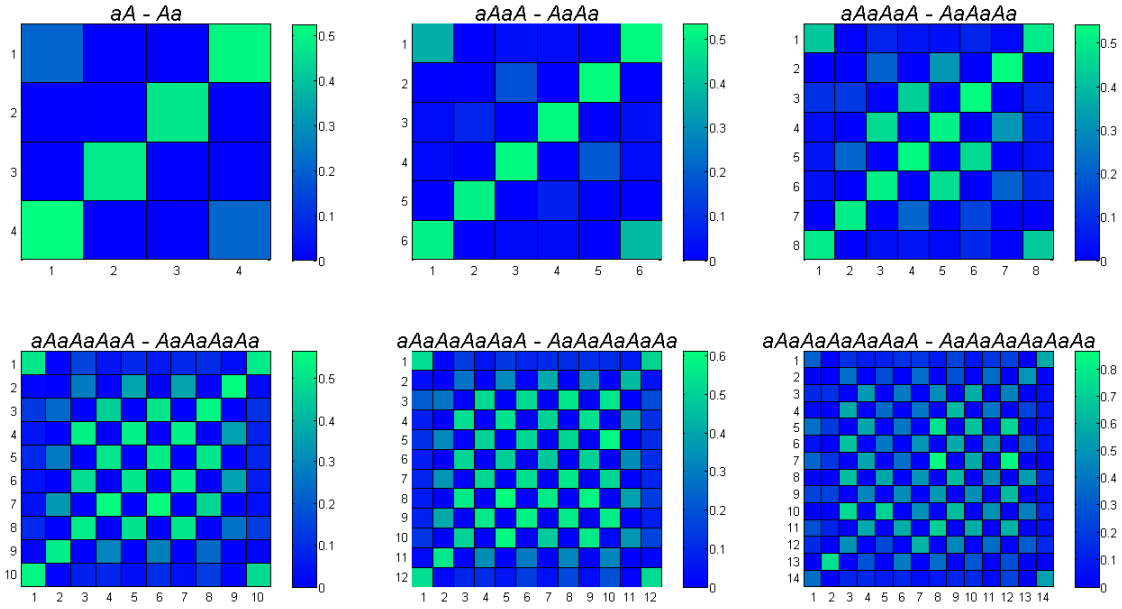

Figure 44 The KS2 test results of the cross comparison of the a and A alternate state pattern with even number of length; the coordinate of the colored patches present the order number of the ISI values which were tested

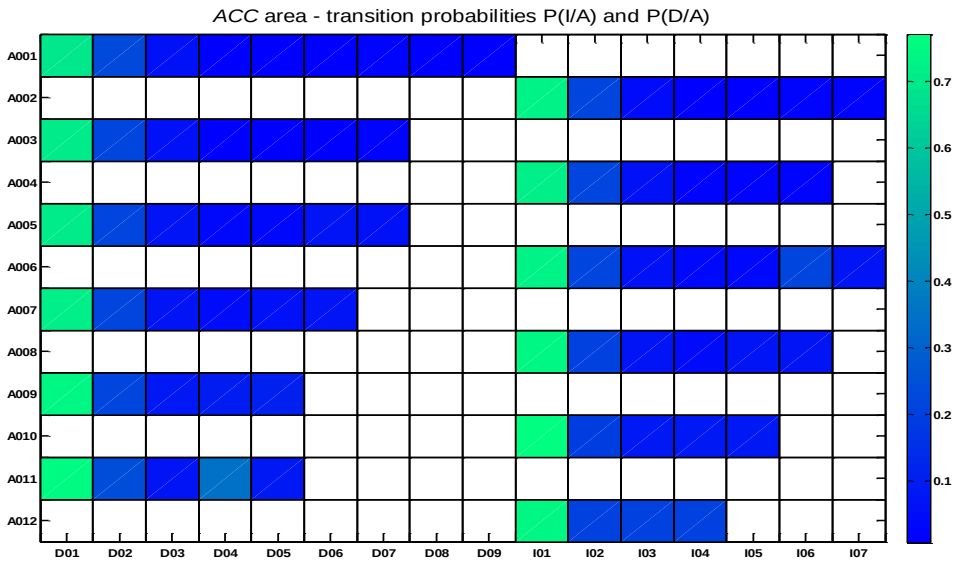

Figure 45 Transition probabilities of the *ACC* brain area

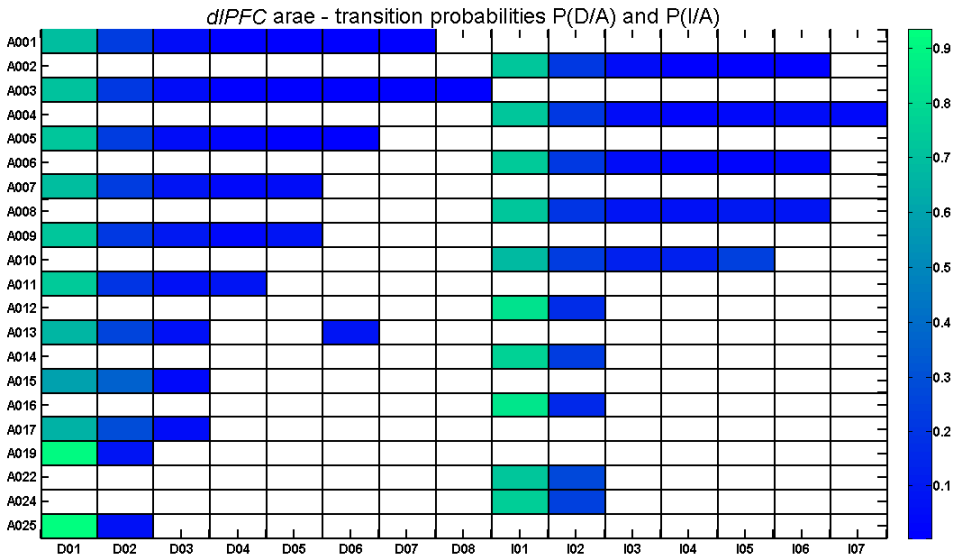

Figure 46 Transition probabilities of the *dlPFC* brain area

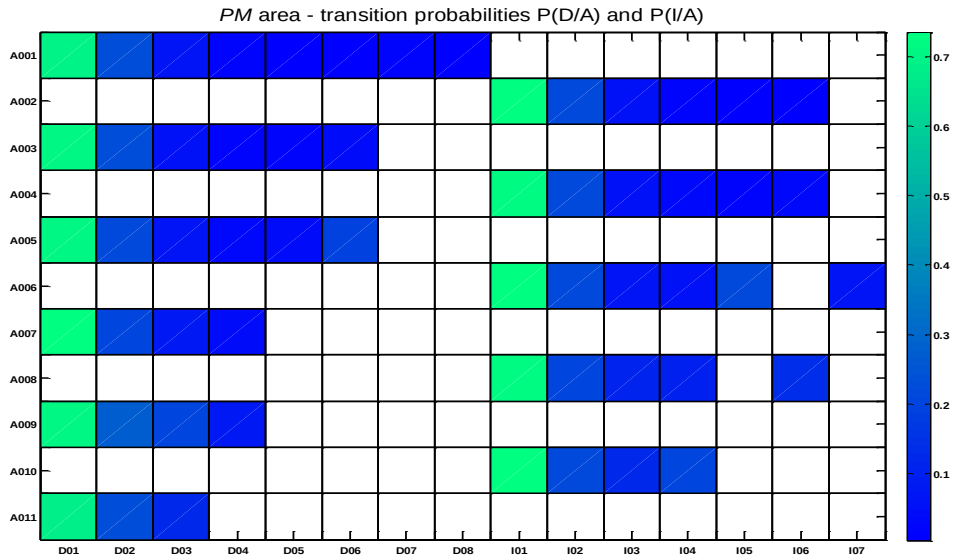

Figure 47 Transition probabilities of the *PM* brain area

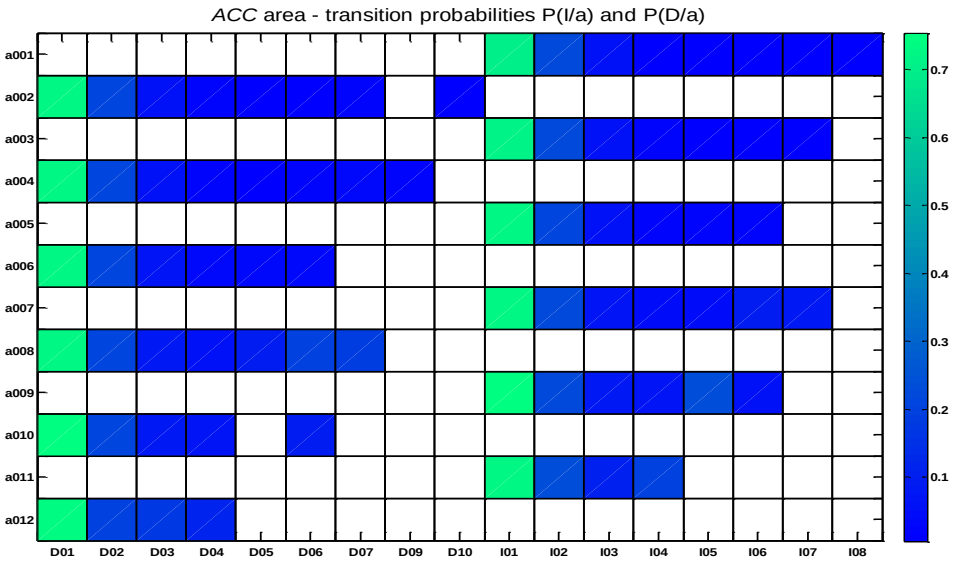

Figure 48 Transition probabilities of the *ACC* brain area

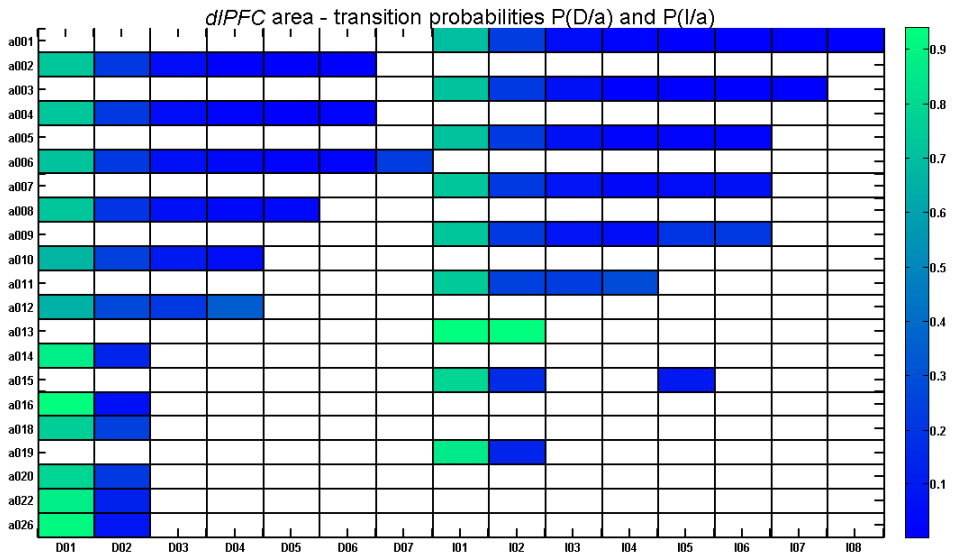

Figure 49 Transition probabilities of the *dlPFC* brain area

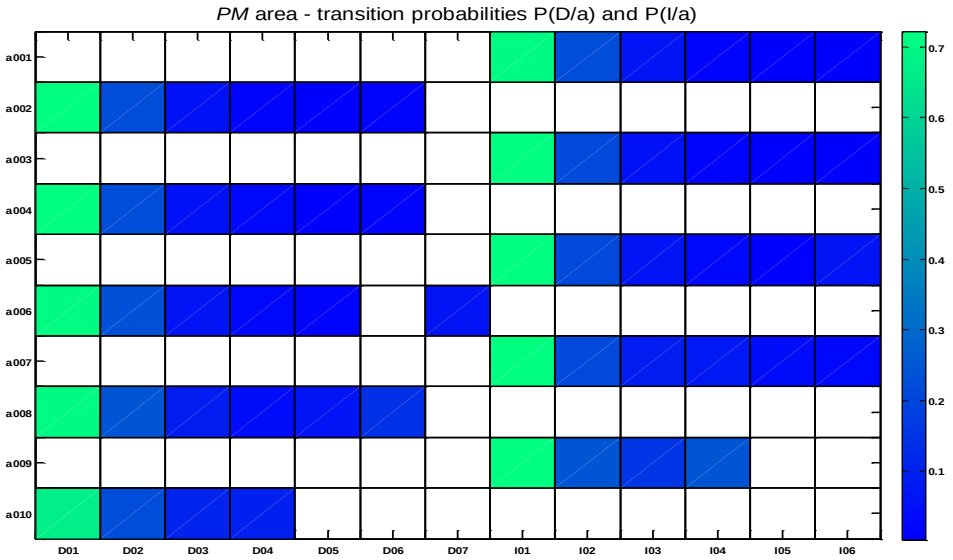

Figure 50 Transition probabilities of the *PM* brain area

5.2.2. The empirical results of the *IP* data set

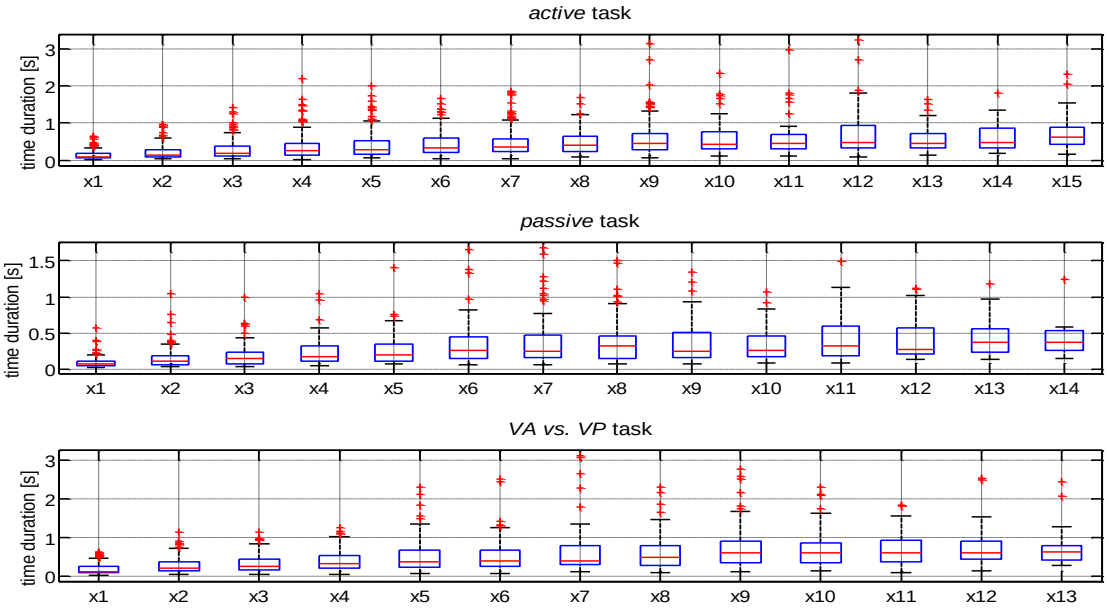

Figure 51 Boxplot diagrams of the time durations of different state patterns of the whole data set; I -increasing state; D -decreasing state; x -aternation state

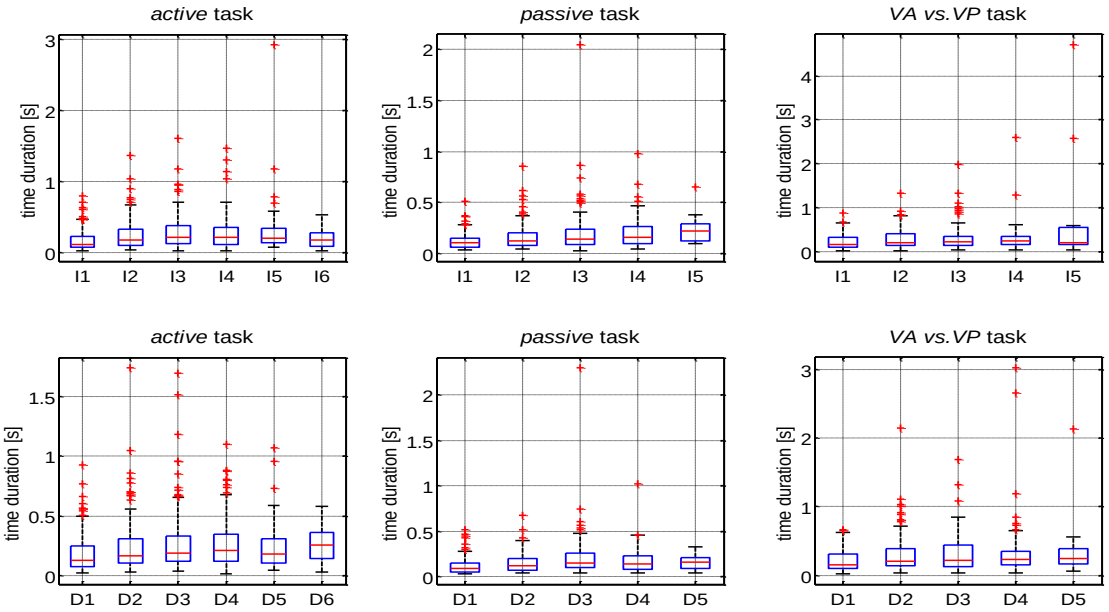

Figure 52 Boxplot diagrams of the time durations for different task; I -increasing state; D -decreasing state

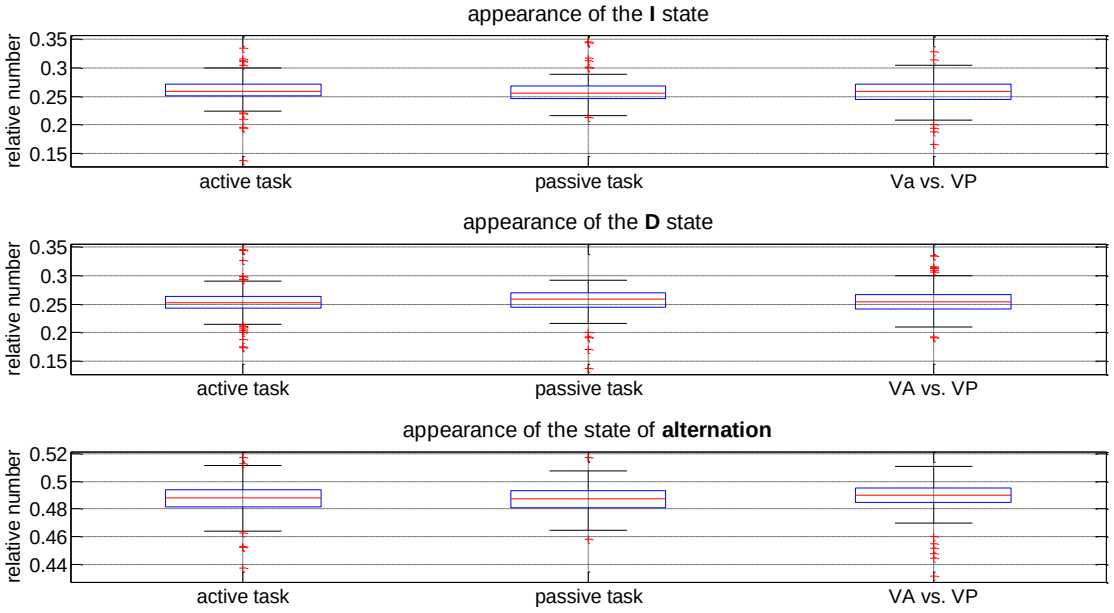

Figure 53 The relative number of appearances of I , D and x states in different taska; I -increasing state; D -decreasing state; x -state of alternation

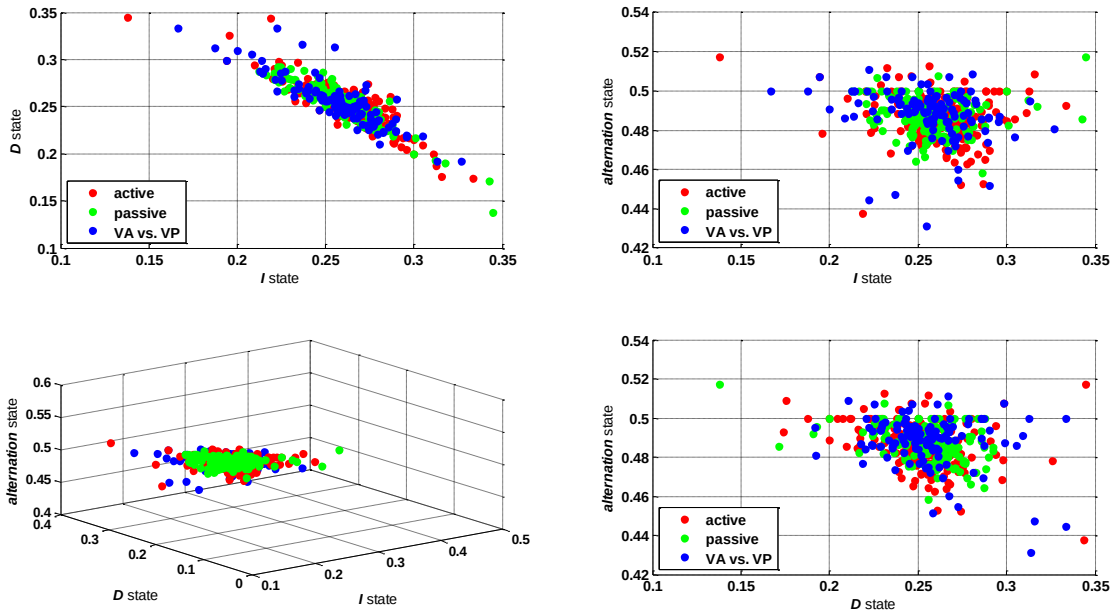

Figure 54 The 3-dimensional presentation of the set of state sequences by the relative number of they I, D and x state contents. Every single point presents a state sequences belonging to one of the three tasks

Table 16 The cross-table statistic to test the independency and homogeneity

CrossTable results $\alpha = 0.05$	degrees of freedom	$\chi^2_{df,\alpha}$	test statistic	Hypothesis
Population	$df = (482-1)\cdot(3-1) = 962$	1035.3	1650.8	Rejected
active task	$df = (225-1)\cdot(3-1) = 448$	498.35	867.61	Rejected
passive task	$df = (138-1)\cdot(3-1) = 274$	313.61	405.82	Rejected
VA vs. VP	$df = (119-1)\cdot(3-1) = 236$	272.84	307.68	Rejected

Table 17 CrossTable between active, passive and VAvsVP tasks, $T = 69.7 > 9.487$

$df = (3-1)\cdot(3-1) = 4$ $\alpha = 0.05$	I state	D state	state of alternation
active task	30987	30124	99776
passive task	13846	14207	48348
VA vs. VP	10922	10579	37212

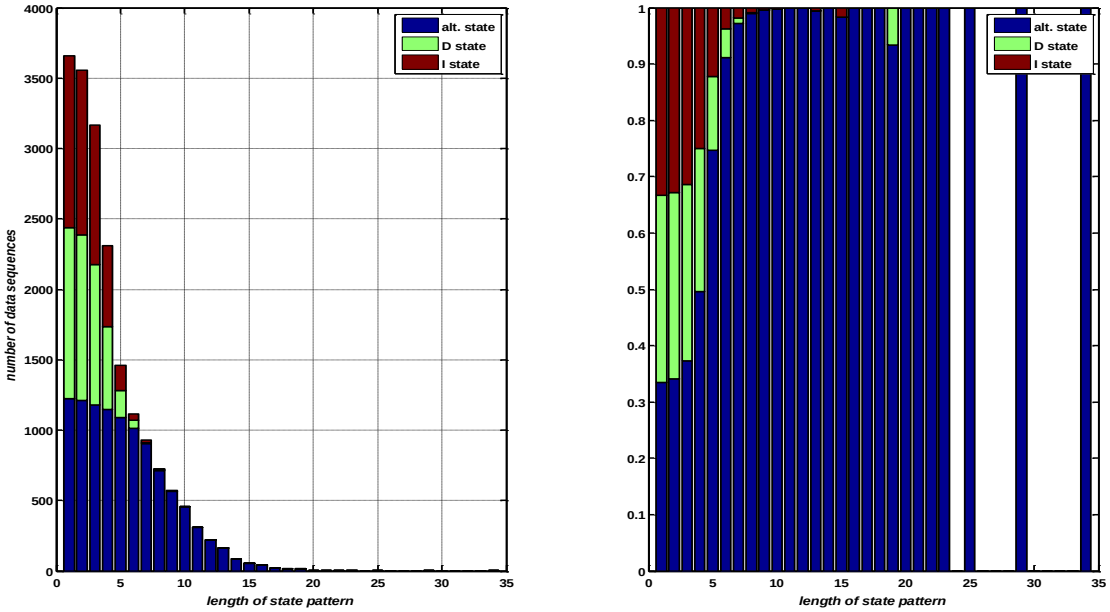

Figure 55 Bar plot of the number of state sequences which contain a specific state pattern; panels at the wrigth column show the relative numbers of these state sequences with the specific state pattern

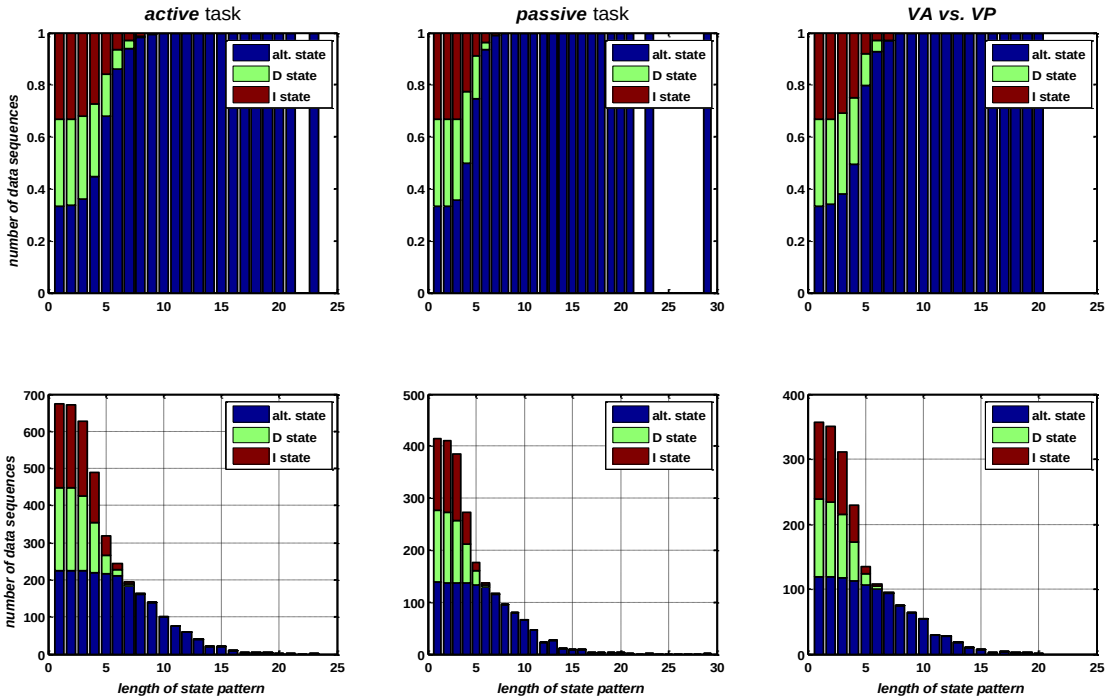

Figure 56 Bar graphs of the state pattern length distribution for different tasks.

Table 18 Cross Table analysis by the different I pattern length

$\alpha = 0.05$	degrees of freedom	$\chi^2_{df,\alpha}$	test statistic	Hypothesis
Active task	$df = (225-1)\cdot(9-1) = 1792$	1891.6	36.6	Accepted
Passive task	$df = (138-1)\cdot(7-1) = 822$	889.81	56.89	Accepted
VA vs. VP	$df = (119-1)\cdot(7-1) = 708$	771.01	28.92	Accepted

Table 19 Cross Table analysis by the different D pattern length

$\alpha = 0.05$	degrees of freedom	$\chi^2_{df,\alpha}$	test statistic	Hypothesis
Active task	$df = (225-1)\cdot(8-1) = 1568$	1661.2	202.4	Accepted
Passive task	$df = (138-1)\cdot(6-1) = 685$	747	360.2	Accepted
VA vs. VP	$df = (119-1)\cdot(6-1) = 590$	647.62	195.1	Accepted

Table 20 Cross Table analysis by the different I , D pattern length and x state

$\alpha = 0.05$	degrees of freedom	$\chi^2_{df,\alpha}$	test statistic	Hypothesis
Active task	$df = (225-1)\cdot(17-1) = 3584$	3724.4	348.3	Accepted
Passive task	$df = (138-1)\cdot(13-1) = 1644$	1739.4	488.2	Accepted
VA vs. VP	$df = (119-1)\cdot(13-1) = 1416$	1504.7	282.9	Accepted

Table 21 The cross table test results of independency and homogeneity by the number of steps between different I pattern length

$\alpha = 0.05$	degrees of freedom	$\chi^2_{df,\alpha}$	test statistic	hypothesis
Active task	$df = (225-1)\cdot(5-1) = 896$	966.75	33099.72	rejected
Passive task	$df = (138-1)\cdot(5-1) = 548$	603.57	16483.07	rejected
PM area	$df = (118-1)\cdot(5-1) = 468$	519.43	16607.68	rejected

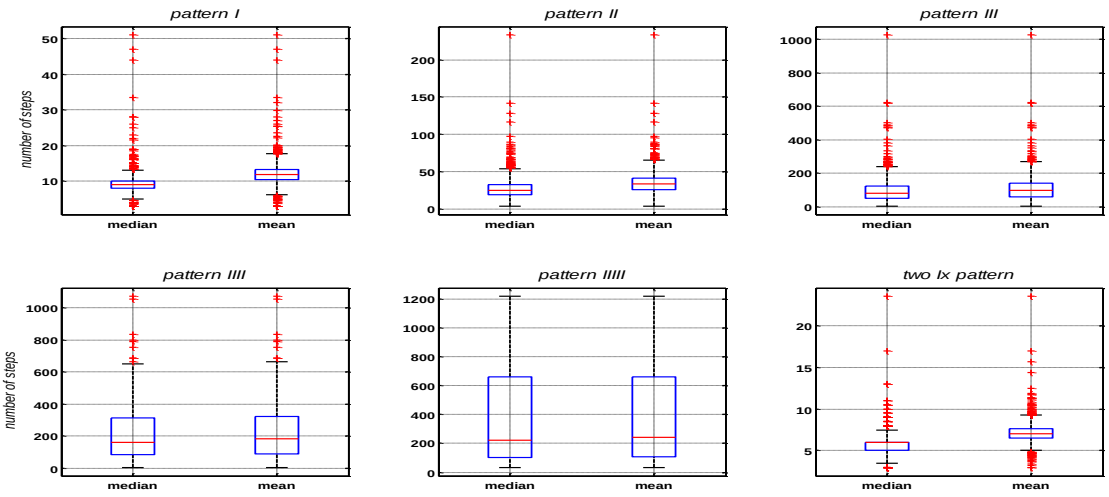

Figure 57 Boxplot diagrams of the number of steps between the same I pattern length; the panel at the lower-wright corner shows the number of steps between any two I state pattern

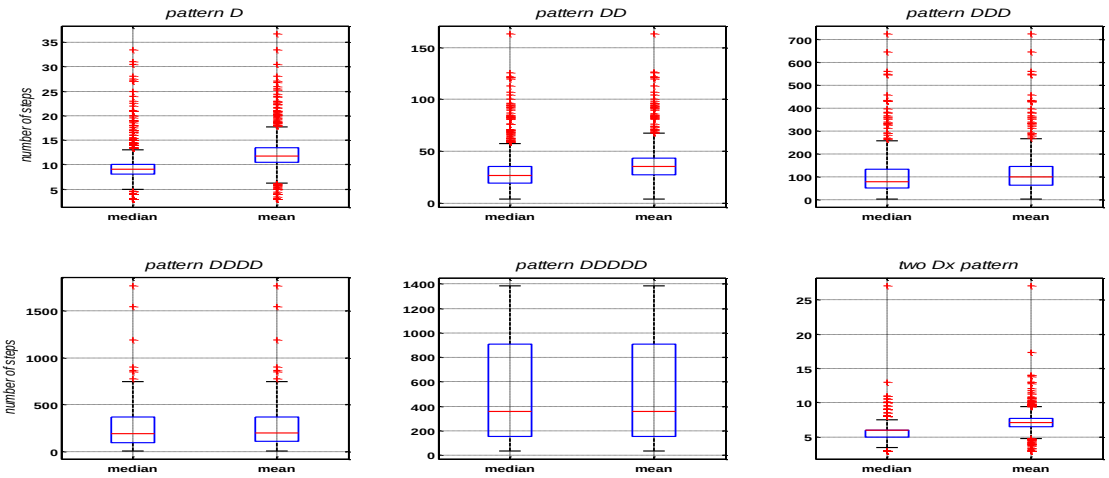

Figure 58 Boxplot diagrams of the number of steps between the same D pattern length; the panel at the lower-wright corner shows the number of steps between any two D state pattern

Table 22 The cross table test results of independency and homogeneity by the number of steps between different D pattern length

$\alpha = 0.05$	degrees of freedom	$\chi^2_{df,\alpha}$	test statistic	Hypothesis
Active task	$df = (225-1)\cdot(5-1) = 896$	966.75	40724.19	Rejected
Passive task	$df = (138-1)\cdot(5-1) = 548$	603.57	21372.62	Rejected
PM area	$df = (119-1)\cdot(5-1) = 472$	523.65	17032.51	Rejected

Table 23 The median of the number of steps between I and D pattern for different tasks

active	D	Dx2	Dx3	Dx4	Dx5	Dx6
I	2	4	6	6	6,5	7
Ix2	4	9	16	18	15	12,5
Ix3	6	17	32	55	56	65
Ix4	6	17	49	111,5	110	103
Ix5	5	18	55	80	216	0
Ix6	8	26,5	30,5	0	0	0

passive	D	Dx2	Dx3	Dx4	Dx5
I	4	4	5	6	5
Ix2	5	10	16	18	11
Ix3	6	16	33	55,5	55
Ix4	4	17,5	60	162	177
Ix5	8	20	39	0	0

VA vs. VP	D	Dx2	Dx3	Dx4	Dx5
I	2	5	6	6	7
Ix2	5	9	16	20	21
Ix3	6	15,5	43	52	47
Ix4	5	20	47,5	99	0
Ix5	8,5	16	0	0	0

Table 24 The mean of the number of steps between I and D pattern for different tasks

active	D	Dx2	Dx3	Dx4	Dx5	Dx6
I	4,91	6,94	8,65	9,23	9,93	9,56
Ix2	7,03	14,06	22,01	25,16	23,27	26,22
Ix3	8,36	22,97	48,42	80,46	73,90	91,80
Ix4	9,53	24,75	72,21	160,26	171,09	184,93
Ix5	8,23	26,64	82,68	155,94	232,50	0,00
Ix6	12,67	28,79	65,75	0,00	0,00	0,00

passive	D	Dx2	Dx3	Dx4	Dx5
I	4,82	6,76	7,41	8,89	9,53
Ix2	6,99	15,45	23,99	26,50	23,26
Ix3	8,54	23,05	51,44	86,13	96,23
Ix4	6,55	25,46	87,35	186,44	249,23
Ix5	10,71	28,52	70,24	0,00	0,00

VA vs. VP	D	Dx2	Dx3	Dx4	Dx5
I	4,73	7,05	7,82	8,34	10,17
Ix2	7,03	14,23	23,11	24,44	28,67
Ix3	8,58	23,04	55,75	74,56	125,14
Ix4	9,95	28,03	73,81	142,20	0,00
Ix5	10,75	19,82	0,00	0,00	0,00

Table 25 The median of the number of steps between D and I pattern for different tasks

active	I	Ix2	Ix3	Ix4	Ix5	Ix6
D	2	5	6	6	6	11,5
Dx2	4	9	14	15	12	9
Dx3	5	15	31,5	59	47	45,5
Dx4	5	16	56,5	77	142	324
Dx5	6	16	76,5	88,5	194	0
Dx6	7	6	53	160	0	0

passive	I	Ix2	Ix3	Ix4	Ix5
D	2	4	6	7	4
Dx2	4	10,5	16	17,5	22
Dx3	6	15	35	66	20
Dx4	4	13	55	87	0
Dx5	4	20	67	242	0

VA vs. VP	I	Ix2	Ix3	Ix4	Ix5
D	2	4	5	6,5	7,5
Dx2	4	10	14,5	15	20
Dx3	5	14	34,5	76	0
Dx4	5,5	16	48	133	0
Dx5	9,5	19	66	0	0

Table 26 The mean number of steps between D and I pattern for different tasks

active	I	Ix2	Ix3	Ix4	Ix5	Ix6
D	4,72	6,84	8,11	8,51	9,46	13,38
Dx2	6,84	13,65	20,18	22,45	23,33	14,56
Dx3	8,12	21,53	46,69	78,66	76,69	69,88
Dx4	7,94	22,87	74,58	137,63	230,39	333,93
Dx5	8,51	23,47	95,57	163,91	270,58	0,00
Dx6	13,05	13,37	51,81	174,91	0,00	0,00

passive	I	Ix2	Ix3	Ix4	Ix5
D	4,61	6,86	7,91	9,41	5,00
Dx2	6,61	14,57	23,98	22,88	27,09
Dx3	8,38	22,84	49,09	77,39	61,94
Dx4	6,87	26,33	74,80	167,38	0,00
Dx5	7,36	35,18	101,85	347,14	0,00

VA vs. VP	I	Ix2	Ix3	Ix4	Ix5
D	4,77	6,82	7,84	8,43	14,08
Dx2	6,90	14,14	21,92	22,06	32,83
Dx3	7,81	19,98	53,57	89,51	0,00
Dx4	7,34	27,30	65,46	210,15	0,00
Dx5	11,17	27,39	104,38	0,00	0,00

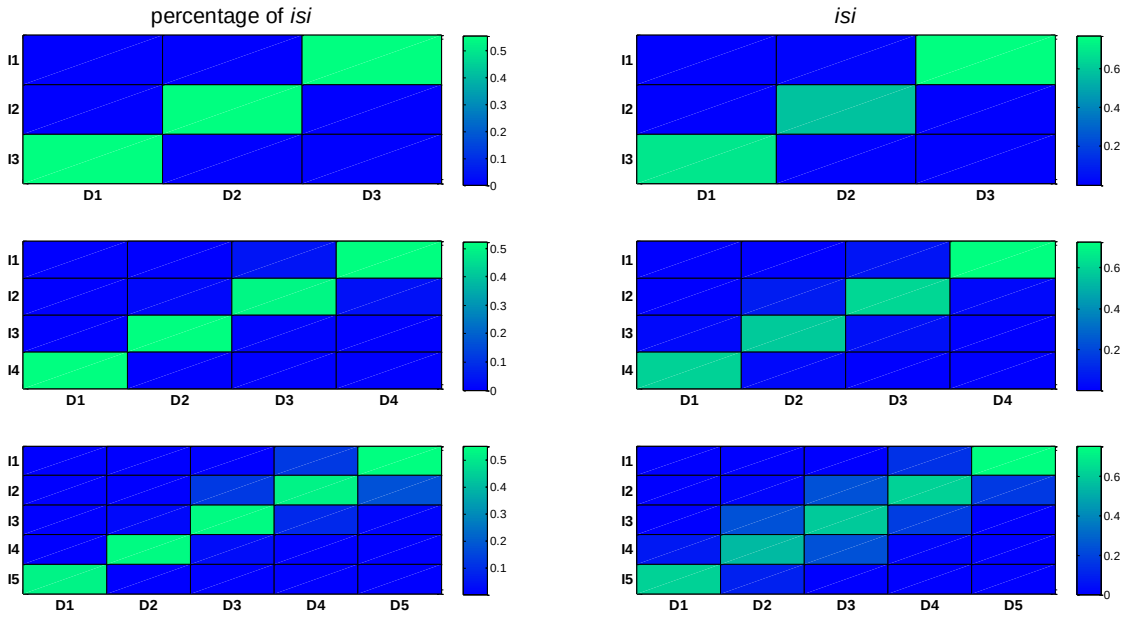

Figure 59 The results of the Kolmogorov-Smirnov twoo sample test (KS2 test) of the percentage of the *ISI* values and raw *ISI* values comparison

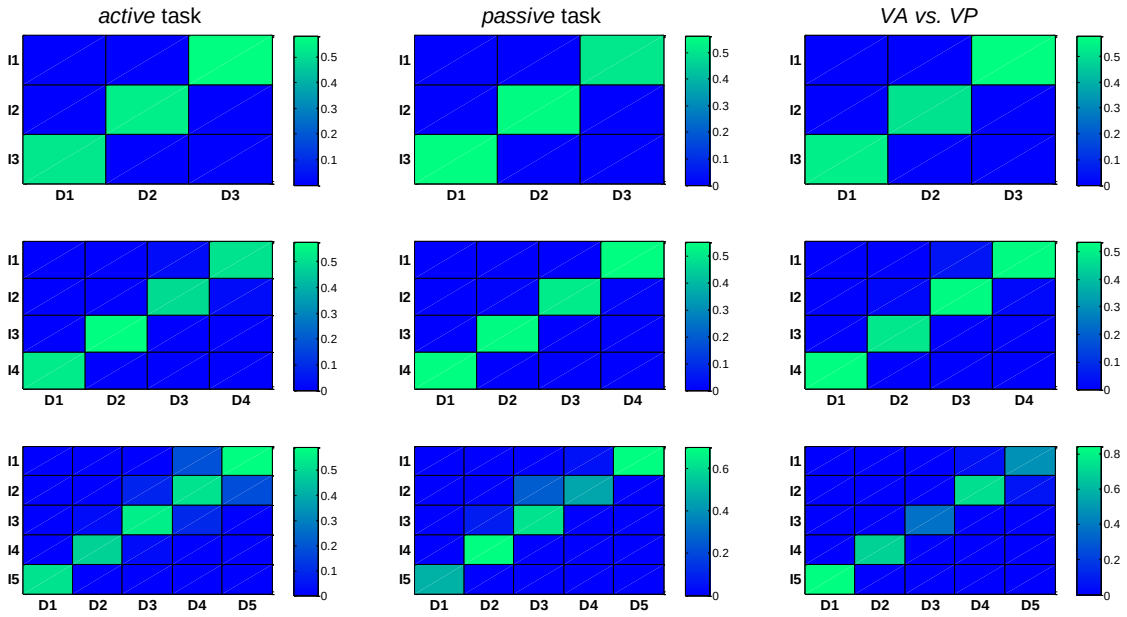

Figure 60 The results of the Kolmogorov-Smirnov twoo sample test (KS2 test) of the percentage of the *ISI* values comparison for different tasks

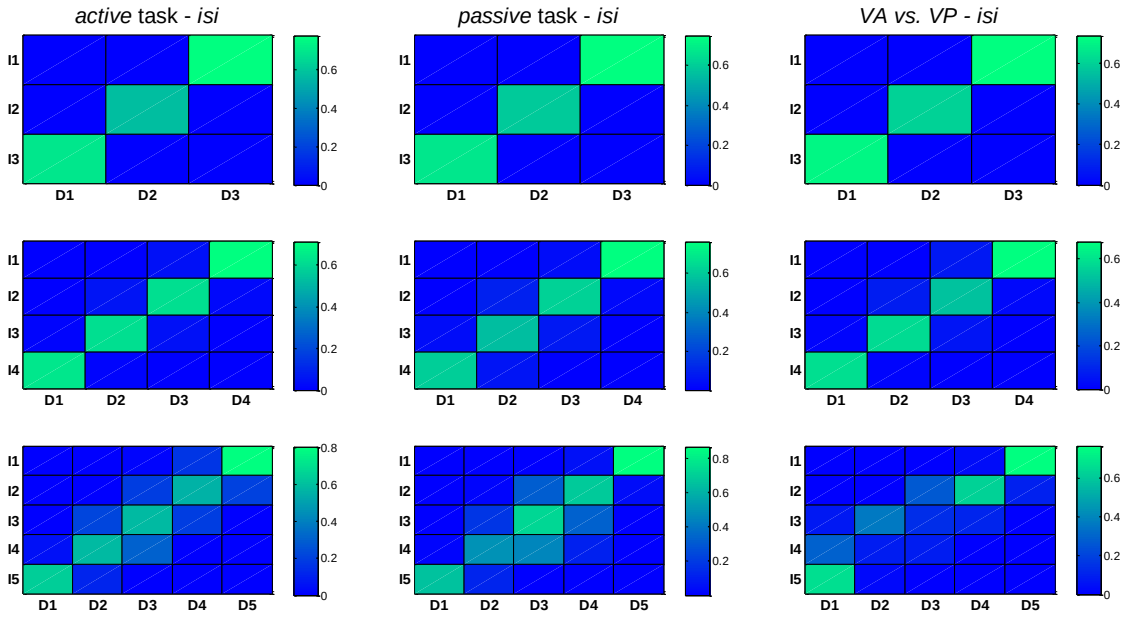

Figure 61 The results of the Kolmogorov-Smirnov twoo sample test (KS2 test) of the raw *ISI* values comparison for different tasks

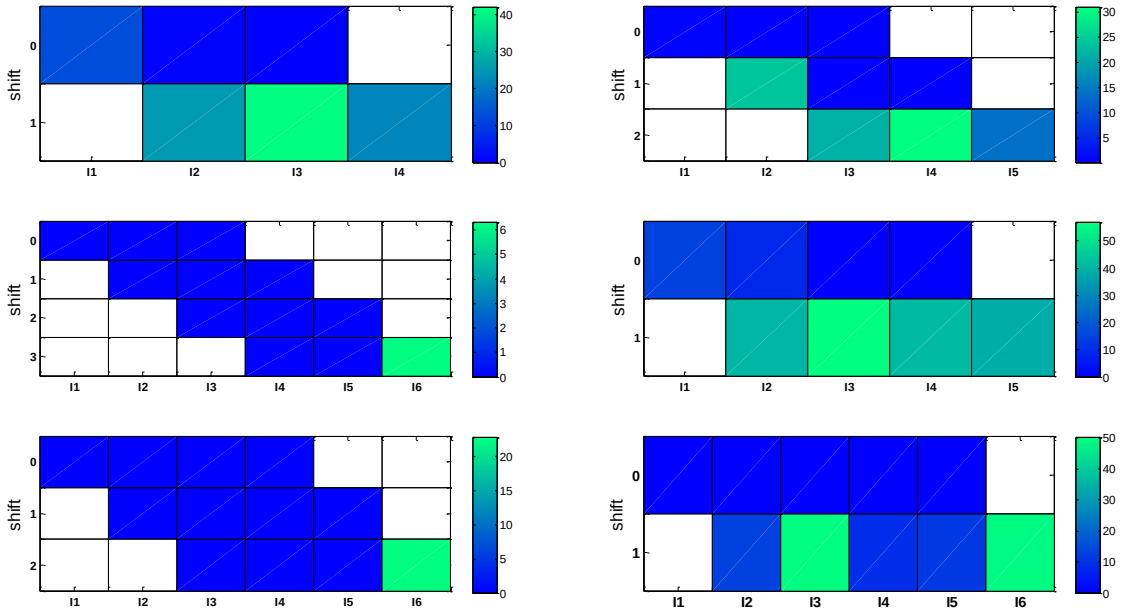

Figure 62 The KS2 test results of comparision between to different legth of *I* state; the y-axes represents the amount of shift of the shorter type state to compare the different percentage *ISI* values.

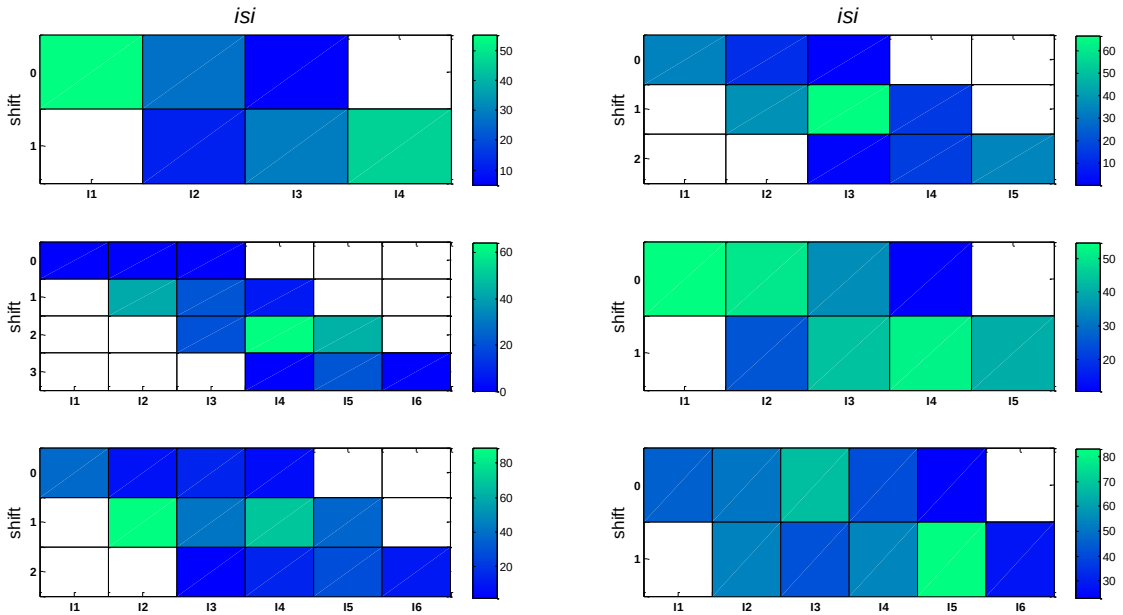

Figure 63 The KS2 test results of comparision between to different legth of *I* state; the y-axes represents of the amount of shift of the shorter type to compare the different raw *ISI* values

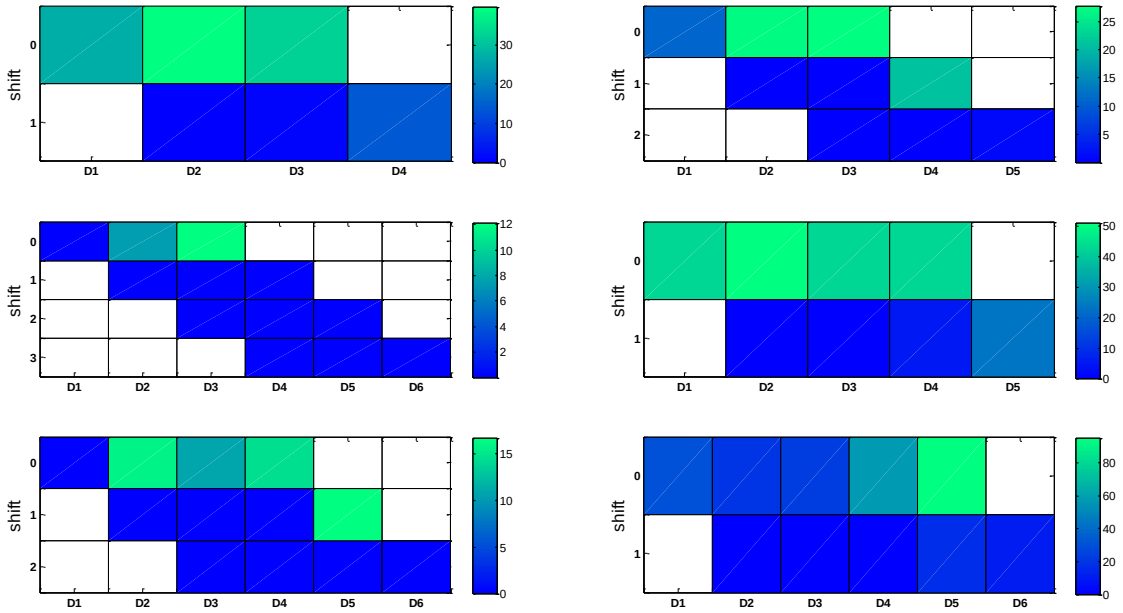

Figure 64 The KS2 test results of comparision between to different legth of *D* state; the y-axes represents of the amount of shift of the shorter type to compare the different percentage *ISI* values.

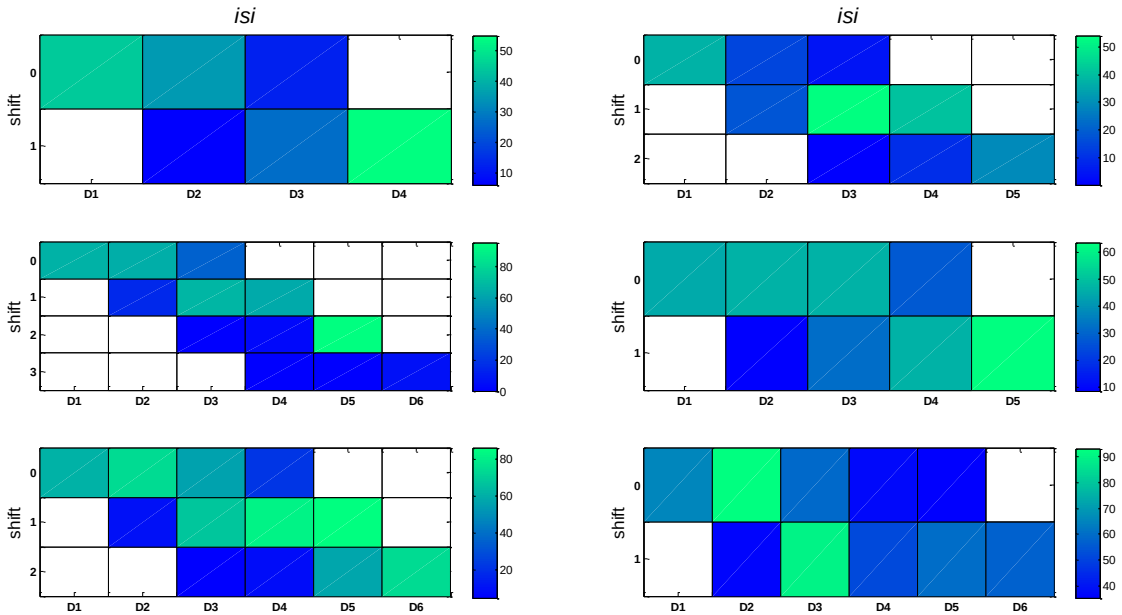

Figure 65 The KS2 test results of comparision between to different legth of D state; the y-axes represents of the amount of shift of the shorter type to compare the different raw ISI values.

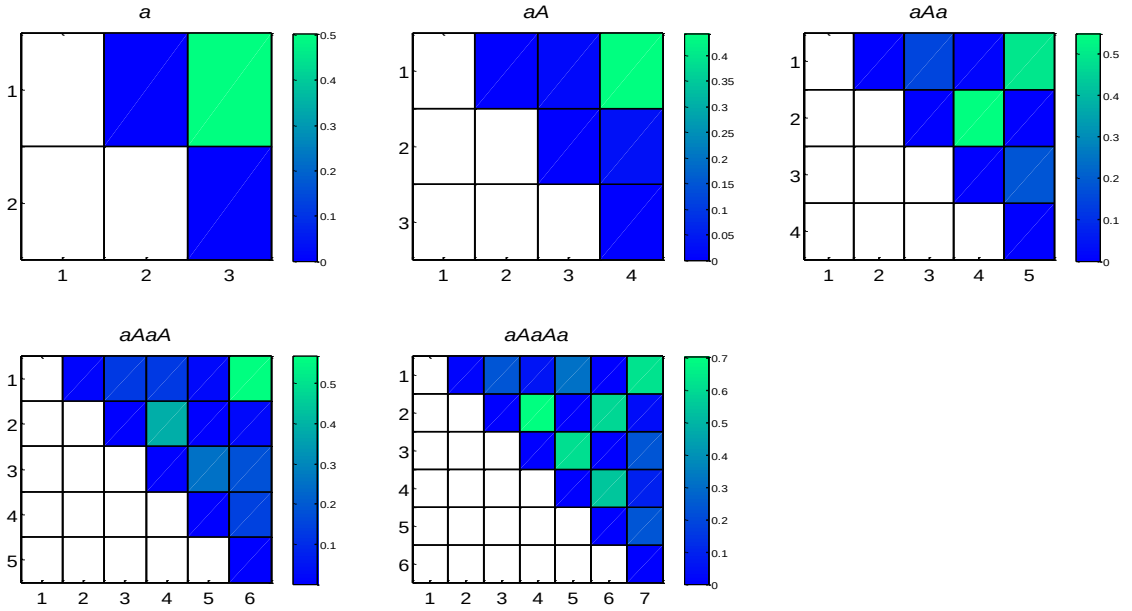

Figure 66 The KS2 test results of the self comparison of the alternate state pattern with different length starting with alternation state a; the coordinate of the colored patches present the order number of the ISI values which were tested

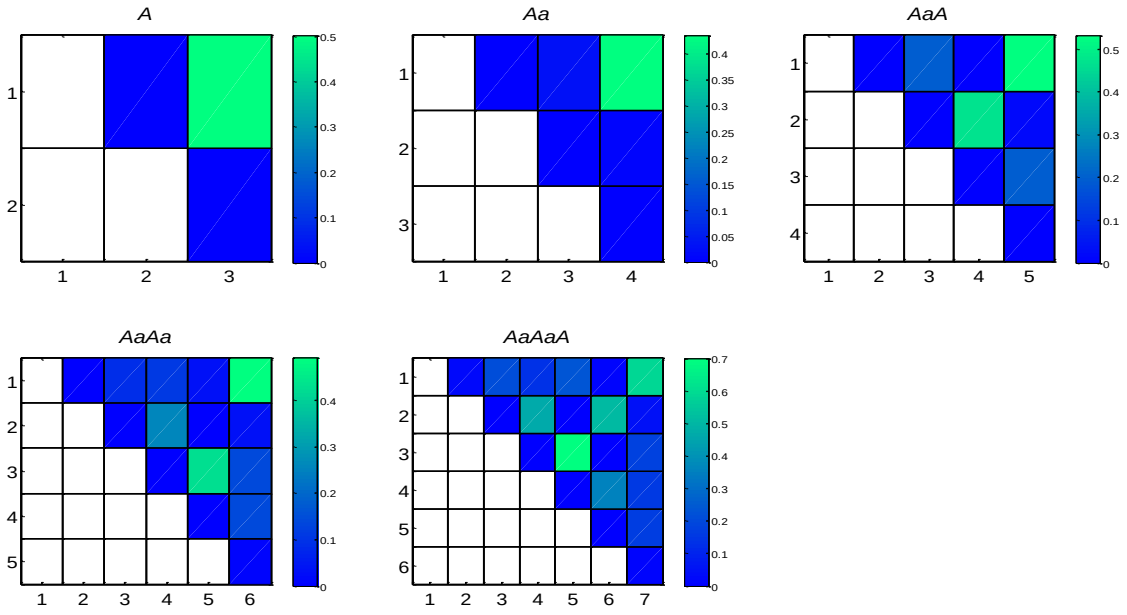

Figure 67 The KS2 test results of the self comparison of the alternate state pattern with different length starting with alternation state A ; the coordinate of the colored patches present the order number of the *ISI* values which were tested

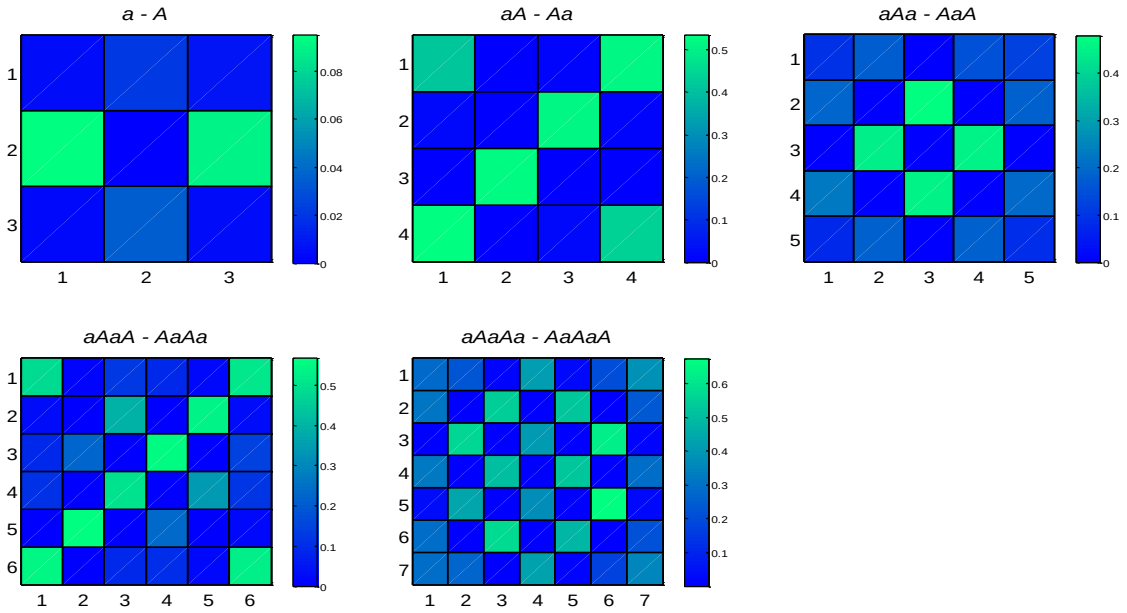

Figure 68 The KS2 test results of the cross comparisons of a and A alternate state pattern; the coordinate of the colored patches present the order number of the *ISI* values which were tested

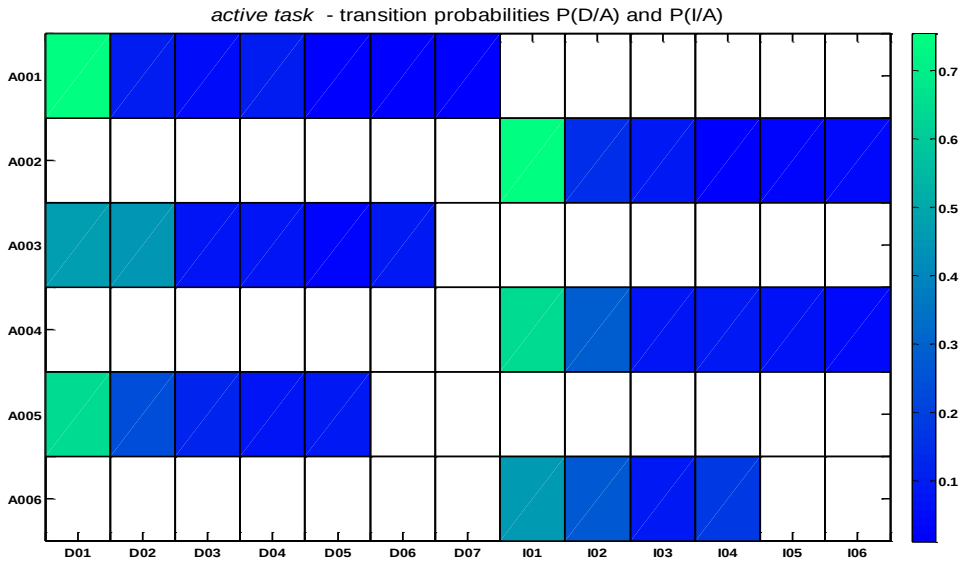

Figure 69 Transition probabilities of the *active* task

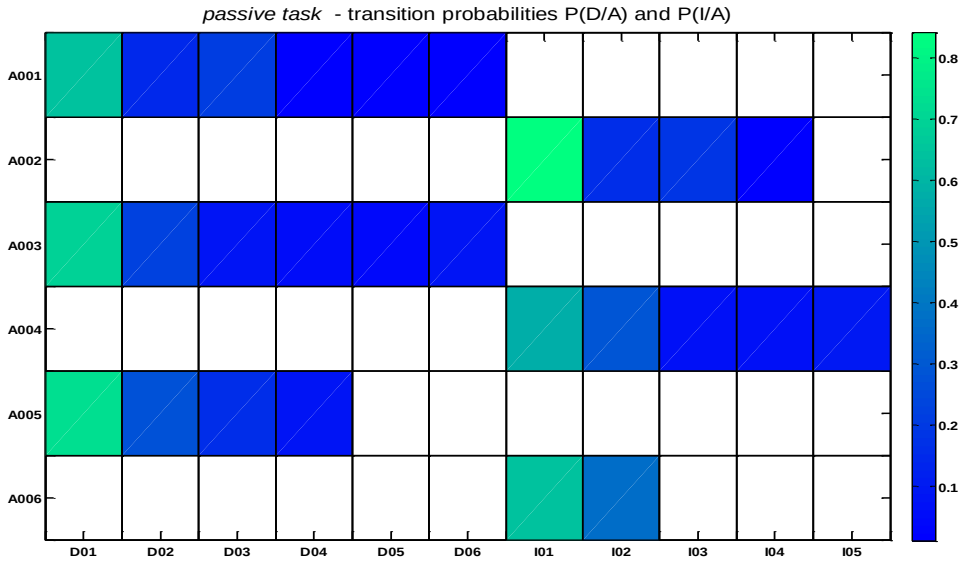

Figure 70 Transition probabilities of the *passive* task

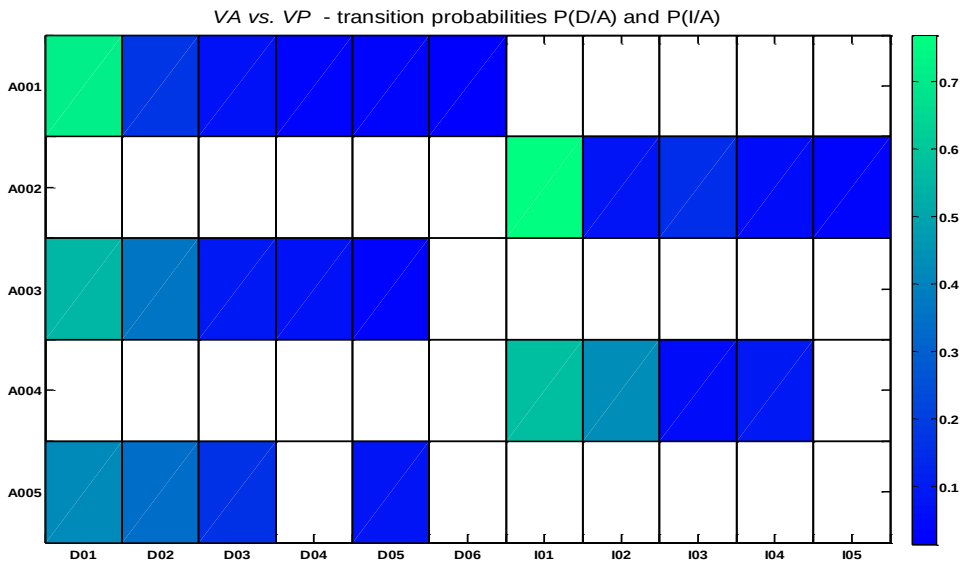

Figure 71 Transition probabilities of the *VA vs. VP* task

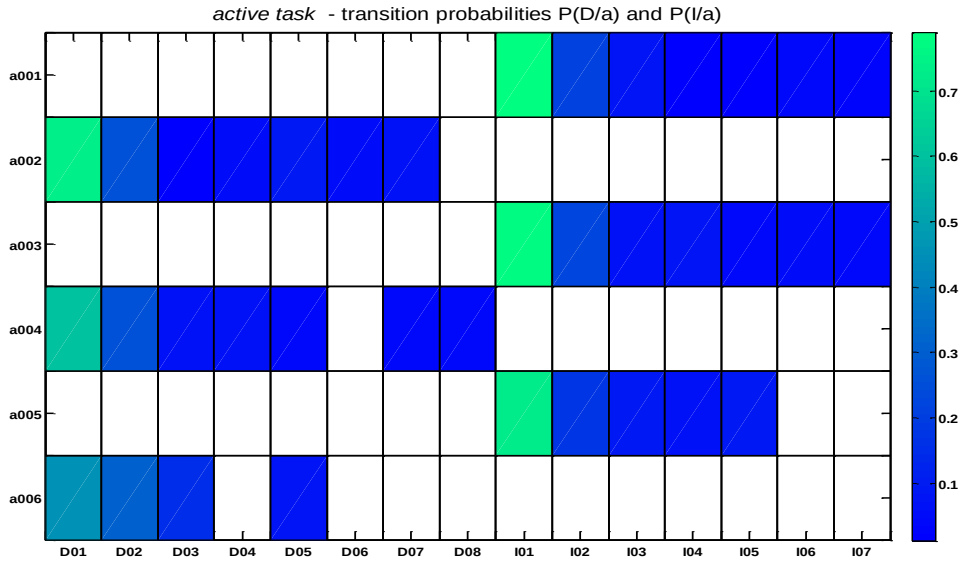

Figure 72 Transition probabilities of the *active* task

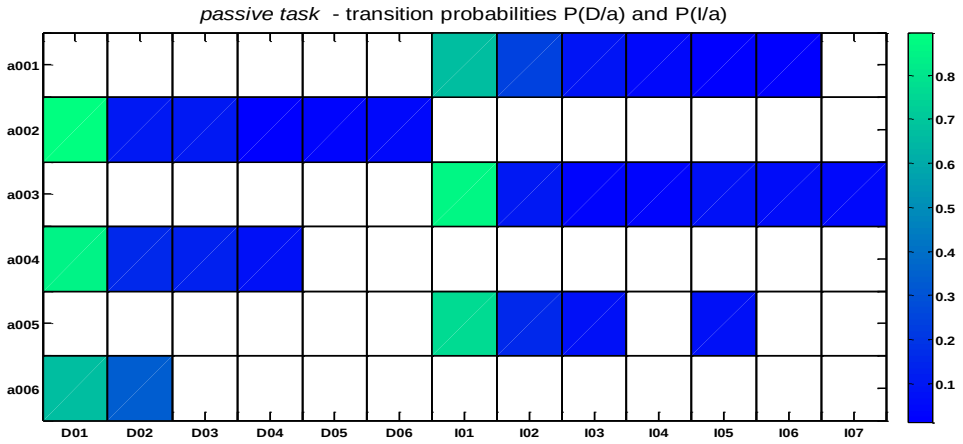

Figure 73 Transition probabilities of the *passive* task

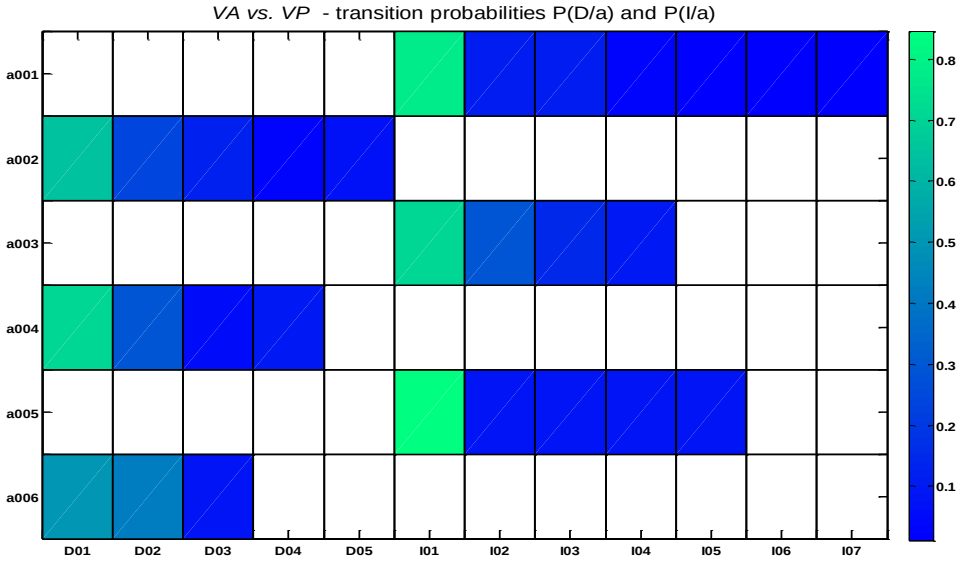

Figure 74 Transition probabilities of the *VA vs. VP* task

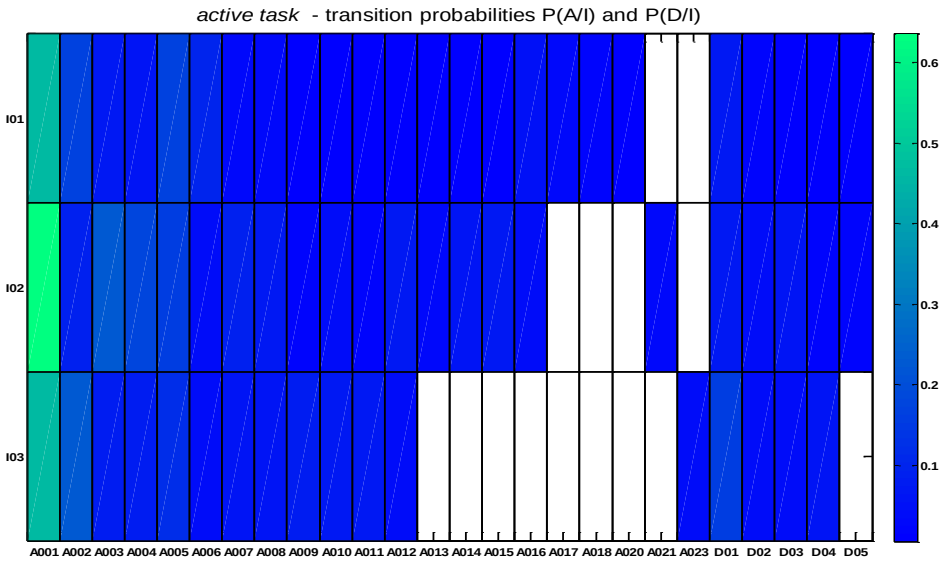

Figure 75 Transition probabilities of the *active* task

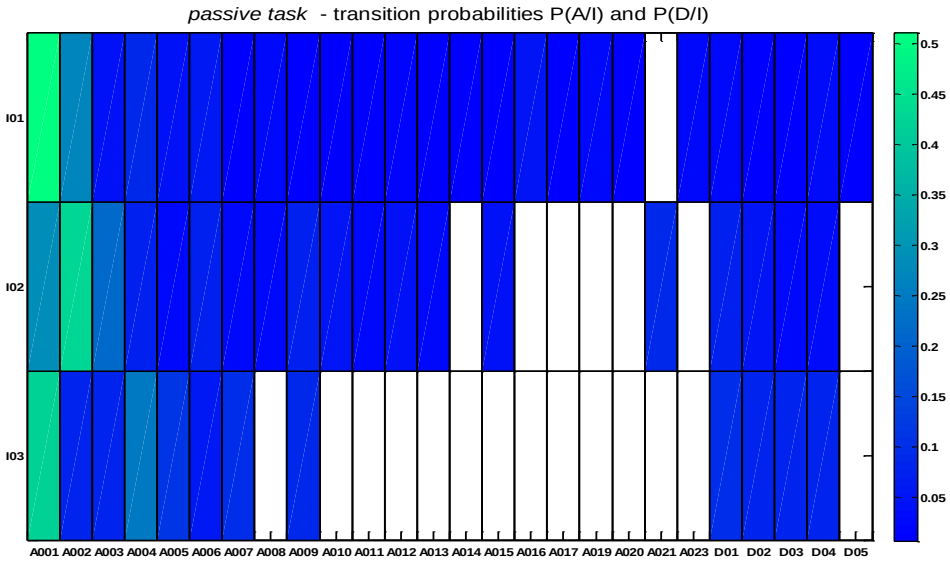

Figure 76 Transition probabilities of the *passive* task

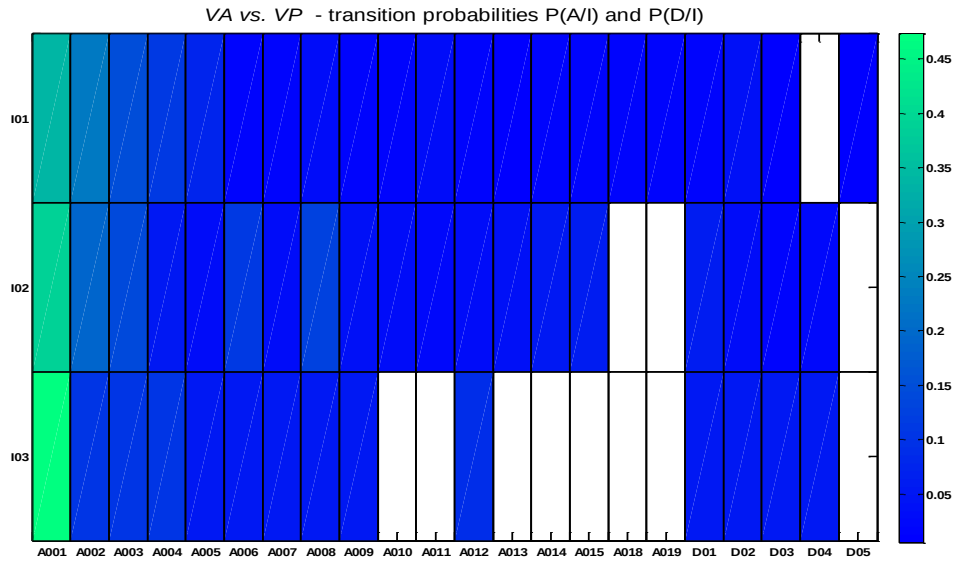

Figure 77 Transition probabilities of the *VA vs. VP* task

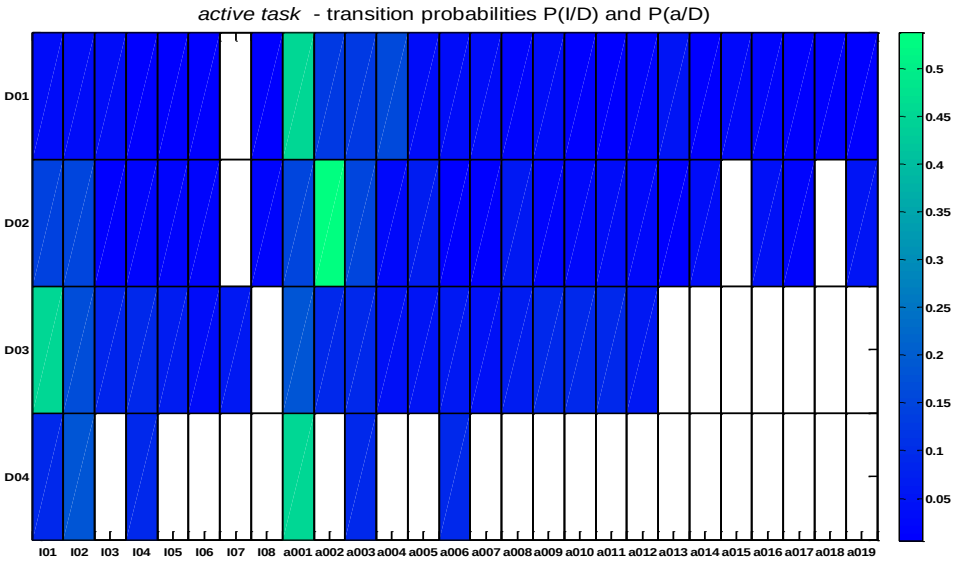

Figure 78 Transition probabilities of the *active* task

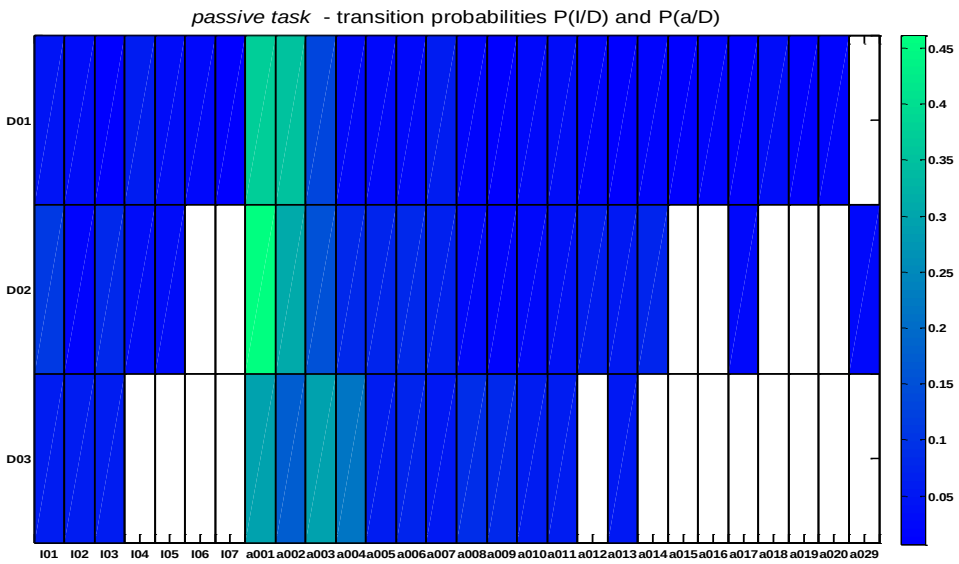

Figure 79 Transition probabilities of the *passive* task

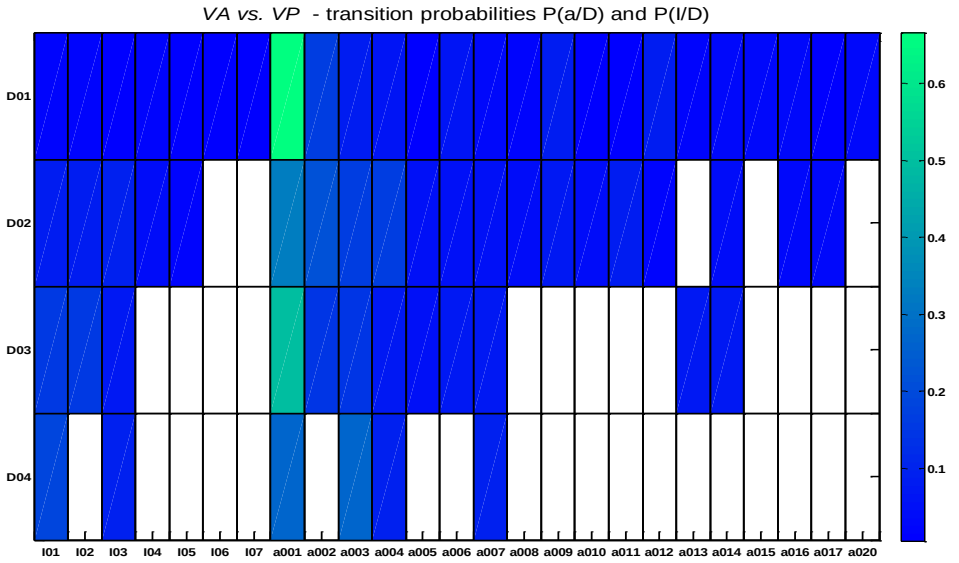

Figure 80 Transition probabilities of the *VA vs. VP* task

6. Discussion

Conclusions obtained from the results of the analysis of the states:

1. the time duration of the I and D states patterns are below of 1 sec.; Figure 9 shows; that the I and D pattern time durations in the same type the specific brain area are very similar; Figure 38 leads to the similar conclusion but for the different tasks; Figure 10 and Figure 37 show a possible stabilization of the time duration of the alternation state as the length of the patern increasing;
2. the distribution of the state of I, D and $alternation$ states over the state sequence population are 25%, 25% and 50% respectively; this result was obtained by counting the appearances of the I, D and x states in state sequences; the length of the specific increasing, decreasing and alternating pattern was not included in the counting process, Figure 11, Figure 39;
3. the three dimensional representations of the state sequences by they increasing, decreasing and alternataion state contents show different characteristics depending on the brain area, Figure 12, and on the different tasks, Figure 40; Figure 12 shows much more consistent distribution of the state sequences over a line; generally the different brain area can not be separated from each other; at Figure 40 the points are more scattered but they do not show any clasterisation to separate the different tasks; however, there are state sequences where the states I and D are missing, all the state sequences contain $alternation$ state,
4. to test the independence and homogeneite of the the state sequences for the different brain area and tasks, the crosstable test was used with minimum discrimination information statistics; Table 1 and Table 13 show that the hypothesis of the independence shoud be rejected at the given significance level;

5. regardless of the brain area, the distribution of the length of the state patterns show the same properties; in most of the state sequences the pattern of length of one state is present; as the length of pattern grows, the number of state sequences which contain the specific pattern length decrease; in case of states I and D the length of the pattern does not reach seven or eight consecutively repeated state; this is true for every brain area and also for the task; the *alternation* patterns are presented with longer length; Figure 13, Figure 14, Figure 41, Figure 42; notice that these figures show only the appearance of the specific state pattern in the sequence population, they do not give information about the number of the pattern in the sequences;
6. the cross table analyses reject the hyphothesis of the independence of the state sequences considering they contents of the pattern length of the increasing, decreasing and alternation states, Table 2, Table 3 and Table 4; only *ACC* brain has different statistical characteristic;
7. however, Table 18, Table 19 and Table 20 show the results of the hypothesis test of independence of the different task; the hypothesis of the independence has been accepted for all three task; the test results suggests that the appearance of the different pattern length of the I, D and alternation state is neither sequences nor task dependent;
8. the median and the average number of steps between two consecutive specific state pattern grows as the pattern length grows; this characteristic is valid for both of the I and D patterns; in all brain area the pattern length one has a shorter waiting time; this conclusion also hold for the different tasks, Figure 15, Figure 16, Figure 43 and Figure 44;
9. the cross table analyses considering the number of steps between the different increasing and decreasing state pattern length show a lack of independency, Table 5, Table 6, Table 18 and Table 19;

Conclusions obtained from the results of the analysis of the ISI statistics of the specific states:

1. the test included only those pattern length, which appear more than ten times in the state sequence;
2. the KS2 test reject the hypothesis of the identical distribution of the ISI values which make states I and D; the same results were obtained for other pattern length too;

3. KS2 test procedure include the cross comparison of ISI values of different pattern length of I state; taking into account the pV values obtained by the test, the results show that the ISI values of two different length of successively repeted I state follow different CDF function; the same results are obtained from the tests of different legth of D state, Figure 35, Figure 36, Figure 37, Figure 38, Figure 62, Figure 63, Figure 64 and Figure 65; these results lead to conclusion that the longer patterns can not be described as a repetition of the I or D state; because these pattern behave like a separate states, it would be suitable to define state spaces for the increasing and decreasing patterns and divide these spaces into parts depending of the number of different pattern length;

4. the results of cross comparison analysis of ISI values between I and D states with different pattern length reject the hypothesis of identical CDF function; statistically these to type of states are generated by different CDF function;

5. in case of the cross comparison analysis of ISI values between I and D states with same pattern length, the KS2 test accepted the hypothesis of the identical CDF function for those ISI values which follows in reverse order in these states; for example let's take the patterns II and DD which contain ISI values denoted as $II = \{I1, I2, I3, I4\}$ and $D = \{D1, D2, D3, D4\}$; the statistically identical CDF are $F(I1) = F(D4)$, $F(I2) = F(D3)$, $F(I3) = F(D2)$, $F(I4) = F(D1)$; the results are presented at Figure 31, Figure 32, Figure 33, Figure 34, Figure 59, Figure 60 and Figure 61; in the context of description given in Paragraph 5, the panels show that at the side diagonals the probabilities that the KS2 tets would give the same result in the same experimental condition are high; it should be emphasize that these specific patterns do not follow each other but appear in a mixed order, so this phenomena requires a careful explanation;

6. the results of the KS2 test analysis of the alternation state pattern have been devided into parts depending on the starting state a or A; these are further devided by the length of the pattern, odd or even number of states in the pattern; Figure 39, Figure 40, Figure 66 and Figure 67 show that the first and the last ISI values came from the same CDF; as the length of the pattern increasing so increasing the number of accepted hypothesis by the KS2 test; Figure 41, Figure 42, Figure 66 and Figure 67 give the same results but for the alternating patterns which begin with state A; it is observabile that for the longer pattern the middle part

of the pattern are independent from the parts with which the pattern begins and ends; from Figure 43, Figure 44 and Figure 68 it is also observabile that the that the twoo type of patterns are independent from the begin state; these observations lead to the conclusion that alternating patterns have short memory (possible one or twoo ISI values); after the short memory time the alternation patterns alternately use twoo type of CDF function to generate corresponding ISI values; the return of the end part to the begin part could be the influence of the input signals of the neuron;

7. Figure 45-50 and Figure 69-70 show that independently from the brain area or tasks, the transition from any length of any type of alternating pattern the most probable transition is to jump to the state $I01$ or $D01$; Figure 75-80 show similar behaviour of the I and D state patterns; the most probabile transition from these states are to states $a01$ and $A01$;

7. References

[1] https://commons.wikimedia.org/w/index.php?curid=36395693,

[2] https://commons.wikimedia.org/w/index.php?curid=1474927,

[3] https://commons.wikimedia.org/w/index.php?curid=2241513,

[4] https://commons.wikimedia.org/w/index.php?curid=19147827,

[5] https://commons.wikimedia.org/w/index.php?curid=4921195,

[6] L.F.Abbott, "Lapicque'sintroduction of the integrate-and-fire modelneuron(1907)", Brain Research Bulletin,Vol.50,Nos.5/6,pp.303–304,1999,

[7] https://en.wikibooks.org/wiki/Sensory_Systems/Computer_Models/NeuralSimulation 2016.06.23. 17.38,

[8] J.A. White, J.T. Rubinstein, A.R. Kay, "Channel noise in neurons.", *Trends Neurosci.*, 23:131-137,

[9] C. van Vreeswijk, H. Sompolinsky, "Chaos in Neural Networks with Balanced Excitatory and Inhibitory Activity", *Science*, Vol. 274, pp. 1724-1726, 1996,

[10] R.B. Stein, E.R. Gossen and K.E. Jones, "Neuronal Variability: Noise or part of the Signal", *Nature Reviews Neuroscience*, Vol. 6, pp. 389-397, 2005,

[11] E. D. Adrian and Yngve Zotterman, "The impulses produced by sensory nerve-endings Part II. The response of a Single End-Organ", J Physiol. 1926 Apr 23; 61(2): 151–171.

[12] Dayan, Peter; Abbott, L. F. (2001). Theoretical Neuroscience: Computational and Mathematical Modeling of Neural Systems. Massachusetts Institute of Technology Press. ISBN 978-0-262-04199-7,

[13] Moss F, Ward LM, Sannita WG (February 2004). "Stochastic resonance and sensory information processing: a tutorial and review of application". Clinical Neurophysiology. **115** (2): 267–81. doi:10.1016/j.clinph.2003.09.014,

[14] T. Lochmann and S. Den`eve "Information transmission with spiking Bayesian neurons" New J of Physics vol. 10, 055019, 2008,

[15] W. J. Ma, J. M. Beck, P. E. L. and A. Pouget, “Bayesian inference with probabilistic population codes” Nature Neurosc 9, pp. 1432 - 1438, doi: 10.1038/nn1790,

[16] J. Beck , W. Ma , P.E. Latham and A. Pouget, “Probabilistic Population Codes and the exponential family of distributions” in Cisek, Drew and Kalaska (Eds.) Progress in Brain Research Vol. 165, Elsevier (2007).

[17] Averbeck BB. Poisson or not Poisson: differences in spike train statistics between parietal cortical areas. Neuron. 2009 May 14;62(3):310-1,

[18] Mizuseki K, Buzsáki G. Preconfigured, skewed distribution of firing rates in the hippocampus and entorhinal cortex. Cell Rep. 2013 Sep 12;4(5):1010-21,

[19] Maimon G, Assad JA. Beyond Poisson: increased spike-time regularity across primate parietal cortex. Neuron. 2009 May 14;62(3):426-40,

[20] Petersen PC, Berg RW. Lognormal firing rate distribution reveals prominent fluctuation-driven regime in spinal motor networks. Elife. 2016 Oct 26;5. pii: e18805.

[21] A. Papoulis, *Probability, Random Variables, and Stochastic Processes*, New York, McGraw-Hill, 1965,

[22] J. Mališić, *Slučajni Procesi, teorija i primene*, IRO Građevinska Knjiga, Beograd, 1989,

[23] J. G. Kemeny, J. L. Snell, *Finite Markov Chains*, Van Nostrand, Princeton, NJ, 1960,

[24] R. Quliodran, M. Rothé and E. Procyk, “Behavioral shifts and action valuation in the anterior cingulated cortex”, *Neuron*, vol. 57, pp. 314-325, 2008,

[25] E. Procyk, P.S. Goldman-Rakic, “Modulation of Dorsolateral Prefrontal Delay Activity during Self-Organized Behavior“, *The Journal of Neuroscienc*, pp. 11313-11323, 2006,

[26] Y. Wang, S. Celebrini, Y. Trotter and P. Barone, “Visuo-auditory interactions in the primary visual cortex of the behaving monkey Electrophysiological evidence“, *BMC Neuroscience*, Volume 9, Number 1, pp. 1-15.

[27] J. Minich, „ISI time series models of electrocorticograph signals“, master (magistar) thesis, FTN, Novi Sad, 2009.